National Institute on Drug Abuse

RESEARCH

MONOGRAPH SERIES

Imaging Techniques in Medications Development: Preclinical and Clinical Aspects

138

U.S. Department of Health and Human Services • Public Health Service • National Institutes of Health

Imaging Techniques in Medications Development: Preclinical and Clinical Aspects

Editors:

Heinz Sorer, Ph.D.
Rao S. Rapaka, Ph.D.

NIDA Research Monograph 138
1994

U.S. DEPARTMENT OF HEALTH AND HUMAN SERVICES
Public Health Service
National Institutes of Health

National Institute on Drug Abuse
5600 Fishers Lane
Rockville, MD 20857

ACKNOWLEDGEMENT

This monograph is based on the papers from a technical review on "Imaging Techniques in Medications Development: Preclinical and Clinical Aspects" held in 1992. The review meeting was sponsored by the National Institute on Drug Abuse.

COPYRIGHT STATUS

National Institute on Drug Abuse
NIH Publication No. 94-3728
Printed 1994

NIDA Research Monographs are indexed in the *Index Medicus.* They are selectively included in the coverage of *American Statistics Index, BioSciences Information Service, Chemical Abstracts, Current Contents, Psychological Abstracts,* and *Psychopharmacology Abstracts.*

Contents

PET, SPECT, and Probes in Drug Design and Development

Henry N. Wagner, Jr.

INTRODUCTION

The technology of nuclear medicine has the potential of bringing together three approaches to drug design and development: genetic, biochemical, and pharmacologic (Burns et al. 1993; Bice et al. 1986; Jefferies et al., submitted; Swann 1988). For example, using polymerase chain reaction, one can synthesize large quantities of complementary RNA related to the production of a specific biochemical such as D_2-dopamine receptors. The structure of the receptor can be determined by means of x-ray crystallography. The essential features of the structure of the receptor that relate to the binding and activation of D_2-dopamine receptors can be determined. Using positron-emitting tracers, one can determine the site, quantity, and degree of occupancy of the receptors and examine the reuptake of dopamine into presynaptic dopaminergic neurons through the dopamine transporter (Gamett et al. 1983; Wagner et al. 1983). Thus, the status of both the presynaptic and postsynaptic neurons can be examined. If one can successfully label oligonucleotides such as the antisense oligonucleotide related to dopamine receptor synthesis, factors affecting the synthesis of D_2-dopamine receptors could be examined. In essence, nuclear medicine makes it possible to relate genotypes, chemotypes, and phenotypes. The essence of modem nuclear medicine is in vivo biochemistry of living human beings.

At the annual meeting of the Society of Nuclear Medicine held in Los Angeles in June 1992, Dewanjee and colleagues (1992) from the University of Miami reported that they had labeled an antisense oligonucleotide with a diethylenetriaminepenta-acetic acid (DTPA) chelate of ^{111}In. When injected intravenously, the tracer bound to leukocytes. Many problems such as nonspecific binding remain to be solved, but, if the oligonucleotide binds successfully to messenger RNA (mRNA), it could represent a major focus of radiotracer

development for in vivo studies. The primary message is that carried by mRNA, which controls the synthesis of polypeptides or proteins.

By looking at the receptors themselves, it is possible to determine the required shape, hydrophilicity, charge, and other factors that result in binding by the receptor with a high affinity. It is possible to design tracers as well as therapeutic agents to conform to the structural requirements. The pharmacokinetics of these agents can be examined and the relationship between structure and function assessed.

Even with complete knowledge of the genome, it would be necessary to examine the biochemical expression of the genome. One important genetic principle is pleotropism, which states that an abnormal gene can result in many different diseases. A defective polypeptide can result in failure of multiple systems, resulting in many different phenotypic manifestations of disease. A second principle is genetic heterogeneity, which states that many different gene abnormalities can result in or produce the same disease manifestations. Thus, the approaches to disease should be genetic, biochemical, and pharmacologic.

USING PET AND SPECT TO TREAT DISEASE

With positron emission tomography (PET) and single photon emission computed tomography (SPECT), researchers can begin to close the circle between brain chemistry and behavior. Not only amine receptors but also polypeptide receptors have been studied successfully. Peptides are bound by specific receptors, are inexpensive to produce by genetic engineering techniques, and are quickly cleared from the blood. Most of the 50-odd peptides are amenable to radiotracer development. One characteristic of peptides is that they do not cross the blood-brain barrier. With the application of the ability to examine various parts of neuroreceptor systems, including the dopamine and opiate systems, it is now possible to examine a whole new approach to drug therapy-the direct installation of amines or peptides into specific regions of the brain. Examples of potential applications of the approach are the treatment of Parkinson's disease (PD) by the infusion of amines or nerve growth factors, of epilepsy by local infusion of drugs (Frost et al. 1985; Mazziotta and Engel 1984), or of intractable

pain by blocking pain receptors. This approach of direct infusion into specific regions of the brain might be useful for the treatment of persons suffering from substance abuse.

PET and SPECT technology could help develop increasingly specific drugs by adding in vivo biochemistry to physiology in drug design and development. The vasopressin story is a prototype. The vaso-constrictive effect of native vasopressin was removed from the antidiuretic effect of vasopressin, which makes it more effective in the treatment of diabetes insipidus. Genetic engineering produces an effective drug that has only an antidiuretic effect. Biochemical tracing and biochemical treatment are two sides of the same coin-molecular medicine. More and more specific tracers directed toward particular biochemical recognition sites have been developed.

From the beginning of the pioneering studies with [^{18}F]deoxyglucose, PET was concerned primarily with bioenergetics (Phelps et al. 1986). Today, both PET and SPECT make it possible to examine intercellular communication in living human beings. Life is maintained because atoms and molecules can recognize each other. More diseases are being characterized as problems with intracellular communication. In the absence of vasopressin receptors, a person develops congenital diabetes insipidus because vasopressin cannot be recognized.

Another example of a disease involving neurotransmission is PD. In the mid-1960s, it was discovered that patients with PD have a deficiency of dopamine in the basal ganglia as a result of degeneration of dopaminergic neurons in the substantia nigra. In 1983, it became possible to image and quantify D_2-dopamine receptors in the living human brain with the tracer [^{11}C]N-methyl spiperone (NMSP). Since that time, both PET and SPECT have been used to examine many aspects of dopamine biochemistry in the human brain. For example, dopamine synthesis can be examined with fluorine-labeled L-dopa. The secretion of dopamine can be measured by its competitive inhibition of tracers that bind to dopamine receptors. It is possible to assess the availability of both presynaptic and postsynaptic receptors, including the presynaptic dopamine transporter involved in the action of cocaine.

Although the state of the art of PET and SPECT imaging has a spatial resolution of about 5 mm, specific chemicals can be used to differentiate the effects of drugs on structures that are only micrometers apart. For example, if one produces a unilateral lesion of presynaptic dopaminergic neurons by injecting the neurotoxin 1-methyl-4-phenyl-1,2,3,6-tetrahydropyridine (MPTP) into a single internal carotid artery, the impairment of presynaptic neurons, but not postsynaptic neurons, can be documented by quantitative imaging of the presynaptic dopamine transporter with [^{11}C]-labeled WIN 45-428 and of the postsynaptic dopamine receptors with [^{11}C]NMSP.

The dopaminergic system has been studied extensively by PET, and the serotonergic system also is becoming a major focus. For example, there is now an effective tracer of the serotonin presynaptic transporter available in both active and inactive isomeric forms that makes possible subtraction images and facilitates quantification.

COMPARISONS BETWEEN PET AND SPECT

What about the relative merits of PET and SPECT in drug design and development? The most fundamental difference lies in the radionuclides that each employs. PET tracers are chiefly those of [^{11}C] and [^{11}F] and, to a lesser degree, ^{12}N and ^{15}O. SPECT primarily uses iodine- 123 ([^{123}I]) or technetium-99m (Tc-99m). The major problem with PET is related to the short half-life of [^{11}C] (20 minutes) and [^{18}F] (2 hours). The half-life of Tc-99m is 6 hours and that of [^{123}I] is 13 hours, which greatly decreases the demands of the study. If a study can be carried out successfully with SPECT, it should be used. Many studies cannot be done with SPECT. The chief advantage of PET is related to [^{11}C]. Chemistry will always be easier with [^{11}C] than it will be with [^{123}I] or Tc-99m, so many new tracers can be developed faster with PET than with SPECT. However, PET successes are translated into more widespread use by extending them to SPECT.

Using PET facilitated the study of D_2-dopamine receptors and transporters. First, [^{11}C]NMSP was developed; its success led to the development of [^{123}I]-labeled benzamides for the study of D_2-dopamine receptors by SPECT. The presynaptic transporter initially was examined with a [^{11}C] tracer that is specific for the dopamine

transporter. The SPECT tracer-[^{123}I] RTI-55-was then developed and found to bind to both serotonin and dopamine presynaptic transporters. The iodinated tracer also was found to have a higher affinity for the transporter than the [^{11}C] compound.

Another advantage of the [^{123}I] tracers is related to their 13-hour half-life, which makes it possible to carry out studies for 24 or more hours after injection of the tracer. By that time, nonspecific binding is less than that observed soon after injection of the [^{11}C]-labeled tracer because of its 20-minute half-life.

USING PET AND SPECT TO PLAN TREATMENT

The purpose of studies with these new tracers of recognition sites is to characterize patients biochemically, as well as physiologically, and then plan treatment for them on the basis of their chemical abnormalities. Because the classification is biochemical, the treatment often can be chemical, and the response to treatment can be assessed chemically. PET and SPECT do not just provide new tests for "old" diseases. They provide a whole new way of looking at disease-an approach based on in vivo biochemistry (i.e., molecular medicine).

An example of an "old" disease is Alzheimer's disease. Dementia is the primary presenting problem; senile plaques and neurofibrillary tangles in histopathological sections of the brain are the basis of classification. Dementia is analogous to heart failure in representing a heterogeneous population. It is naive to search for a single biological marker that will characterize all patients who meet the phenotypical criteria for schizophrenia as described in *the Diagnostic and Statistical Manual of Mental Disorders* (American Psychiatric Association 1987). Schizophrenics are also a very heterogeneous population of patients. The status of specific neuronal systems, the perturbation of which may help the patients, must be determined. In vivo chemistry can be used to try to answer the five basic questions that describe the practice of medicine:

- What is wrong with the patient?
- How did it happen?
- What is going to happen?

- What can be done about it?
- Is the problem being solved?

The approach to movement disorders is a good example. In patients with typical idiopathic PD, both D_1- and D_2-dopamine receptors are intact, and patients benefit from being given L-dopa to increase dopamine synthesis or bromocriptine to stimulate the intact D_2-receptors. Other patients with movement disorders involving nigrostriatal degeneration have impaired D_2-dopamine receptors and will not be helped by either L-dopa or bromocriptine treatment.

The development of a SPECT tracer of D_2-dopamine receptors called [^{123}I]iodobenzamide extended the PET studies to larger numbers of patients with movement disorders. A recent study (Dewanjee et al. 1992) included 60 patients with idiopathic PD, 17 controls, and 30 patients with Parkinson's syndrome. Quantification with PET was more accurate than with SPECT. Some investigators (e.g., Dewanjee et al. 1992) have used simple indices such as the basal ganglia to frontal cortex activity ratios in [^{123}I]iodobenzamide studies of D_2-dopamine receptors. There is a dangerous tendency to oversimplify when a method becomes simple. SPECT studies should be carried out drawing on the lessons learned from decades of PET. Attenuation correction, positioning, errors related to the limitations in spatial resolution, and many other technical factors are as important for SPECT as for PET.

ROLE OF SOMATOSTATIN RECEPTORS IN CANCER DIAGNOSIS

An example of an advance made recently in SPECT is the study of somatostatin receptors by Krenning and colleagues (1992*a*) from the Netherlands. They used an 8-amino acid polypeptide analog of somatostatin, a growth suppressor. The tracer, octreotide-111, was labeled with an ^{111}In DTPA chelate. Developed in Sandoz Research Institute, the labeled octreotide was investigated initially at the University of Rotterdam by Krenning and colleagues. To date, they have studied more than 1,000 patients with various types of neuroendocrine and other tumors. Among the findings was the fact

that 70 percent of 70 patients with carcinoma of the breast had somatostatin receptors.

Somatostatin receptor imaging should not be considered a test for breast cancer. It is a test for somatostatin receptors. If a tumor has somatostatin receptors, the patient is a candidate for somatostatin therapy. Somatostatin is a stable drug.

An important finding by Krenning and colleagues (1992*b*) was that patients with hyperthyroidism and exophthalmus have large numbers of somatostatin receptors in the T lymphocytes behind the eyes. The degree of accumulation of octreotide-111 behind the eyes was related to the degree of the malignant exophthalmus. This finding is important in planning treatment. If the disease is active, the patient can be treated with steroids or an immunosuppressive drug. If there is no evidence of activity of the disease, the exophthalmus is treated better by surgery to remove the fibrous tissue behind the eyes. Thus, again, one sees the sequence: chemical characterization of the disease, planning of treatment, and monitoring of treatment on the basis of chemistry.

An example of how effectively PET and SPECT technology can be used to study the action of drugs is the recent report of Dewey and colleagues (1992) from Brookhaven National Laboratory, who studied the effects of a suicide inhibitor of the enzyme that breaks down γ-aminobutyric acid (GABA), an inhibitory neurotransmitter. Inhibition of the metabolizing enzyme resulted in decreased production of GABA. This in turn disinhibited the dopaminergic neurons, so synaptic dopamine secretion increased. The secretion of dopamine competed with the binding of [^{11}C]raclopride by the D_2-dopamine receptors, so more dopamine receptors were available for binding [^{11}C]raclopride. Dopamine secretion inhibited the release of acetylcholine by cholinergic neurons; this inhibition was reflected in increased binding of [^{11}C]benzotropine because less acetylcholine was bound to the acetylcholine receptor. Thus, Dewey and colleagues (1992) were able to demonstrate serial neurochemical effects among three neurotransmitters-GABA, dopamine, and acetylcholine. Their studies were also a demonstration of how endogenous neurotransmitter release can be measured by competitive inhibition of radioligand binding.

SIMPLE PROBE SYSTEM USES

Some types of problems do not need the spatial resolution provided by PET or SPECT. Much simpler dual-detector systems can be used to look at either the entire brain or specific regions such as the frontal lobes or cerebellum. The use of the simple probe systems shows that it is not necessary to use expensive high-spatial-resolution PET or SPECT imaging to solve problems in which spatial resolution does not have to be high. Probes are simple and less expensive by a factor of 30 or 50. The radiation dose also is reduced by orders of magnitude compared with high-resolution imaging, in which the statistical limitations are related to the number of counts per picture element.

Particularly in the study of drug effects, it is often not necessary to have a high degree of spatial resolution. For example, a high-resolution system is not needed to measure the quantitative effect of naltrexone or naloxone on opiate receptors. The antagonists affect all the u-type opiate receptors regardless of location. Conversely, in a problem such as temporal lobe epilepsy, in which the search is for a focus in the temporal or frontal lobe, a high degree of spatial resolution is required.

A probe device developed at The Johns Hopkins University has been used to study mice, rats, dogs, baboons, and human beings. For example, in living mice it was possible to obtain a dose/response curve showing the blocking effect of haloperidol on the binding of [^{11}C]NMSP. Similar dose/response curves were obtained in human beings, and the results correlated well with PET studies of the same persons. One study (Brust et al. 1992) examined the effect of vasopressin on [^{11}C]methionine accumulation in the brain of living dogs. When nonradioactive phenylalanine was given before the dose of [^{11}C]methionine, the rate of transport of methionine decreased because of competitive inhibition. The purpose of the vasopressin study was to test the hypothesis that vasopressin's effect on memory might be through amino acid transport because vasopressin itself does not cross the blood-brain barrier. Vasopressin administration did inhibit [^{11}C]methionine transport,

Another study (Lee et al. 1988) addressed the question of how long a 50-mg dose of naltrexone blocks opiate receptors. When

[^{11}C]carfentanil was used at various times after the administration of an oral 50-mg dose of naltrexone, it was found that the half-time of blockade of the receptors was 72 hours. Thus, even though a 50-mg dose blocks the p-opiate receptors for about a week, it is recommended that the dose be given every day, primarily because of the rapid blood clearance of the drug. By examining the state of the receptors themselves, one can get closer to the site of action of the drug than one can get by measuring only plasma concentrations of the drug. This study exemplifies the marriage of nuclear medicine technology and drug design and development.

Probe-based systems have the potential of opening up PET and SPECT studies to basic neuroscientists. It is unlikely that human-oriented PET or SPECT scanners can be provided to basic neuroscientists, but simpler systems can be used to take advantage of the new tracers rapidly being developed. Probe studies also can be carried out safely and effectively in public health studies. In the author's laboratory, for example, the effects of lead toxicity on brain neurochemistry are being investigated. At present, only laboratory animals are being studied, but it is hoped that the studies soon will extend to human beings. It is unlikely that PET imaging could be used in public health studies.

Another direction is the development of less expensive imaging devices for the study of animals. Green and colleagues (1992) at the National Institutes of Health have developed a SPECT scanner for animals that costs less than $50,000.

CONCLUSION

The main engine of nuclear medicine technology is the cyclotron because of its chemical capabilities, chiefly [^{11}C] and [^{18}F]. PET studies are beginning to be used in community hospitals and research centers from centrally located cyclotrons, some under commercial sponsorship. One commercial supplier of cyclotron-produced radiotracers is in Los Angeles; another is in Phoenix, where PET imaging is carried out in community hospitals and health centers using tracers supplied from a central cyclotron. More research and patient studies can be carried out with Tc-99m and [^{123}I] because of their longer half-lives. The half-lives of these tracers will never

change—for [^{11}C], 20 minutes; for [^{18}F], 2 hours; for Tc-99m, 6 hours; and for [^{123}I], 13 hours. At the 1992 Society of Nuclear Medicine meeting mentioned previously, 51 papers were based on the use of [^{11}C] compounds. Forty papers (not all discussing [^{11}C]) involved the dopaminergic system, and 125 papers involved [^{18}F]. Ninety papers were based on [^{18}F]deoxyglucose to study bioenergetics. Half of the nearly 900 papers presented at the meeting involved PET or SPECT.

The number of studies of neuroreceptors continues to increase every year. Blood flow and metabolism also are important topics. A major area of research is the study of drug effects. Someday, a psychiatrist or other physician will be measuring brain chemistry with simple probe detectors the way physicians now use the sphygmomanometer to measure blood pressure.

A description of a patient who presented with a lesion of the brain that was seen in a magnetic resonance imaging study illustrates the use of various imaging techniques. Was it a tumor? Was it radiation necrosis? A [^{18}F]deoxyglucose study showed that the lesion was hypometabolic and therefore not a tumor. The pituitary was very hypermetabolic, indicating a tumor. The next question was whether the tumor had dopamine receptors on its membrane, as is the case with many pituitary tumors. If a pituitary tumor manifests dopamine receptors, dopamine receptor agonists are helpful because the dopaminergic system is inhibitory of cell growth, acting through prolactin-secreting cells. This tumor contained dopamine receptors, so bromocriptine (a dopamine agonist) therapy was begun. By studying the metabolism of either deoxyglucose or amino acids, in 1 day it was determined whether the metabolic activity of the tumor had been reduced. If the metabolism was not affected, there was no reason to treat the patient for months, waiting for anatomical changes to occur. Thus, in 1 day it was possible to characterize the tumor, plan the treatment, and monitor the effect of the treatment (Di Chiro, personal communication, 1992).

Is there a competition between PET and SPECT? Their synergism is documented by that fact that, as noted above, the use of both has been increasing to the point that they were discussed in 50 percent of the papers presented at the 1992 Society of Nuclear Medicine meeting. PET and SPECT are like two hands with which complicated problems

can be approached. To emphasize one without the other is like tying one hand behind the back. If SPECT can solve a problem, it should be used; but PET will always be able to do things that SPECT cannot do because this is a world of carbon, and there never will be a good SPECT tracer for carbon. That is physics, and that is forever. There is a PET and SPECT continuum, in which both will flourish and in which SPECT extends PET. Yet, advances often will be made initially by SPECT because of the greater simplicity and greater numbers of patients who can be studied. PET, however, is unique in the possibility of labeling pharmacological compounds without changing their pharmacological behavior. Evaluating the behavior of a drug in vivo through time is now a PET domain.

REFERENCES

American Psychiatric Association. *Diagnostic and Statistical Manual of Mental Disorders* 3rd ed. Washington, DC: American Psychiatric Press, 1987.

Brust, P.; Shaya, E.K.; Jeffried, K.J.; Gjedde, A.; Dannals, R.F.; Ravert, H.T.; Wilson, A.A.; Wagner, H.N., Jr.; Ermisch, A.; and Wong, D.F. Effects of vasopressin on blood-brain transfer of methionin in dogs. *J Neurochem* 59: 1421-1429, 1992.

Dewanjee, M.K.; Ghafouripour, A.K.; Kapadvanjwala, M.; Glenn, S.; Serafini, A.N.; Sfakianakis, G.N. A new direct method of cell-labeling in whole blood by administration of In-111 labeled anti-sense oligonucleotide. Abstract. *J Nucl Med* 33:980, 1992.

Dewey, S.L.; Brodie, J.D.; Smith, G.; Logan, J.; MacGregor, R.R.; King, P.T.; Fowler, J.S.; Wolf, A.P.; Volkow, R.A.; and Ferrieri, R.A. GABAergic modulation of endogenous dopamine and acetylcholine release measured in vivo with positron emission tomography. Abstract. *J Nucl Med* 33:847, 1992.

Frost, J.J.; Wagner, H.N., Jr.; Dannals, R.F.; Ravert, H.T.; Links, J.M.; Wilson, A.A.; Bums, D.H.; Wong, D.F.; McPherson, R.W.; Rosenbaum, A.E.; Kuhar, M.J.; and Snyder, S.H. Imaging opiate receptors in the human brain by positron tomography. *J Comput Assist Tomogr* 9(2):231-236, 1985.

Gamett, E.S.; Firnau, G.; and Nahmias, C. Dopamine visualized in the basal ganglia of living man. *Nature* 305:137-138, 1983.

Green, M.V.; Markowitz, A.; Tedder, T.E.; Andrich, M.P.; Owens, ES.; and Neumann, R.D. SPECT imaging in small animals. Abstract. *J Nucl Med* 33:852, 1992.

Krenning, E.P.; Bakker, W.H.; Kooij, P.P.M.; Breeman, W.A.P.; Oei, H.Y.; de Jong, M.; Reubi, J.-C.; Visser, T.J.; Bums, C.; Kwekkeboom, D.J.; Reijs, A.E.M.; van Hagen, P.M.; Koper, J.W.; and Lamberts, S.W.J. Somatostatin receptor scintigraphy with [^{111}In-DTPA-Phe^{1}] octreotide in man: Metabolism, dosimetry and comparison with [^{123}1-Ty^{3}]-octreotide. *J Nucl Med* 33:652-658, 1992*a*.

Krenning, E.P.; Oei, H.Y.; Kooij, P.P.M.; Wijnngaarde, R.; Lamberts, S.W.J.; Wiersinga, W.M.; Prummel, M.F.; and van Royer, R.M.L. Thyroid and orbital radiolabelled somatostatin accumulation in Graves' disease and Graves' ophthalmopathy. Abstract. *J Nucl Med* 33:894, 1992*b*.

Lee, M.C.; Wagner, H.N., Jr.; Tanada, S.; Frost, J.J.; Bite, A.N.; and Dannals, R.F. Duration of occupancy of opiate receptors by naltrexone. *J Nucl Med* 29:1207-1211, 1988.

Mazziotta, J.C., and Engel, J., Jr. Advanced neuro-imaging techniques in the study of epilepsy: PET, SPECT and NMR-CT. In: Pedley, T., and Meldrum, B., eds. *Recent Advances in Epilepsy.* Vol. 2. Edinburgh, UK: Churchill, Livingstone, 1984.

Phelps, M.E.; Mazziotta, J.C.; and Schelbert, H.R., eds. *Positron Emission Tomography and Autoradiography: Application in the Brain and Heart.* New York: Raven Press, 1986.

Swann, J.P. *Academic Scientists and the Pharmaceutical Industry.* Baltimore: The Johns Hopkins University Press, 1988.

Wagner, H.N., Jr.; Bums, H.D.; Dannals, R.F.; Wong, D.F.; Langstrom, B.; Duelfer, T.; Frost, J.J.; Ravert, H.T.; Links, J.M.; Rosenbloom, S.B.; Lukas, SE.; Kramer, A.V.; and Kuhar, M.J. Imaging dopamine receptors in the human brain by positron tomography. *Science* 221:1264-1266, 1983.

AUTHOR

Henry N. Wagner, Jr., M.D.
Professor
Divisions of Nuclear and Radiation Health Sciences
The Johns Hopkins Medical Institutions
615 North Wolfe Street, Room 2001
Baltimore. MD 21205-1279

Positron Emission Tomography in Studies of Drug Abuse

Edythe D. London

INTRODUCTION

Positron emission tomography (PET) is a nuclear medicine procedure that uses radiopharmaceuticals that are labeled with positron-emitting radionuclides such as [^{15}O], [^{13}N], [^{11}C], and [^{18}F]. In human volunteers, PET scanning can be used to map and quantitate biochemical processes in the brain. Applications include the labeling of receptors for drugs and neurotransmitters, or functional studies, such as assessments of regional cerebral blood flow and glucose metabolism. This chapter focuses on how studies of glucose metabolism have been applied to understanding the euphoriant actions of drugs of abuse.

USING PET TO MEASURE CEREBRAL GLUCOSE METABOLISM

The metabolic rate for glucose is an index of brain function because glucose is the major metabolic substrate of the adult brain (Sokoloff 1972; Siesjö 1978). Physiological perturbations that increase energy metabolism of the brain also increase the metabolism of glucose, although nonoxidative metabolism of glucose also can be stimulated (Lear and Ackermann 1989). A method for measuring the regional cerebral metabolic rate(s) for glucose (rCMRglc) in intact animals was developed using ex vivo autoradiography (Sokoloff et al. 1977). The procedure involves the intravenous injection of radiolabeled 2-deoxy-D-glucose and the collection of timed arterial blood samples for estimation of radioactivity and glucose in plasma. An operational equation allows calculation of rCMRglc from these data and tissue radioactivity, as determined by quantitative autoradiography of individual brain regions. This method had been adapted for non-invasive use in human subjects with PET scanning and the use of

[^{18}F]fluorodeoxy-glucose (FDG) (Phelps et al. 1979; Reivich et al. 1979) or [^{11}C]deoxyglucose (Reivich et al. 1982).

Studies of glucose metabolism can provide important insights into normal brain function as well as the pathophysiology of diseases (Reivich et al. 1983). For example, in patients with Alzheimer's disease, there are rCMRglc deficits in the temporoparietal cortex (Friedland et al. 1983) and correlations between asymmetries in rCMRglc and neuropsychological performance (Grady et al. 1986). The FDG method also has been used to study regional brain function in schizophrenia (Farkas et al. 1980; Gur et al. 1987) and in neurological diseases, including stroke, neurodegenerative disorders, and epilepsy (Kuhl 1983; Engel et al. 1983).

Measurements of rCMRglc obtained by the FDG method also have been useful in drug abuse research. Studies of the acute cerebral metabolic responses to drugs of abuse have been performed using this method in human volunteers. Although only some of these studies were designed to elucidate the neurobiological determinants of drug-induced euphoria, the results from all of them provide information about the mechanisms by which drugs of abuse produce their effects on mood and feeling state. Drugs that have been studied in this way include morphine (London et al. 1990*a*), psychomotor stimulants (Wolkin et al. 1987; London et al. 1990*b*), A^9-tetrahydrocannabinol (Volkow et al. 1991), benzodiazepines (Buchsbaum et al. 1987; Foster et al. 1987; de Wit et al. 1991), nicotine (Stapleton et al. 1992), and alcohol (de Wit et al. 1990; Volkow et al. 1990).

In PET scan studies of substance abuse at the Addiction Research Center, most of the subjects were male polydrug abusers who resided on a closed research ward. The subjects underwent screening procedures, including psychological and medical assessments. After a drug-free period of several weeks, the subjects participated in simulation sessions designed to reduce the novelty of the procedures and also to provide training in the completion of specific questionnaires. Each subject received either an x-ray computed tomography scan or a magnetic resonance imaging scan. These structural images were used to exclude individuals with frank structural brain abnormalities and to aid in localization of specific regions of interest in the functional images obtained by PET.

The subjects participated in two PET sessions, with placebo or active drug administered in random sequence. During the measurement of rCMRglc, subjective self-reports of mood and feeling state were obtained. Questionnaires that are sensitive to the effects of psychoactive drugs were administered before and after the PET scan measurements and, in some cases, during the radiotracer uptake period. These included the Addiction Research Center Inventory, composed of the following three subscales:

- Morphine-Benzedrine Group subscale, which is sensitive to the positive (euphoriant) properties of opioids and psychomotor stimulants;

- Pentobarbital Chlorpromazine Alcohol Group subscale, which is sensitive to fatigue and low motivation; and

- Lysergic Acid Diethylamide (LSD) subscale, which contains items that reflect weird feelings, increased awareness of somatic sensations, and depersonalization (Haertzen 1974).

The Cocaine-Sensitive Scale (Sherer 1988; Muntaner et al. 1989) was administered during the radiotracer uptake period after the injection of either cocaine or placebo.

The responses to 30 mg morphine, injected intramuscularly, included elevations on the Morphine-Benzedrine and Pentobarbital Chlorpromazine Alcohol Group subscales of the Addiction Research Center Inventory, indicating the presence of euphoria and, to a lesser extent, of sedation and disorientation (London et al. 1990*a*). At the same time, global cerebral glucose metabolism was reduced (10 percent reduction from placebo values), with statistically significant decrements in six of the cortical areas assayed when controlling for the contribution of $PaCO_2$ by partial correlation analysis. The major conclusion from this study was that opioid euphoria involved a reduction of cortical activity, as indicated by rCMRglc. It seems reasonable that reduced cortical activity could be a necessary component of the production of opioid euphoria or that, alternatively, the reduced activity is a response to the positive affective state that is produced.

When polydrug abusers with histories of intravenous use of cocaine were tested similarly, self-report ratings on items of the Cocaine-Sensitive Scale indicated intense "rush" immediately after the injection of cocaine; the response declined to negligible values within 20 min (London et al. 1990*b*). Similarly, subjects reported feeling high, pleasant, and powerful. These subjective ratings were accompanied by an increase in beta activity in the spontaneous electroencephalogram (R. Herning, R.L. Phillips, B. Glover, and E.D. London, unpublished observations). Simultaneous measures of cerebral glucose utilization showed a global decrease (mean reduction of 14 percent), and most of the regions of interest that were assayed showed statistically significant decrements in rCMRglc (5 percent to 26 percent). Thus, the intravenous dose of cocaine that was used produced a more widespread decrease in rCMRglc than the morphine dose used in the previous study.

It is intriguing that drugs as different as morphine and cocaine would produce similar effects on cerebral metabolism. While morphine produces a constellation of effects, including sedation and decreases in body temperature, cocaine produces restlessness, cardiovascular stimulation, and increases in body temperature. Nonetheless, these drugs share the common property of inducing a positive affective state, termed "euphoria." It is now a common view that this euphoria is linked to a common brain mechanism, involving systems that use dopamine as a transmitter. A variety of evidence, obtained from studies in animal models for human drug abuse, suggests that the primary sites in the brain that mediate reinforcement due to opiates and psychomotor stimulants are different (for reviews, see Koob and Bloom 1988; Hubner and Koob 1993). Specifically, studies in rats suggest that opiates produce reinforcement by primary actions in the ventral tegmental area, which contains the cell bodies of mesolimbic dopaminergic neurons (Broekkamp and Phillips 1979; Bozarth and Wise 1980; Joyce et al. 1981). In contrast, psychomotor stimulants such as amphetamine and cocaine appear to produce reward by primary actions on the terminals of mesolimbic dopaminergic neurons (Carr and White 1983; Goeders and Smith 1983). Nonetheless. irrespective of the initial target sites, the effect of opioid or psychomotor stimulant action would be the same in that both classes of drugs would increase intrasynaptic dopamine in terminal fields of the mesolimbic dopamine system. Thus, the overall reduction of cerebral

glucose metabolism, particularly in the cortex, could result from enhanced dopaminergic activity.

If one extends an examination of the effects of drugs of abuse on cerebral glucose metabolism beyond studies of acute morphine and cocaine effects, the emergent finding is that almost all euphoriants that are compulsively self-administered reduce cerebral glucose utilization (table 1). This statement derives from observations that amphetamine (Wolkin et al. 1987) benzodiazepines (Buchsbaum et al. 1987; Foster et al. 1987; de Wit et al. 1991), and ethanol (de Wit et al. 1990; Volkow et al. 1990) all reduce rCMRglc. Similarly, preliminary studies at the Addiction Research Center also indicate that intravenous nicotine (Stapleton et al. 1992) and buprenorphine (Walsh et al. 1992) produce liking and other positive subjective self-reports while decreasing rCMRglc in experienced users of tobacco products and opioids, respectively. An exception is the finding that an intoxicating dose of Δ^9-tetrahydrocannabinol does not consistently reduce rCMRglc. Instead the most robust finding with Δ^9-tetrahydrocannabinol is a stimulation of rCMRglc in the cerebellum (Volkow et al. 1991), an area that shows a high density of cannabinoid receptors (Herkenham et al. 1990). Additional studies with euphorigenic doses of Δ^9-tetrahydrocannabinol may be warranted. In general, the aforementioned findings indicate that a decrease in cerebral glucose metabolism may be a fundamental component of drug-induced euphoria.

TABLE 1. *Reduction of rCMRglc by drugs of abuse*

Morphine (London et al. 1990*a*)
Cocaine (London et al. 1990*b*)
Amphetamine (Wolkin et al. 1987)
Nicotine (Stapleton et al. 1992)
Benzodiazepines (Buchsbaum et al. 1987; Foster et al. 1987; de Wit et al. 1991)
Ethanol (de Wit et al. 1990; Volkow et al. 1990)
Barbiturates (Theodore et al. 1986)

CONCLUSION

PET scanning is a valuable approach to understanding the brain mechanisms that support drug abuse in human subjects. In particular, functional studies using the FDG method have revealed that drugs of abuse generally reduce rCMRglc when the drugs are given at euphorigenic doses. Future investigations of brain mechanisms in substance abuse might use such methodology to study the physiological processes in the brain that underlie persistent states such as craving and physiological dependence that are induced by drugs of abuse.

REFERENCES

Bozarth, M.A., and Wise, R.A. Intracranial self-administration of morphine into the ventral tegmental area in rats. *Life Sci* 28:551-555, 1980.

Broekkamp, C.L., and Phillips, A.G. Facilitation of self-stimulation behavior following intracerebral microinjections of opioids into the ventral tegmental area. *Pharmacol Biochem Behav* 11:289-295, 1979.

Buchsbaum, MS.; Wu, J.; Haier, R.; Hazlett, E.; Ball, R.; Katz, M.; Sokolski, K.; Lagunas-Solar, M.; and Langer, D. Positron emission tomography assessment of effects of benzodiazepines on regional glucose metabolic rate in patients with anxiety disorder. *Life Sci* 40:2393-2400, 1987.

Carr, G.D., and White, N.M. Conditioned place preference from intra-accumbens but not intracaudate amphetamine injections. *Life Sci* 33:2551-2557, 1983.

de Wit, H.; Metz, J.; and Cooper, M. Effects of ethanol, diazepam and amphetamines on cerebral metabolic rate: PET studies using FDG. In: Harris, L., ed. *Problems of Drug Dependence 1990: Proceeding of the 52nd Annual Scientific Meeting.* National Institute on Drug Abuse Research Monograph 105. DHHS Pub. No. (ADM)91-1753. Washington, DC: Supt. of Docs., U.S. Govt. Print. Off., 1991. pp. 61-67.

de Wit, H.; Metz, J.; Wagner, N.; and Cooper, M. Behavioral and subjective effects of ethanol: Relationship to cerebral metabolism using PET. *Alcohol Clin Exp Res* 14:482-489, 1990.

Engel, J., Jr.; Kuhl, D.E.; Phelps, M.E.; Rausch, R.; and Nuwer, M. Local cerebral metabolism during partial seizures. *Neurology* 33:400-413, 1983.

Farkas, T.; Reivich, M.; Alavi, A.; Greenberg, J.H.; Fowler, J.S.; MacGregor, R.R.; Christman, D.R.; and Wolf, A.P. The application of [^{18}F]2-deoxy-2-fluoro-D-glucose and positron emission tomography in the study of psychiatric conditions. In: Passonneau, J.V.; Hawkins, R.A.; Lust, W.D.; and Welsh, F.A., eds. *Cerebral Metabolism and Neural Function.* Baltimore: Waverly Press, Inc., 1980. pp. 403-408.

Foster, N.L.; VanDerSpek, A.F.L.; Aldrich, M.S.; Berent, S.; Hichwa, R.H.; Sackellares, J.C.; Gilman, S.; and Agranoff, B.W. The effect of diazepam sedation on cerebral glucose metabolism in Alzheimer's disease as measured using positron emission tomography. *J Cereb Blood Flow Metab* 7:415-420, 1987.

Friedland, R.P.; Budinger, T.F.; Ganz, E.; Yano, Y.; Mathis, C.A.; Koss, B.; Ober, B.A.; Huesman, R.H.; and Derenzo, SE. Regional cerebral metabolic alterations in dementia of the Alzheimer type: Positron emission tomography with [^{18}Flfluorodeoxyglucose. *J Comput Assist Tomogr* 7:590-598, 1983.

Goeders, N.E., and Smith, J.E. Cortical dopaminergic involvement in cocaine reinforcement. *Science* 221:773-775, 1983.

Grady, CL.; Haxby, J.V.; Schlageter, N.L.; Berg, G.; and Rapoport, S.I. Stability of metabolic and neuropsychological asymmetries in dementia of the Alzheimer type. Neurology 36:1390-1392, 1986.

Gur, R.E.; Resnick, S.M.; Alavi, A.; Gur, R.C.; Caroff, S.; Dann, R.; Silver, F.L.; Saykin, A.J.; Chawluk, J.B.; Kushner, M.; and Reivich, M. Regional brain function in schizophrenia: I. A positron emission tomography study. *Arch Gen Psychiatry* 44:119-125, 1987.

Haertzen, C.A. *An Overview of Addiction Research Center Inventory Scales (ARCI): An Appendix and Manual of Scales.* National Institute on Drug Abuse. U.S. Department of Health, Education, and Welfare. DHEW Pub. No. (ADM)74-92. Rockville, MD: Supt. of Docs., U.S. Govt. Print. Off., 1974.

Herkenham, M.; Lynn, A.B.; Little, M.B.; Johnson, R.M.; Melvin, L.S.; de Costa, B.N.; and Rice, K.C. Cannabinoid receptor localization in brain. *Proc Natl Acad Sci U S A* 87:1932-1936, 1990.

Hubner, C.B., and Koob, G.F. Neurobiological substrates mediating the reinforcing effects of psychomotor stimulant and opiate drugs. In: London, E.D., ed. *Imaging Drug Action in the Brain.* Boca Raton, FL: CRC Press, 1993. pp. 1-48.

Joyce, E.M.; Koob, G.F.; Strecker, R.; Iversen, S.D.; and Bloom, F.E. The behavioral effects of enkephalin analogues injected into the ventral tegmental area and globus pallidus. *Brain Res* 221:359-370, 1981.

Koob, G.F. and Bloom, F.E. Cellular and molecular mechanisms of drug dependence. *Science* 242:715-723, 1988.

Kuhl, D.E. Mapping local cerebral glucose metabolism in stroke, degenerative diseases, and epilepsy. In: Magistretti, P.L., ed. *Functional Rodionuclide Imaging of the Brain.* New York: Raven Press, 1983. pp. 257-267.

Lear, J.L., and Ackermann, R.F. Why the deoxyglucose method has proven so useful in cerebral activation studies: The unappreciated prevalence of stimulation-induced glycolysis. *J Cereb Blood Flow Metab* 9:911-913, 1989.

London, E.D.; Broussolle, E.P.M.; Links, J.M.; Wong, D.F.; Cascella, N.G.; Dannals, R.F.; Sano, M.; Heming, R.; Snyder, F.R.; Rippetoe, L.R.; Toung, T.J.K.; Jaffe, J.H.; and Wagner, H.N., Jr. Morphine-induced metabolic changes in human brain: Studies with positron emission tomography and [fluorine 18]fluorodeoxyglucose. *Arch Gen Psychiatry* 47:73-81, 1990*a*.

London, E.D.; Cascella, N.G.; Wong, D.F.; Phillips, R.L.; Dannals, R.F.; Links, J.M.; Heming, R.; Grayson, R.; Jaffe, J.H.; and Wagner, H.N., Jr. Cocaine-induced reduction of glucose utilization in human brain. A study using positron emission tomography and [fluorine 18]fluorodeoxyglucose. *Arch Gen Psychiatry* 47:567-574, 1990*b*.

Muntaner, C.; Cascella, N.G.; Kumor, K.M.; Nagoshi, C.; Heming, R.; and Jaffe, J. Placebo responses to cocaine administration in humans: Effects of prior administration and verbal instructions. *Psychopharmacology* 99:282-286, 1989.

Phelps, M.E.; Huang, S.C.; Hoffman, E.J.; Selin, C.; Sokoloff, L.; and Kuhl, D.E. Tomographic measurement of local cerebral glucose metabolic rate in humans with (F-18)2-fluoro-2-deoxy-D-glucose: Validation of method. *Ann Neurol* 6:371-388, 1979.

Reivich, M.; Alavi, A.; Wolf, A.; Greenberg, J.H.; Fowler, J.; Christman, D.; MacGregor, R.; Jones, S.C.; London, J.; Shiue, C.; and Yonekura, Y. Use of 2-deoxy-D[1-^{11}C]glucose for the determination of local cerebral glucose metabolism in humans: Variation within and between subjects. *J Cereb Blood Flow Metab* 2:307-319, 1982.

Reivich, M.; Kuhl, D.; Wolf, A.; Greenberg, J.; Phelps, M.; Ido, T.; Casella, V.; Fowler, J.; Hoffman, E.; Alavi, A.; Som, P.; and Sokoloff, L. The [^{18}F]fluorodeoxyglucose method for the measurement of local cerebral glucose utilization in man. *Circ Res* 44:127-137, 1979.

Reivich, M.; Rosen, A.D.; Kushner, M.; Gur, R.C.; and Alavi, A. Local cerebral glucose consumption in man in health and disease. In: Magistretti, P.L., ed. *Functional Radionuclide Imaging of the Brain.* New York: Raven Press, 1983. pp. 311-318.

Sherer, M.A. Intravenous cocaine: Psychiatric effects, biological mechanisms. *Biol Psychiatry* 24:865-885, 1988.

Siesjö, B.K. *Brain Energy Metabolism.* New York: Wiley, 1978.

Sokoloff, L. Circulation and energy metabolism of the brain. In: Siegel, G.J.; Albers, R.W.; Katzman, R.; and Agranoff, B.W., eds. *Basic Neurochemistry.* Vol. 2. Boston: Little, Brown and Co., 1972. pp. 338-413.

Sokoloff, L.; Reivich, M.; Kennedy, C.; Des Rosiers, M.H.; Patlack, C.S.; Pettigrew, K.D.; Sakurada, O.; and Shinohara, M. The [^{14}C]deoxyglucose method for the measurement of local cerebral glucose utilization: Theory, procedure, and normal values in the conscious and anesthetized albino rat. *J Neurochem* 28:897-916, 1977.

Stapleton, J.M.; Henningfield, J.E.; Wong, D.F.; Phillips, R.L.; Gilson, SF.; Grayson, R.F.; Dannals, R.F.; and London, E.D. Effects of nicotine on cerebral metabolism and subjective responses in human volunteers. *Soc Neurosci Abstr* 18:1074, 1992.

Theodore, W.H.; DiChiro, G.; Margolin, R.; Fishbein, D.; Porter, R.J.; and Brooks, R.A. Barbiturates reduce human cerebral glucose metabolism. *Neurology* 36:60-64, 1986.

Volkow, N.D.; Gillespie, H.; Mullani, N.; Tancredi, L.; Grant, C.; Ivanovic, M.; and Hollister, L. Cerebellar metabolic activation by delta-9-tetrahydrocannabinol in human brain: A study with positron emission tomography and ^{18}F-2-fluoro-2-deoxyglucose. *Psychiatry Res* 40:69-78, 1991.

Volkow, N.D.; Hitzemann, R.; Wolf, A.P.; Logan, J.; Fowler, J.S.; Christman, D.; Dewey, S.L.; Schlyer, D.; Burr, G.; Vitkun, S.; and Hirschowitz, J. Acute effects of ethanol on regional brain glucose metabolism and transport. *Psychiatry Res* 35:39-48, 1990.

Walsh, S.L.; Stapleton, J.M.; Preston, K.L.; Sullivan, J.T.; Dannals, R.F.; Grayson, R.; Phillips, R.L.; Bigelow, G.E.; Jasinski, D.R.; and London, E.D. Acute effects of buprenorphine on cerebral glucose utilization in human substance abusers. *Soc Neurosci Abstr* 18:371, 1992.

Wolkin, A.; Angrist, B.; Wolf, A.; Brodie, J.; Wolkin, B.; Jaeger, J.; Cancro, R.; and Rotrosen, J. Effects of amphetamine on local cerebral metabolism in normal and schizophrenic subjects as determined by positron emission tomography. *Psychopharmacology* 92:241-246, 1987.

AUTHOR

Edythe D. London, Ph.D.
Chief
Neuroimaging and Drug Action Section
Neuroscience Branch
Addiction Research Center
National Institute on Drug Abuse
National Institutes of Health
Baltimore, MD 21224
and
Associate Professor of Radiology
Department of Radiology
School of Medicine
The Johns Hopkins University
Baltimore, MD 2 1204
and
Adjunct Associate Professor
Department of Pharmacology and Experimental Therapeutics
School of Medicine
University of Maryland
Baltimore, MD 21201

Imaging Brain Function in Animals To Understand Drugs of Abuse and Potential Pharmacotherapies

M. F. Piercey

INTRODUCTION

Most central nervous system (CNS) drugs, including those involved in drug abuse, act by enhancing or depressing activities in specific brain pathways. Some of these pathways are involved in acute reinforcing properties such as euphoric or psychostimulant phenomena. Others are involved with alterations in sensory perception or autonomic drug effects. Thus, to understand functional effects of drugs of abuse, as well as to design potential pharmacotherapies to treat drug abusers, it is critical to define which neuronal structures are altered and how they are altered (i.e., stimulated or inhibited).

Evaluating specific brain structures is challenging because of the large number of such structures, many of which are extremely small. Indeed, drugs frequently affect parts of the same structure differently. To solve this problem, animal neuroscientists have turned to autoradiography to map the functional neuroanatomy of the brain. The development of positron emission tomography (PET) for imaging the functional neuroanatomy of the human brain has at the same time opened opportunities for evaluating how specific neuronal circuits altered in animals are affected by the same drugs in humans.

IMAGING TECHNIQUES

Receptor binding autoradiography, usually carried out in vitro, is used to determine the distribution of a specific receptor subtype among the myriad brain structures (Kuhar 1985). When used in vivo, the anatomy of receptor occupancy can be determined at doses known to

have biological effects. Receptor binding autoradiography uses specific high-affinity radioligands to identify receptor sites. When ligands interact with more than one receptor site, other drugs can sometimes be used to mask the complicating receptors. Additionally, drugs without apparent high affinity for any one site can be evaluated for their ability to displace high-affinity ligands for well-documented sites.

Nonspecific binding of radioactive ligands represents a potential contaminating influence in receptor binding autoradiography. Nonspecific binding can be isolated by removal of specific binding with a nonlabeled ligand competing for the same receptor. Since receptor-specific binding is saturable, whereas nonspecific binding is not, cold ligand can be used to mask specific binding of the identical radioactive ligand. Using adjacent brain sections and computer imaging techniques, nonspecific binding is removed pixel by pixel to yield the specific receptor binding image. Receptor binding identifies where a drug can potentially act, but it does not actually reveal whether any meaningful effect occurs.

2-Deoxyglucose (2-DG) autoradiography (Sokoloff et al. 1977) can be used to determine drug effects, both stimulatory and inhibitory, on brain energy metabolism, an indirect measure of neuronal activity. This technique relies upon the fact that brain energy metabolism is totally dependent upon blood glucose, since the brain does not store glycogen. A steady state exists whereby glucose metabolism is equal to glucose transported into the neurons. Tracer amounts of C^{14} 2-DG enter brain neurons by competing with glucose for the transporter. Once inside neurons, 2-DG is phosphorylated but not metabolized further. 2-DG phosphate cannot diffuse outside cells, so radioactivity accumulates at a rate proportional to glucose metabolism. If one knows 2-DG and glucose concentrations, one needs only their transporter affinities to obtain absolute amounts of glucose metabolized. In practice, this is done by measuring timed samples of arterial plasma glucose and radioactivity, measuring total radioactivity in each brain region, and plugging the values into the equation developed by Sokoloff and colleagues (1977) to quantitatively measure glucose metabolism.

2-DG autoradiography measures not only a drug's direct effects at sites where its receptors are located but also its indirect effects occurring downstream from these receptor sites. For example, phencyclidine (PCP, "angel dust") receptors are located throughout the circuit of Papez, except in the mammillary body (MB). Nonetheless, PCP intensely excites the MB by recruitment through activation of the entire Papez circuit. Interestingly, indirect activation of the MB may be important for PCP's psychotropic effects (Piercey and Ray 1988*a,* 1988*b*; Piercey and Hoffmann 1989).

A major advantage of 2-DG imaging over receptor binding autoradiography is that one does not need to know the mechanistic effects or the receptor identity of the drug under study. In addition, this technique does not require the development of a new high-affinity ligand since C^{14} 2-DG is readily available. However, because brain energy metabolism occurs in all tissues, including those not responding to a drug, 2-DG imaging patterns are superimposed over an active background, which tends to "blur" the image. In contrast, receptor binding imaging negates nonspecific binding of its ligands. Thus, receptor binding images are presented over essentially uniform inactive black backgrounds. For this reason, receptor binding gives "sharper" images that pinpoint active sites more clearly than 2-DG imaging.

In addition to receptor binding and 2-DG autoradiography, other brain imaging techniques also are used. In particular, radiolabeled genetic probes for in situ hybridization of messenger ribonucleic acid (mRNA) (Uhl 1986) are being used with increasing frequency, particularly for those receptors for which high-affinity receptor ligands are not available. However, it must be remembered that receptor mRNA is a measure of receptor synthesis, which quantitatively can be quite different from the actual distribution of receptor protein. Antibody staining of receptors occasionally has been used with some success (McVittie et al. 1991). In addition to autoradiography and PET, magnetic resonance imaging has some potential for evaluating drug effects on some measures of brain function (Eastwood et al. 1985).

SITES OF DRUG ACTION

Receptor binding autoradiography, although dependent upon some knowledge of the drug receptors activated by a drug, is probably the most accurate method for identification of specific brain sites directly affected by a drug. PCP, for example, binds to specific high-affinity binding sites throughout the limbic system, especially the circuit of Papez and the dopaminergic system (Gundlach et al. 1986*a*). Interestingly, this high-affinity PCP receptor is codistributed with the NMDA receptor subtype for the excitatory amino acid neurotransmitter, glutamate (Maragos et al. 1988). Electrophysiology experiments confirm that PCP can block activation of NMDA ion channels (Anis et al. 1983). The nonopioid sigma receptor has been suggested as another major receptor involved in PCP's pharmacological effects. This receptor is distributed more caudally than the high-affinity PCP receptor, with particularly high receptor concentrations in the brain stem (Gundlach et al. 1986*b*).

Receptor binding autoradiography identifies where a drug binds to its receptors but not necessarily where a drug induces its major biological effects. By means of 2-DG autoradiography, PCP was found to induce very large increases in energy metabolism in the forebrain, particularly in the cerebral cortex, the dopaminergic system, and the limbic system (especially the circuit of Papez). These excitatory effects were not observed in the caudal brain or brain stem, although inhibitory effects were seen occasionally (e.g., in the inferior colliculus) (Piercey and Ray 1988*a*, 1988*b*; Piercey and Hoffmann 1989). Comparison of binding and 2-DG data demonstrated a positive correlation between PCP's excitatory effects and those sites where the high-affinity PCP receptor (i.e., NMDA channel) was located. In contrast, there was a negative correlation between these sites for PCP excitation and those where high concentrations of sigma receptors were found. It was concluded that PCP's stimulant effects are evoked through the high-affinity PCP site (Piercey and Ray 1988*a*, 1988*b*).

Knowing where a drug acts often can give great insight into how a drug could produce some of its specific effects. For example, excitation in dopaminergic areas could be responsible for many of the psychotomimetic effects of PCP (Luisada 1978) since hyperactivity in dopaminergic systems is thought to represent a major neurobiological

basis of schizophrenia (Matthysse and Sugarman 1978). However, some of the more bizarre aspects of PCP intoxication could involve excitatory effects in Papez' circuit. Papez himself thought the circuit to be involved in the integration of emotional sensation and expression, with the MB in particular being critical for emotional outbursts (Papez 1937).

Where a drug acts is often dependent upon dose. High-dose effects sometimes can be used to get an overall view of the pattern of actions of a drug. Such patterns are particularly useful when using brain imaging to identify what pharmacological class a drug belongs to (see below, "Identification of Pharmacological Class"). Conversely, lower doses may more specifically activate neuronal pathways responsible for the dominant behavioral effects of the drug. For example, Porrino and colleagues (1988) found that, at an intravenous (IV) dose of 0.5 mg/kg, cocaine excited only the medial prefrontal cortex and nucleus accumbens. Higher cocaine doses led to broader stimulation of dopamine-related structures, especially those in the extrapyramidal regions, accompanied by increases in locomotor activity. Porrino and colleagues (1988) concluded that the nucleus accumbens and prefrontal cortex may be involved in the reinforcing effects of cocaine and that the extrapyramidal areas are more involved in the general stimulant effects of the drug. Many of these conclusions are consistent with the dopaminergic theory of drug reinforcement (Wise and Rompre 1989).

Other factors affecting sites of drug action include route and sometimes time of injection relative to injection of the 2-DG. For example, using intraperitoneal injections, London and colleagues (1986) found that cocaine did not excite the nucleus accumbens at all. Hoffmann and colleagues (1991) also did not observe excitation of the nucleus accumbens or many of the other major dopaminergic areas when cocaine was injected intravenously 10 minutes prior to the injection of the 2-DG label. By comparison, Porrino and colleagues (1988) injected cocaine only 2 minutes prior to 2-DG. Subsequent (unpublished) experiments in the author's laboratory in which cocaine was injected 2 minutes prior to 2-DG resulted in a pattern of stimulation extremely similar to that reported by Porrino and colleagues (1988). Such sensitivity to timing seems likely to be related to the short duration of action for cocaine, particularly regarding its reinforcing effects (Gawin 1991).

A rarely discussed additional issue is the fact that, while most imaging scientists would probably agree that a certain section of the brain can be identified as a given brain nucleus, the specific component of that nucleus used in the evaluation of the image probably varies greatly among laboratories. This represents a problem since drug receptors and responses to drugs often are not uniform within a brain area. For example, even when cocaine is injected 2 minutes prior to the 2-DG injection, this author's laboratory did not see excitatory effects in the nucleus accumbens measured at two different levels. However, neither of these levels were as anterior as the area where Porrino and colleagues (1988) observed the high nucleus accumbens sensitivity (Porrino, personal communication, 1992). Thus, it probably would be useful for authors to publish the atlases to identify precisely where they analyze each brain area. In some cases, standardization might be useful. However, this needs to be weighed against the need to explore more brain regions.

IDENTIFICATION OF PHARMACOLOGICAL CLASS

Drugs acting through common mechanisms can be expected to affect similar or identical brain areas. MK-801, like PCP, is an NMDA channel blocking agent (Woodruff et al. 1987). Like PCP, MK-801 excites dopaminergic structures, Papez' circuit, and other limbic and cortical structures (Piercey et al. 1988). However, other psychostimulants such as amphetamine and cocaine excite dopaminergic structures but have relatively fewer effects than MK-801 and PCP in limbic areas (Porrino et al. 1988; Piercey and Hoffmann 1989). It is interesting that amphetamine and cocaine, both of which increase synaptic dopamine (albeit by different receptor mechanisms), in general excite similar structures, according to 2-DG autoradiography. It also is interesting that all of the psychostimulants excite dopaminergic structures. This observation is consistent with the hypothesis that a dopamine reward system may be responsible for the reinforcing effects of these and possibly other agents (Wise and Rompre 1989). Also, as noted previously, the fact that all of these drugs stimulate dopaminergic structures may account for some of the psychotomimetic effects common to this group of compounds.

Identification of pharmacological class is not limited to psychostimulants; it applies to other classes of drugs as well. For example, the hypnotic zolpidem acts through benzodiazepine receptors, even though it is chemically not a benzodiazepine (Langer et al. 1988). In 2-DG autoradiography experiments, it was demonstrated that zolpidem and triazolam (a benzodiazepine hypnotic) depressed metabolism in precisely the same regions of the brain (Piercey et al. 1991). Indeed, a strong positive linear correlation was demonstrated to exist between the percent of depression exerted by both drugs over all regions of the brain, whether or not the level of depression was statistically significant. Thus, the distribution of pharmacological effects is linked inextricably to what receptor is affected and not to the precise chemical nature of the ligand.

DRUG INTERACTIONS

The 2-DG autoradiography method allows evaluation of the interactions between centrally acting drugs, Such interactions can occur between drugs acting at the same receptor and those acting at different receptors. Receptor binding autoradiography can be used to establish whether interacting drugs interact at the same receptor since, when this is true, both will displace the same radioactive ligand.

Numerous imaging studies have demonstrated interactions between drugs acting at the same receptors. McCulloch and colleagues (1982) showed that the dopamine receptor antagonist, haloperidol, completely eliminated the effects of the dopamine receptor agonist, apomorphine, in all brain regions where apomorphine affected brain energy metabolism. Similarly, flumazenil, a benzodiazepine receptor antagonist, eliminates the effects of the benzodiazepine agonist, diazepam (Ableitner et al. 1985). The benzodiazepine receptor partial agonist, U-78875, also antagonized the effects of the benzodiazepine agonist, alprazolam (Piercey et al. 1990). However, in this case, antagonism was observed only in those brain areas where the drug had low efficacy of its own. Areas of high efficacy presumably have large receptor reserves, allowing full agonist effects even with low intrinsic activity.

Meaningful interactions also occur between drugs acting on similar systems but through different receptors. Piercey and Ray (1988*b*) demonstrated that haloperidol altered the effects of PCP, particularly in areas where dopamine is thought to be a major neurotransmitter. Hoffmann and colleagues (1991) showed that cocaine's stimulant effects could be altered by treatment with a stimulant dopamine antagonist. In both these studies, the antagonist interacted directly with dopamine receptors, but the agonists' actions at these sites were mediated indirectly through dopamine released from endogenous stores.

Interactions also can be demonstrated between agonists acting at different receptors. Ray and colleagues (1992), for example, found that the dopamine D_1 receptor agonist, SKF 38393, and the dopamine D_2 receptor agonist, quinpirole, have different actions and interactions, depending upon brain site. In some areas, there are clear synergistic interactions, whereas in others there are antagonistic interactions. Yet, in other brain areas, one of the drugs produced significant alterations, whereas the other did not affect metabolism either by itself or interact with the active drug.

ANIMAL/HUMAN CORRELATIONS

One of the more exciting opportunities for brain imaging is the possibility of comparing effects observed in animals to those observable in humans. It has been demonstrated, for example, that there is a positive correlation between rodent and human brains when comparing energy metabolism among different brain regions in the two species (Blinn et al. 1991). When comparing drug effects, it is interesting that while the distribution of effects may, in general, be similar between animals and man, the directions of these pharmacological effects are sometimes opposite. For example, whereas PCP, amphetamine, and cocaine mostly increase energy metabolism in rodents, they produce predominantly inhibitory effects in humans (Wolkin et al. 1987; London et al. 1990).

IMAGING OF POTENTIAL PHARMACOTHERAPIES FOR DRUG ADDICTION

It is hoped that through greater understanding of how drugs of abuse act, it will be possible to design specific pharmacotherapies to treat drug abuse as a clinical disorder.

Knowledge that stimulation of dopaminergic structures is a common finding for euphoric psychostimulants suggests that dopamine antagonists might be therapeutic in this condition. Unfortunately, in addict populations, dopamine antagonists tend to promote the anhedonias (inability to perceive pleasure) associated with drug craving (Gawin 1991). Thus, some alternative approach is probably necessary. Whatever the approach, imaging experiments can, along with a full battery of pharmacological evaluations, be helpful in appreciating the proposed mechanism of any pharmacotherapy being considered for human testing. In addition, by comparing autoradiographic imaging in animals to PET scans in humans, imaging experiments almost uniquely can be used to determine if the critical neurobiological effects observed in animals actually occur in man as well.

One possible mechanism for treating cocaine and other psychostimulant abuse is the use of a dopamine partial agonist. To date, no imaging experiments involving dopamine partial agonists have been published. However, 2-DG autoradiography potentially can be used to demonstrate partial agonist and antagonist pharmacology, as has been done with the benzodiazepine partial agonist U-78875 (Piercey et al. 1990). It is hoped that benzodiazepine partial agonists will lack the drug dependence associated with full agonists.

Another drug class with potential for use in treating cocaine abuse is the stimulant dopamine antagonists such as (±)-AJ 76. The mechanism for (±)-AJ 76's stimulant effects is not clearly delineated, but the stimulant effects may be due to a preferential blockade of dopamine autoreceptors (Svensson et al. 1986). Although it antagonizes amphetamine and cocaine locomotor activity, (±)-AJ 76 weakly increases locomotor activity like a weak psychostimulant (Svensson et al. 1986; Piercey et al. 1992). (±)-AJ 76 partially generalizes to cocaine's subjective cue (Callahan et al. 1992) but antagonizes cocaine self-administration (Richardson et al., in press). In 2-DG experiments,

(±)-AJ 76 by itself sometimes weakly excites dopaminergic structures, but it antagonizes the excitatory effects of cocaine and amphetamine (Hoffmann et al. 1988, 1991; table 1). Because it can weakly stimulate dopaminergic structures, it is possible that (±)-AJ 76 will not produce anhedonias like other dopamine antagonists (Gawin 1991).

TABLE 1. *Antagonism of cocaine stimulation by (+)-AJ 76*[1]

	Control	Cocaine[2]	Cocaine + (+)-AJ 76[3]
Subthalamus	100 ± 10	138 ± 6*	103 ± 2+
AV Thalamus	100 ± 12	132 ± 3*	97 ± 7+
VL Thalamus	100 ± 9	138 ± 3*	107 ± 6+
Lateral Septum	100 ± 6	147 ± 3*	108 ± 8+
PAG	100 ± 5	138 ± 8*	136 ± 8+
Dorsal Horn	100 ± 12	125 ± 5*	112±4+

[1]Glucose utilization, µmole/100 g brain/min expressed as percent control.
[2]Cocaine, 5 mg/kg IV injection, 10 min before 2-DG injection plus vehicle IV injection at 5 min before 2-DG injection.
[3]Cocaine, 5 mg/kg IV injection, 10 min before 2-DG injection plus (+)-AJ 76, 15 mg/kg IV injection, 5 min before 2-DG injection.
* $p < 0.05$ versus control, ANOVA.
+ $p < 0.05$ versus cocaine alone, ANOVA.

Piercey and Ray (1988*b*) noted that haloperidol either significantly reduced or destroyed PCP's effects in dopaminergic areas. However, the importance of this finding may be more related to treatment of behavioral toxicity rather than the drug abuse itself.

Drug development begins with chemical synthesis and pharmacological testing. Brain imaging experiments in animals represent only one component of the pharmacological evaluation of a drug. Only one compound of many thousands synthesized is generally found to have a sufficiently delineated mechanism of action combined with good pharmacokinetic and toxicological profiles to justify evaluation in

humans. New chemical entities tested in humans do not always produce the desired effect. It is not always clear whether this is due to differences in drug pharmacokinetics and distribution, to some altered pharmacological properties in humans, or to a general failure of the proposed mechanism for treatment. The complexity of the nervous system has made it difficult for both animal and clinical scientists to compare their results to answer these questions. However, with the parallel development of brain imaging techniques in both animals and humans, it is now possible to compare a drug's effects across species. It seems likely that brain imaging techniques will, over time, play a larger role in the development of drugs to treat psychiatric conditions such as drug abuse.

SUMMARY

Brain imaging studies can be used to enhance current understanding of how CNS drugs act. Because the brain is in reality a collection of independent, albeit interconnected, neural organs, identification of sites of brain action are critical to an appraisal of how each drug exerts its different behavioral and physiological effects. For new drugs not yet tested in humans, identification of which neuronal structures are affected by a drug can give clues as to what to expect from the drug if it is eventually exposed to clinical testing.

Receptor binding autoradiography, more than any other technique, pinpoints the distribution of those sites at which a given drug acts. When combined with 2-DG autoradiography, the intensity and direction of the action at each of these sites, as well as the impact of these actions on additional sites, can be appreciated. In addition to identification of sites of drug action, brain imaging studies can be used to identify classes of drug action, interactions between drugs, and, perhaps more than any other technique, enhance the appreciation of the similarities and differences between the effects in animals and those in humans.

When applied to drugs of abuse, brain imaging studies can be used to help identify key physiological events underlying drug reinforcement as well as those important for various physiological effects of each drug. Armed with such information, brain imaging techniques can

play a unique role as one component of an effort to discover pharmacotherapies for drug abuse.

REFERENCES

Ableitner, A.; Wuster, M.; and Herz, A. Specific changes in local cerebral glucose utilization in the rat brain induced by acute and chronic diazepam. *Brain Res* 359:49-56, 1985.

Anis, N.A.; Berry, S.C.; Burton, N.R.; and Lodge, D. The dissociative anesthetics, ketamine and phencyclidine, selectively reduce excitation of central mammalian neurones by N-methyl aspartate. *Br J Pharmacol* 79:1565-575, 1983.

Blinn, J.; Ray, C.A.; Chase, T.C.; and Piercey, M.F. Regional cerebral glucose metabolism compared in rodents and humans. *Brain Res* 568:215-222, 1991.

Callahan, P.M.; Piercey, M.F.; and Cunningham, K.A. Effects of the putative dopamine autoreceptor antagonists AJ 76 and UH 232 on the discriminative stimulus properties of cocaine. *Psychopharmacology* 107:73-77, 1992.

Eastwood, L.M.; Hutchinson, J.M.S.; and Besson, J.A.O. Nuclear magnetic resonance (NMR): I. Imaging biochemical change. *Br J Psychiatry* 146:26-35, 1985.

Gawin, F.H. Cocaine addiction: Psychology and neurophysiology. *Science* 251:1580-1586, 1991.

Gundlach, A.L.; Largent, B.L.; and Snyder, S.H. Phencyclidine (PCP) receptors: Autoradiographic localization in brain with the selective ligand, ^{3}H-TCP. *Brain Res* 386:266-279, 1986*a*.

Gundlach, A.L.; Largent, B.L.; and Snyder, S.H. Autoradiographic localization of sigma receptor binding sites in guinea pig and rat central nervous system with (=)-3-H-3-(3-hydroxyphenyl)-N-(l-propyl)piperidine. *J Neurosci* 6:1757- 1770, 1986*b*.

Hoffmann, W.E.; Lum, J.T.; and Piercey, M.F. Electrophysiological and metabolic effects of (+)-AJ 76, a selective antagonist of dopamine autoreceptors. Neurosci *Abstr* 14:935, 1988.

Hoffmann, W.E.; Svensson, K.; Callahan, P.; Cunningham, K.; Mead, B.; Lum, J.T.; and Piercey, M.F. Interactions between cocaine and the presumed preferential dopamine autoreceptor antagonists, (+)-AJ 76 and (+)-UH 232. Neurosci *Abstr* 17:681, 1991.

Kuhar, M.J. Receptor localization with the microscope. In: Yamamuru, H.I.; Enna, S.J.; and Kuhar, M.J., eds. Neurotransmitter Receptor Binding. 2nd ed. New York: Raven Press, 1985. pp. 153-175.

Langer, S.Z.; Arbilla, S.; Scatton, B.; Niddam, R.; and Dubois, A. Receptors involved in the mechanism of action of zolpidem. In: Savvanet, J.P.; Langer, S.Z.; and Morselli, P.L., eds. *Imidazopyridines* in Sleep Disorders. New York: Raven Press, 1988. pp. 55-70.

London, E.D.; Cascella, N.G.; Wong, D.F.; Phillips, R.L.; Dannals, R.F.; Links, J.M.; Herning, R.; Grayson, R.; Jaffe, J.H.; and Wagner, H.N., Jr. Cocaine-induced reduction of glucose utilization in human brain: A study using positron emission tomography and fluorine18-fluorodeoxyglucose. *Arch Gen Psychiatry* 47:567-574, 1990.

London, E.D.; Wilkerson, G.; Goldberg, S.R.; and Risner, M.E. Effects of l-cocaine on local cerebral glucose utilization in the rat. *Neurosci Lett* 68:173-78, 1986.

Luisada, P.F. The phencyclidine psychosis: Phenomenology and treatment. In: Petersen, R.C., and Stillman, R.C., eds. Phencyclidine (PCP) Abuse: An Appraisal. National Institute on Drug Abuse Research Monograph 21. DHHS Pub. No. (ADM)017-024-00785-4. Washington, DC: Supt. of Docs., U.S. Govt. Print. Off., 1978. pp. 19-43.

Maragos, W.F.; Penney, J.B.; and Young, A.B. Anatomic correlation of NMDA and ^{3}H-TCP-labeled receptors in rat brain. *J Neurosci* 8:493-501, 1988.

Matthysse, S., and Sugarman, J. Neurotransmitter theories of schizophrenia. In: Iversen, L.L.; Iversen, S.D.; and Snyder, S.H., eds. *Neuroleptics and Schizophrenia.* New York: Plenum Press, 1978. pp. 221-242.

McCulloch, J.; Savaiki, H.E.; and Sokoloff, L. Distribution of effects of haloperidol in energy metabolism in the rat brain. Brain Res 243:81-90, 1982.

McVittie, L.D.; Ariano, M.A.; and Sibley, D.R. Characterization of anti-peptide antibodies for the localization of D2 dopamine receptors in rat striatum. *Proc Natl Acad Sci U S A* 88:1441-1445, 1991.

Papez, J.W. A proposed mechanism of emotion. *Arch Neurol Psychiatry* 38:724-743, 1937.

Piercey, M.F., and Hoffmann, W.E. Cerebral pathways activated by PCP-like compounds: Relevance to neurotransmitters and their receptors. In: Harris, L.S., ed. *Problems of Drug Dependence.* National Institute on Drug Abuse Research Monograph 95. DHHS Pub. No. (ADM)90-1663. Washington, DC: Supt. of Docs., U.S. Govt. Print. Off., 1989. pp. 264-269.

Piercey, M.F.; Hoffmann, W.E.; and Cooper, M. The benzodiazepine hypnotics triazolam and zolpidem have identical metabolic effects throughout the brain: Implications for benzodiazepine receptor subtypes. *Brain Res* 554:224-252, 1991.

Piercey, M.F.; Kasckovsky, P.; and Hoffmann, W.E. MK-801A, a potential antistroke agent, stimulates PCP receptors in limbic and cortical areas. *Psychopharmacology* 96:561-562, 1988.

Piercey, M.F.; Lum, J.T.; Hoffmann, W.E.; Carlsson, A.; Ljung, E.; and Svensson, K. Antagonism of cocaine's pharmacological effects by the stimulant dopaminergic antagonists, (+)-AJ 76 and (+)-UH 232. *Brain Res* 588:217-222, 1992.

Piercey, M.F.; Nielsen, E.O.; Honore, T.; and Hoffmann, W.E. U-78875 is a benzodiazepine agonist in some brain sites and an antagonist in others: A 2-DG autoradiography study. *Pharmacologist* 32: 136, 1990.

Piercey, M.F., and Ray, C.A. Dramatic stimulation of limbic and cortical structures via high-affinity PCP receptors. *Life Sci* 43:379-385, 1988*a.*

Piercey, M.F., and Ray, CA. Evidence from 2-DG autoradiography that phencyclidine's functional effects are mediated by specific PCP rather than sigma receptors. In: Domino, E.F., and Kamenka, J.-M., eds. *Sigma Opioid Phencyclidine-like Compounds as Molecular Probes in Biology.* Ann Arbor: NPP Press, *19886.* pp. 285-295.

Porrino, L.J.; Domer, F.R.; Crane, A.M.; and Sokoloff, L. Selective alterations in cerebral metabolism within the mesocorticolimbic dopaminergic system produced by acute cocaine administration in rats. *Neuropsychopharmacology* 1:109-117, 1988.

Ray, C.A.; Strutt, M.; Camacho-Ochoa, M.; and Piercey, M.F. Synergistic and antagonistic interactions of dopamine D1 and D2 agonists: A 2-deoxyglucose autoradiography study. *Neurosci Abstr* 18:995, 1992.

Richardson, N.R.; Piercey, M.F.; Svensson, K.; Collins, R.J.; Myers, J.E.; and Roberts, D.C.S. An assessment of the reinforcing and anti-cocaine effects of the preferential dopamine autoreceptor antagonist, (+)-AJ 76. *Brain Res,* in press.

Sokoloff, L.; Reivich, M.; Kennedy, C.; Des Rosiers, M.H.; Patlak, C.S.; Pettigrew, K.D.; Sakurada, O.; and Shinohara, M. The [^{14}C]deoxyglucose method for the measurement of local cerebra1 glucose utilization: Theory, procedure, and normal values in the conscious and anesthetized albino rat. *J Neurochem* 28:897-916, 1977.

Svensson, K.; Johansson, A.M.; Magnusson, T.; and Carlsson, A. (+)-AJ 76 and (+)-UH 232: Central stimulants acting as preferential dopamine autoreceptor antagonists. *Naunyn Schmiedeberg Arch Pharmacol* 334:234-245, 1986.

Uhl, G.R. *In Situ Hybridization in Brain.* New York: Plenum Press, 1986.

Wise, R.A., and Rompre, P.-P. Brain dopamine and reward. *Annu Rev Psychol* 40:191-225, 1989.

Wolkin, A.; Angrist, B.; Wolf, A.; Brodie, J.; Wolkin, B.; Jaeger, J.; Cancro, R.; and Rotrosen, J. Effects of amphetamine on local cerebral metabolism in normal and schizophrenic subjects as determined by positron emission tomography. *Psychopharmacology* 92:241-246, 1987.

Woodruff, G.N.; Foster, A.C.; Gill, R.; Kemp, J.A.; Wong, E.H.F.; and Iversen, L.L. The interaction between MK-801 and receptors for N-methyl-D-aspartate: Functional consequences. *Neuropharmacology* 26:903-909, 1987.

ACKNOWLEDGMENTS

Cathy Ray and Bill Hoffmann played major roles in the imaging experiments carried out in The Upjohn Company laboratory. Brenda Mead was instrumental in the (+)-AJ 76 experiments with cocaine.

AUTHOR

M.F. Piercey
CNS Research 725 1-209-4
The Upjohn Company
301 Henrietta Street
Kalamazoo, MI 49001

Brain-Imaging Studies of the Combined Use of Cocaine and Alcohol and of the Pharmacokinetics of Cocaethylene

Nora D. Volkow and Joanna S. Fowler

INTRODUCTION

The simultaneous use of cocaine and alcohol is one of the most frequent patterns of combined drug use (Grant and Harford 1990; Sands and Ciraulo 1992). Alcohol is combined with cocaine to reduce the dysphoria experienced after a cocaine binge (crash) and also to prolong the euphoria. Recent epidemiological studies have shown that combined use of cocaine and alcohol may be synergistically toxic (Boag and Havard 1985). It has been estimated that the combined use of cocaine and alcohol results in an eighteenfold increase in the risk of sudden death (Rose et al. 1990). Although the factors mediating the increased risk associated with the combined use of cocaine and alcohol are not fully understood, recent studies have suggested that cocaethylene, a metabolite of cocaine formed in the presence of alcohol, may contribute to enhanced morbidity and mortality (Hear-n et al. 1991*a*). Preclinical neurochemical and behavioral data on cocaethylene have shown that it has pharmacological properties similar to those of cocaine (Hearn et al. 1991*a*). Cocaethylene, like cocaine, binds to the dopamine transporter, inhibiting dopamine uptake and indirectly increasing the presynaptic concentration of dopamine (Jatlow et al. 1991; Woodward et al. l991), and it has been shown to be more toxic than cocaine (Hearn et al. 1991*b*; Katz et al. 1992).

Although cocaine and cocaethylene are similar in structure, differences in physical properties such as lipophilicity, plasma protein binding, and the ability to serve as substrates for cholinesterases in plasma might be expected to result in a different uptake and residence time in target

organs. Differences in availability could result in higher drug-tissue concentrations and longer drug duration, which could accentuate and prolong the effects of cocaine.

However, other factors also could explain the enhanced behavioral and toxic properties of cocaine when combined with alcohol. The enhanced behavioral effects could relate to the combination of two drugs that enhance dopamine concentrations in the nucleus accumbens (Ritz et al. 1987; Seeman and Lee 1974; Di Chiara and Imperato 1988). Also, cocaine's metabolism and pharmacokinetics could be changed in the presence of ethanol, leading to higher and longer lasting concentrations of cocaine or active metabolites. Such an effect of alcohol in drug pharmacokinetics has been demonstrated for amphetamine where coadministration with alcohol prolongs the blood and brain levels of amphetamine (Jonsson and Lewander 1973) and for cocaine where coadministration with alcohol results in higher blood levels of cocaine (Perez-Reyes and Jeffcoat 1992). The direct actions of cocaine and alcohol on target organs such as the heart also could account for the synergistic toxicity (Masur et al. 1989).

Positron emission tomography (PET) is a nuclear-imaging technique that allows the direct measurement of drug distribution and pharmacokinetics in the living human brain and body (Fowler et al. 1990). Investigations on the uptake and pharmacokinetics of [^{11}C]cocaine in the living human and nonhuman primate brain using PET have been done (Fowler et al. 1989, 1992*a)*. In the current study, the authors used [^{11}C]-labeled cocaethylene to investigate the pharmacokinetics of cocaethylene in the baboon brain, heart, and plasma; the findings were compared with those for [^{11}C]cocaine (Fowler et al. 1992*b*). To assess whether alcohol affects the pharmacokinetics of cocaine, the authors have performed PET studies with [^{11}C]cocaine in human subjects scanned without alcohol and during alcohol intoxication.

MATERIALS AND METODS

Baboon Studies

The baboon studies were designed to investigate the properties of [^{11}C]cocaethylene as they compare with those of [^{11}C]cocaine. Radiotracers synthesis occurred as follows: [N-^{11}C-methyl]cocaine was prepared by the methylation of norcocaine with [^{11}C]methyliodide (Langstrom and Lundqvist 1976; Fowler et al. 1989). [N-^{11}C-methyl]cocaethylene was prepared by the methylation of norcocaethylene (Fowler et al. 1992*a*). Cocaine, norcocaine, and cocaethylene were supplied by the National Institute on Drug Abuse (NIDA).

Five adult female baboons *(Papio Anubis)* were anesthetized, catheterized, and prepared for the PET study (Dewey et al. 1990). Scanning was carried out on a CTI 931-08 Computer Technologies, Inc., tomograph (spatial resolution of 6x6x6.5 mm full width half maximum). Each baboon was scanned twice, 2 hours apart, to compare [^{11}C]cocaine with [^{11}C]cocaethylene. Seven paired studies were done, five with [^{11}C]cocaine preceding [^{11}C]cocaethylene and two scans with [^{11}C]cocaethylene preceding [^{11}C]cocaine. For the studies, [^{11}C]cocaethylene (5 to 8 mCi:3 to 10 μg) or cocaine (5 to 8 mCi:4 to 6 μg) were injected sequentially. Dynamic scans were started immediately after injection of the tracer and were continued for 50 minutes.

Plasma analyses were done on arterial samples to measure total radioactivity and unchanged labeled tracer. Also, procedures regarding blood sampling and analysis were done (Fowler et al. 1992*a*). The concentration of the unchanged labeled tracer in plasma was used for the data analysis. The amount of [^{11}C]cocaine and [^{11}C]cocaethylene bound to plasma proteins also was determined for these studies (Fowler et al. 1992*a*).

For the analysis of the PET images, regions of interest were drawn directly on the images. An approximate value for whole brain uptake was obtained by averaging the activity in the five central slices. Regions for the striatum, cerebellum, and thalamus were obtained in the various slices where the regions were identified (Dewey et al.

1990). The activity in these regions of interest was used to obtain the time-activity curve for regional tissue concentration. The time-activity curves for tissue concentration and for unchanged tracer in plasma were used to calculate the transport constant between plasma and tissue (K_1) and to obtain the distribution volume for the various regions using a graphical analysis technique (Logan et al. 1990). The distribution volume is a measure of Bmax/Kd.

Human Studies

Seven normal male volunteers (ages 22 to 26 years) were studied with [^{11}C]cocaine (Fowler et al. 1989, 1992*b*). Subjects were screened for absence of medical, psychiatric, and neurological disease. Subjects with a past or present history of alcohol or other drug abuse in themselves or in first-degree relatives were excluded from the investigation. Urine samples were taken prior to the PET scan to ensure lack of psychoactive substance consumption. Each subject received two scans with [^{11}C]cocaine. The first scan was done with no pharmacological intervention, and the second scan was done 2 hours later during alcohol intoxication. Alcohol was given orally as 1 g/kg of ethanol during a 45-minute period, and scans were done 40 minutes later. For three subjects, scans were obtained for their brains; for four subjects, scans were obtained for their hearts.

Blood samples from a radial artery were obtained to quantitate total radioactivity, unchanged [^{11}C]cocaine, and blood alcohol concentration. A plasma sample drawn 10 minutes after injection of [^{11}C]cocaine was subjected to high-pressure liquid chromatography analysis to quantitate for labeled cocaethylene (Fowler et al. 1992*b*).

Regions of interest were obtained directly on the emission scans. Regions for striatum, cerebellum, thalamus, and frontal cortex were drawn on the various planes where they were identified, and a "composite" value was obtained using their weighted average (Fowler et al. 1989). Regions in the heart were obtained for the left ventricle, septum, and left atrium (Volkow et al. 1992). The tissue and plasma concentrations of tracer were used to calculate the distribution volume as described for the baboon studies.

RESULTS

Baboon Studies

Figures 1 and 2 show brain images for [^{11}C]cocaine and for [^{11}C]cocaethylene taken 3 to 6 minutes and 24 to 54 minutes after tracer injection. The pattern of distribution for both tracers in the brain was similar during the early scanning period (3 to 6 minutes). Maximal uptake for both tracers was obtained in the basal ganglia. Kinetic analysis of [^{11}C]cocaine and [^{11}C]cocaethylene in the brain revealed that peak uptake occurred for both tracers between 3 and 5 minutes for striatum and between 2 and 5 minutes for cortex, thalamus, and cerebellum. The peak uptake for these two tracers (expressed as percent dose/cm^3 of tissue) was not significantly different for any of the brain regions analyzed. In contrast to the similar pattern of uptake for these two tracers, significant differences were observed for their clearance; [^{11}C]cocaethylene cleared more slowly than [^{11}C]cocaine from the brain.

Figure 3 shows the time-activity curve for [^{11}C]cocaine and [^{11}C]cocaethylene in the whole brain (global), basal ganglia, and cerebellum and illustrates the slower clearance for [^{11}C]cocaethylene (CE) relative to that of [^{11}C]cocaine (C). The averages of the clearance half-time are shown in table 1.

Analyses of the rate of unchanged tracer in plasma revealed that there was a significantly higher percentage of unchanged tracer for [^{11}C]cocaethylene than for [^{11}C]cocaine. Average percentages of unchanged tracer in plasma at 10 minutes were C = 32±9.4 percent and CE = 39.7±8.9 percent; at 30 minutes they were C=16.6±6.8 percent and CE = 22.3±4.1 percent.

The values for the distribution volume in basal ganglia were not significantly different for [^{11}C]cocaine (7.4±1.9 mL/g) and [^{11}C]cocaethylene (7.7±1.9 mL/g). However, they were significantly larger for [^{11}C]cocaethylene than for [^{11}C]cocaine in the whole brain, basal ganglia, thalamus, and cerebellum. The distribution volume values are shown in table 2.

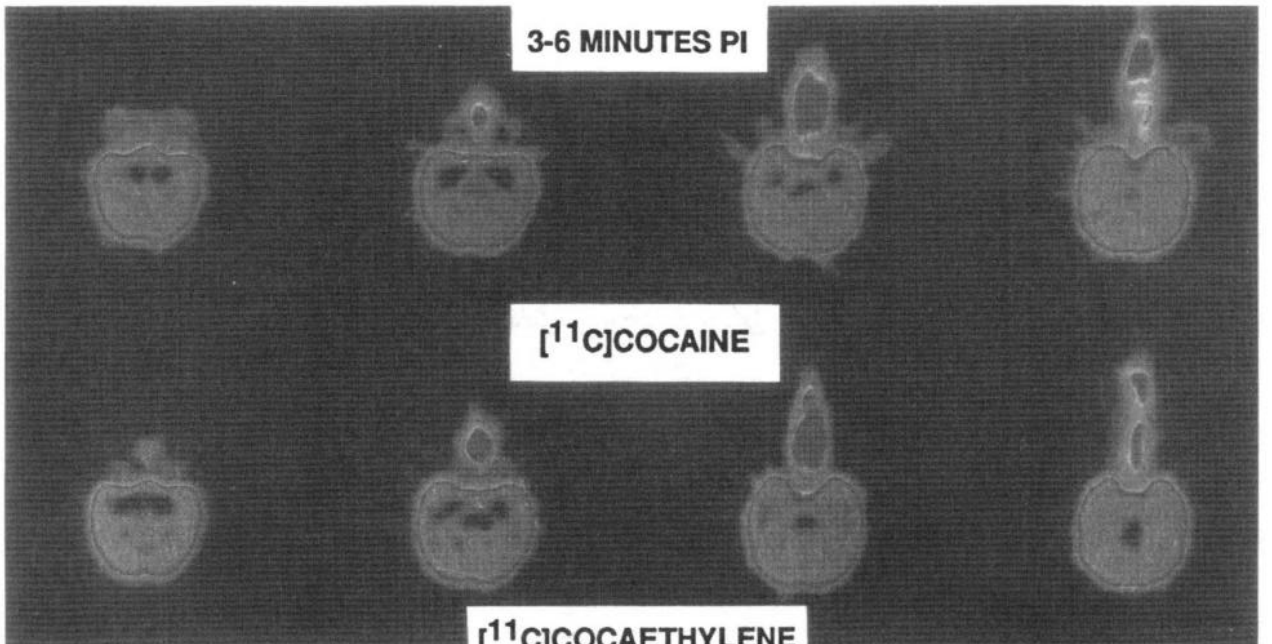

FIGURE 1. *Brain images for [^{11}C]cocaine and [^{11}C]cocaethylene obtained 3 to 6 minutes postinjection (PI). Brain images correspond to sequential planes at the level where the basal ganglia are located. Darker areas denote the brain regions with the highest uptake. For both tracers, highest uptake occurs in basal ganglia and, secondly, in thalamus.*

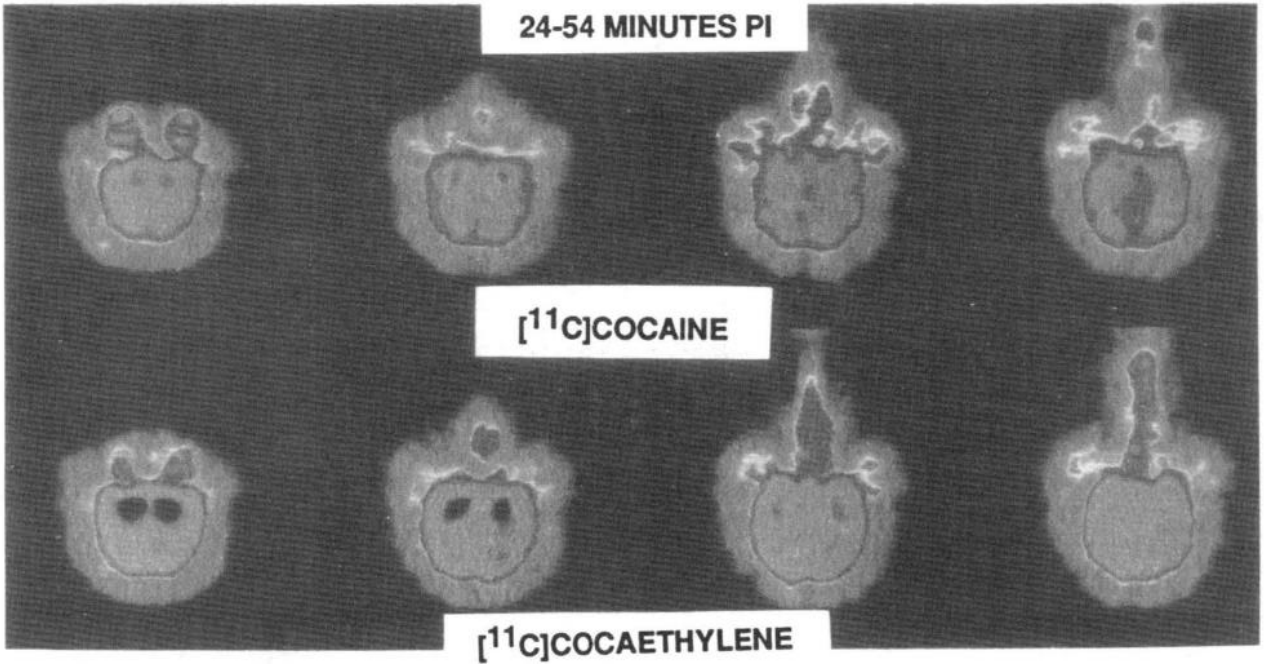

FIGURE 2. *Brain images for [^{11}C]cocaine and [^{11}C]cocaethylene obtained 24 to 54 minutes PI. Brain images correspond to the same planes as for figure 1. Notice the clearance of [^{11}C]cocaine in basal ganglia, whereas there is still a high concentration of [^{11}C]cocaethylene.*

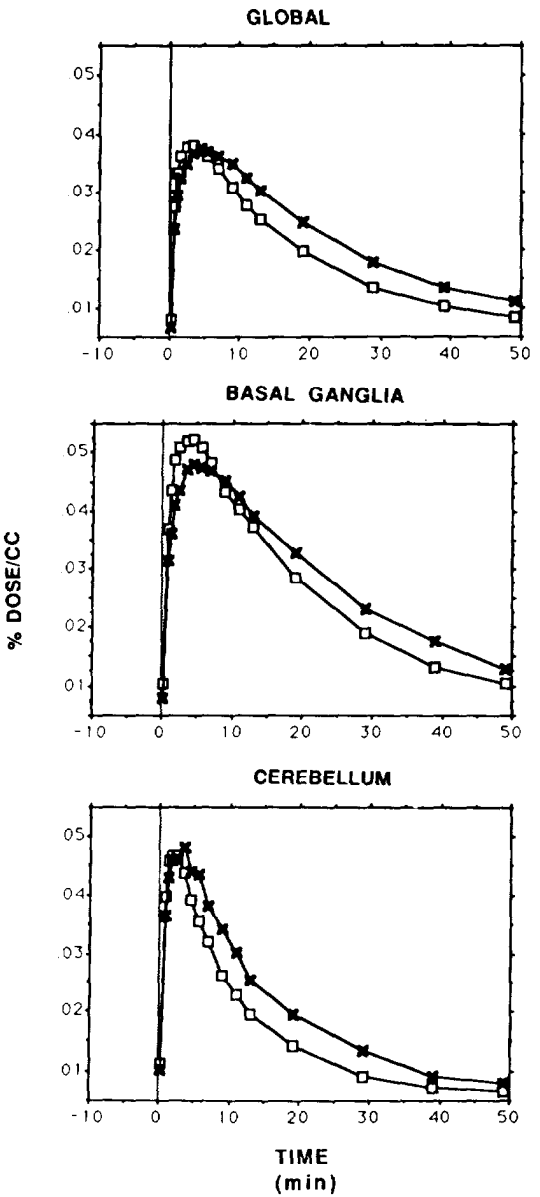

FIGURE 3. *Time-activity curves for [^{11}C]cocaine(□) and [^{11}C]cocaethylene (X) in whole brain (global), basal ganglia, and cerebellum. Notice the slower clearance of [^{11}C]cocaethylene than of [^{11}C]cocaine.*

TABLE 1. *Averages of the clearance half-time in min*

REGION	CLEARANCE HALF-TIME AVERAGES
Whole Brain	C = 14.3 ± 4.3 CE = 9.13 ± 4.7
Striatum	C = 17.2 ± 4.5 CE = 22.8 ± 3.2
Thalamus	C = 10.7 ± 3 CE = 315.4 ± 4
Cerebellum	C = 7.9 ± 1.9 CE = 12.0 ± 2.4

KEY: C = cocaine; CE = cocaethylene

Incubation of samples of labeled cocaine and labeled cocaethylene with baboon plasma for 40 minutes at room temperature, followed by thin-layer chromatography analysis, showed that cocaine is metabolized at a faster rate than cocaethylene. After 40 minutes, hydrolysis of cocaine to ecgonine methyl ester is 45-percent complete, whereas hydrolysis of cocaethylene to ecgonine ethyl ester is 15-percent complete. The plasma-free fraction for cocaine was 33.5 percent, and for cocaethylene it was 30.5 percent (Fowler et al. 1992*b*).

Human Studies

Alcohol intoxication did not significantly affect [^{11}C]cocaine pharmacokinetics as reflected by the rate of uptake and clearance of cocaine from the brain and heart. Also, alcohol intoxication did not affect the pattern of distribution of [^{11}C]cocaine nor its uptake in the brain or heart, nor did it affect rate of metabolism of [^{11}C]cocaine in plasma.

TABLE 2. *Values for the distribution volume in mL/g*

REGION	DISTRIBUTION VOLUME VALUES
Whole Brain	C = 4.9 ± 1 CE = 5.5 ± 1.3
Basal Ganglia	C = 7.4 ± 1.9 CE = 7.7 ± 1.9
Thalamus	C = 5.8 ± 1.3 CE = 6.7 ± 1.7
Cerebellum	C = 4.6 ± 1.1 CE = 5.4 ± 1.4

KEY: C = cocaine; CE = cocaethylene

NOTE: $p < 0.01$ paired *t*-test, two-tail

Distribution volumes before and during alcohol intoxication for the brain regions were not significantly different from each other and were within the variations previously reported for studies done on the same subject without intervention (Logan et al. 1990). The 10-minute plasma sample did not detect the presence of labeled cocaethylene (Fowler et al. 1992*b*).

DISCUSSION

The similar rate of uptake of [^{11}C]cocaethylene in the brain to that of [^{11}C]cocaine suggests that both drugs cross the blood-brain barrier to the same extent. The distribution of [^{11}C]cocaethylene in the baboon brain was also similar to that of [^{11}C]cocaine. For both tracers, the highest uptake was basal ganglia > thalamus > cortex = cerebellum. Both these drugs reached peak concentration in the brain at the same time (average 2 to 5 minutes after injection). The high uptake of [^{11}C]cocaethylene in the basal ganglia probably represents binding to

the dopamine transporter as shown for [^{11}C]cocaine by Fowler and colleagues (1989). This is likely because pharmacological studies have shown that the affinity of cocaethylene for the dopamine transporter is similar to that of cocaine (Heam et al. 1991*a*). Thus, differences between cocaine and cocaethylene do not seem to be due to either a difference in (1) the rate or speed of brain uptake or (2) their pattern of regional distribution. Interestingly, the rate of clearance of [^{11}C]cocaethylene from the brain was slower than that of [^{11}C]cocaine. This slower clearance could prolong the pharmacological effects when cocaine and alcohol are taken in combination. Similarly, the slower clearance in plasma of cocaethylene than that of cocaine could lead to more prolonged effects. However, the extent to which the differences in pharmacokinetics and metabolism between the two drugs could explain the enhanced behavioral and toxic effects of cocaine is not clear because tolerance to cocaine develops rapidly, and decreased cardiovascular and behavioral responses are observed even with steady-state plasma concentrations of cocaine (Ambre 1989).

The human studies were unable to document an effect of alcohol intoxication on the pharmacokinetics and distribution of [^{11}C]cocaine. This is different from what has been reported for alcohol and amphetamines. Also, these studies were unable to document the presence of labeled cocaethylene during the 10 minutes after administration of [^{11}C]cocaine.

In interpreting these results, one has to realize that the studies differ from real-life situations in the following manner: (1) a tracer dose of [^{11}C]cocaine was used rather than a pharmacologically active dose; (2) alcohol was administered prior to cocaine, and usually drug abusers consume alcohol after they have been administering cocaine; (3) a single administration of [^{11}C]cocaine was given as opposed to the repeated "binge" administration of cocaine by cocaine abusers; and (4) the study does not reproduce the conditions of the chronic drug abuser in whom metabolism of cocaine or alcohol may be impaired by long-term exposure to these drugs.

The inability to detect [^{11}C]cocaine and cocaethylene 10 minutes after injection of [^{11}C]cocaine during alcohol consumption is consistent with a recent study in humans showing that cocaethylene does not peak until 90 to 120 minutes after coadministration of cocaine and alcohol.

The amount of cocaethylene seen at peak is relatively low, corresponding to one-sixth of that for cocaine (McCance-Katz et al. 1991). Another study (Perez-Reyes and Jeffcoat 1992) reported a similar low conversion, which is consistent with a recent study on the enzymatic transesterification of cocaine in the presence of ethanol (Boyer and Petersen 1992).

Although cocaethylene may play a role in the amount of toxicity seen in cocaine and alcohol coadministration, other variables are probably as important and need to be considered. In fact, it may be the direct action of cocaine and alcohol, not their interactions, that is mainly responsible for the enhanced toxicity when used in combination. For example, the cardiovascular enhanced toxicity could relate to the fact that both these drugs (1) are directly toxic to the myocardium (Urbano-Marquez et al. 1989; Przywara and Dambach 1989), (2) release catecholamines from adrenals (Pohorecky and Brick 1988; Chiueh and Kopin 1978), and (3) induce vasoconstriction (Pohorecky and Brick 1988). Similarly, the acute behavioral effects of cocaine and alcohol could result from their effects on the same brain reward systems (Seeman and Lee 1974; Di Chiara and Imperato 1988).

In explaining the enhanced behavioral and toxic effects seen with coadministration of cocaine and alcohol and relating them to the formation of cocaethylene, one has to be aware that these effects are not specific to this particular drug combination. In fact, combination of other stimulant drugs with alcohol or other sedative hypnotics, such as benzodiazepines, has been shown to enhance behavioral and toxic effects of the individual drug (Rech et al. 1976; Iverson et al. 1975; Coleman and Evans 1975). The latter studies and the current findings emphasize the need to consider the direct actions of alcohol and of cocaine as one of the underlying mechanisms for their enhanced toxicity when used in combination.

REFERENCES

Ambre, J.J. Cocaine kinetics in humans. In: Redda, K.K.; Walker, CA.; and Bemett, *G.,* eds. *Cocaine, Marijuana, Designer Drugs: Chemistry, Phamtacology, and Behavior.* Boca Raton, FL: CRC Press, 1989. pp. 53-70.

Boag, F., and Havard, C.W.H. Cardiac arrhythmia and myocardial ischemia related to cocaine and alcohol consumption. *Postgrad Med J* 61:997-999, 1985.

Boyer, C.S., and Petersen, D.R. Enzymatic basis for the trans-esterification of cocaine in the presence of ethanol: Evidence for the participation of carboxylesterases. *J Pharmacol Exp Ther* 260:939-945, 1992.

Chiueh, C.C., and Kopin, I.J. Endogenous epinephrine and nor-epinephrine from the sympathoadrenal medullary system of anesthetized rats. *J Phamacol Exp Ther* 205:148-154, 1978.

Coleman, J.H., and Evans, W.E. Drug interactions with alcohol. *Med Times* 103:145-150, 1975.

Dewey, S.L.; MacGregor, R.R.; Brodie, J.D.; Bendriem, B.; King, P.T.; Volkow, N.D.; Schlyer, D.J.; Fowler, J.S.; Wolf, A.P.; Gately, S.J.; and Hitzemann, R. Mapping muscarinic receptors in human and baboon brain using [N-^{11}C-methyl]-benztropine. *Synapse* 5:213-223, 1990.

Di Chiara, G., and Imperato, A. Drugs abused by humans preferentially increase synaptic dopamine concentrations in the mesolimbic systems of freely moving rats. *Proc Natl Acad Sci U S A* 85:5274-5278, 1988.

Fowler, J.S.; Volkow, N.D.; Logan, J.; MacGregor, R.R.; Wang, G.-J.; and Wolf, A.P. Alcohol intoxication does not change [^{11}C]cocaine pharmacokinetics in human brain and heart. *Synapse* 12:228-235, 1992*b*.

Fowler, J.S.; Volkow, N.D.; MacGregor, R.R.; Logan, J.; Dewey, S.L.; Gatley, S.J.; and Wolf, A.P. Comparative PET studies of the kinetics and distribution of cocaine and cocaethylene in baboon brain. *Synapse* 12:220-227, 1992*a*.

Fowler, J.S.; Volkow, N.D.; Wolf, A.P.; Dewey, S.L.; Schlyer, D.J.; MacGregor, R.R.; Hitzemann, R.; Logan, J.; Bendriem, B.; Gatley, S.J.; and Christman, D. Mapping cocaine binding sites in human and baboon brain in vivo. *Synapse* 4:371-377, 1989.

Fowler, J.S.; Wolf, A.P.; and Volkow, N.D. New directions in positron emission tomography-Part II. *Annu Rep Med Chem* 25:261-269, 1990.

Grant, B.F., and Harford, T.C. Concurrent and simultaneous use of alcohol with cocaine: Results of national survey. *Drug Alcohol Depend* 25:97-104, 1990.

Hearn, W.L.; Flynn, D.D.; Hime, G.W.; Rose, S.; Cofino, J.C.; Mantero-Atienza, E.; Wetli, C.V.; and Mash, D.C. Cocaethylene: A unique cocaine metabolite displays high affinity for the dopamine transporter. *J Neurochem* 56:698-701, 1991*a*.

Heam, W.L.; Rose, S.; Wagner, J.; Ciarleglio, A.; and Mash, D.C. Cocaethylene is more potent than cocaine in mediating lethality. *Pharmacol Biochem Behav* 39:531-533, 1991*b*.

Iverson, F.; Coldwell, B.B.; Downie, R.H.; and Whitehouse, L.W. Effect of ethanol on toxicity and metabolism of amphetamine in the mouse. *Experientia* 31:679-680, 1975.

Jatlow, P.; Elsworth, J.D.; Bradberry, C.W.; Winger, G.; Taylor, J.R.; Russell, R.; and Roth, R.H. Cocaethylene: A neuropharmacologically active metabolite associated with concurrent cocaine-ethanol ingestion. *Life Sci* 48:1787-1794, 1991.

Jonsson, J., and Lewander, T. Effects of diethyldithiocarbamate and ethanol on the in vivo metabolism and pharmacokinetics of amphetamine in the rat. *J Pharm Pharmacol* 25:589-591, 1973.

Katz, J.L.; Terry, P.; and Witkin, J.M. Comparative behavioral pharmacology and toxicology of cocaine and its ethanol-derived metabolite, cocaine ethyl ester (cocaethylene). *Life Sci* 50: 1351-1361, 1992.

Langstrom, B., and Lundqvist, H. The preparation of "C-methyl iodide and its use in the synthesis of ^{11}C-methyl-L-methionine. *Int J Appl Radial Isotope* 27:357-363, 1976.

Logan, J.; Fowler, J.S.; Volkow, N.D.; Wolf, A.P.; Dewey, S.L.; Schlyer, D.; MacGregor, R.R.; Hitzemann, R.; Bendriem, B.; Gatley, S.J.; and Christman, D.R. Graphical analysis of reversible radioligand binding time-activity measurements applied to [N-^{11}C-methyl]-(-)-cocaine PET studies in human subjects. *J Neurochem* 10:740-747, 1990.

Masur, J.; Souza-Formigoni, M.L.O.; and Pires, M.L.N. Increased stimulatory effect by the combined administration of cocaine and alcohol in mice. *Alcohol* 6:181-182, 1989.

McCance-Katz, E.F.; Price, L.H.; McDougle, C.J.; Marek, G.J.; Kosten, T.R.; and Jatlow, P.I. Cocaethylene formation following sequential administration of cocaine and ethanol to humans: Pharmacological, physiological, and behavioral studies. *Soc Neurosci Abstr* 349.1:890, 1991.

Perez-Reyes, M., and Jeffcoat, A.R. Ethanol/cocaine interaction: Cocaine and cocaethylene plasma concentrations and their relationship to subjective and cardiovascular effects. *Life Sci* 51:1553-563, 1992.

Pohorecky, L.A., and Brick, J. Pharmacology of ethanol. *Pharmacol Ther* 36:1335-427, 1988.

Przywara, D.A., and Dambach, G.E. Direct action of cocaine on cardiac cellular activity. *Circ Res* 65:185-192, 1989.

Rech, R.H.; Vomachka, M.K.; and Rickert, D. Interactions between amphetamine and alcohol and their effect on rodent behavior. *Ann N Y Acad Sci* 281:426-440, 1976.

Ritz, M.C.; Lamb, R.J.; Goldberg, S.R.; and Kuhar, M.J. Cocaine receptors on dopamine transporters are related to self-administration of cocaine. *Science* 237:1219-1223, 1987.

Rose, S.; Heam, W.L.; Hime, G.W.; Wetli, C.V.; Ruttenber, A.I.; and Mash, D.C. Cocaine and cocaethylene concentrations in human post mortem cerebral cortex. *Soc Neurosci Abstr* 11.6:14, 1990.

Sands, B.F., and Ciraulo, D.A. Cocaine drug-drug interactions. *J Clin Psychopharmacol* 12:49-55, 1992.

Seeman, P., and Lee, T. The dopamine-releasing actions of neuroleptics and ethanol. *J Pharmcol Exp Ther* 190:131-140, 1974.

Urbano-Marquez, A.; Estruch, R.; Navarro-Lopez, F.; Grau, J.M.; Mont, L.; and Rubin, E. Effects of alcoholism on skeletal and cardiac muscle. *N Engl J Med* 320:409-415, 1989.

Volkow, N.D.; Fowler, J.S.; Wolf, A.P.; Wang, G.-J.; Logan, J.; MacGregor, R.R.; Dewey, S.L.; Schlyer, D.; and Hitzemann, R. Distribution and kinetics of carbon- 11 -cocaine in human body measured with PET. *J Nucl Med* 33:521-525, 1992.

Woodward, J.J.; Mansbach, R.; Carroll, F.I.; and Balster, R.L. Cocaethylene inhibits dopamine uptake and produces cocaine-like actions in drug discrimination studies. *Eur J Pharmacol* 197: 235-236, 1991.

ACKNOWLEDGMENTS

This research was supported by NIDA grants RID-A06891 and RID-A06278 and by the U.S. Department of Energy under contract DE-AC02-76CH00016.

AUTHORS

Nora D. Volkow, M.D.
Scientist
Medical Department

Joanna S. Fowler, Ph.D.
Senior Chemist

Brookhaven National Laboratory
Building 490
30 Bell Avenue
Upton, NY 11973

Positron Emission Tomography of Cocaine Binding Sites on the Dopamine Transporter

Bertha K. Madras, David R. Elmaleh, Peter C. Meltzer, Anna Y. Liung, Gordon L. Brownell, and Anna-Liisa Brownell

INTRODUCTION

Abuse of the highly addictive drug cocaine results in adverse psychological and medical consequences. The addictive properties of the drug appear to be related, in part, to the rapid entry of the drug into the brain, association with the brain's dopamine systems, and short duration of action. Swift metabolism leads to multiple and frequent dosing with the drug, which is an added risk for getting Acquired Immunodeficiency Syndrome (AIDS) by the intravenous route. These sequelae have catalyzed efforts to develop drug therapeutic approaches for cocaine addiction, particularly in view of the reported benefits of methadone and nicotine replacement for heroin and tobacco addictions.

Brain imaging techniques can contribute to and expedite the development of therapeutic agents, Positron emission tomography (PET) imaging is a sensitive method for localizing drug receptors in living brain tissue. The method can be applied to detect receptor occupancy of candidate therapeutic drugs and to determine whether occupancy is associated with therapeutic benefit. This chapter surveys preliminary studies by the authors to apply PET imaging to medications development. As converging evidence suggests that brain dopamine systems are principal targets of cocaine in the brain, the authors' studies focused on these systems.

PARAMETERS OF THE STUDIES

The Dopamine Transporter

The dopamine transporter is localized on dopamine neurons and suspends the effects of dopamine by transporting the neurotransmitter back into the terminals from which it was released. Although cocaine is a relatively nonselective inhibitor of the dopamine, serotonin, and norepinephrine transport, blockade of the dopamine transporter is strongly implicated in mediating the reinforcing properties of the drug (Ritz et al. 1987; Madras et al. 1989*a*; Bergman et al. 1989). Imaging of the dopamine transporter in vivo may be useful for monitoring behaviorally relevant cocaine recognition sites in the brain and for monitoring occupancy of potential drug therapies.

Cocaine Analogs as Probes for the Dopamine Transporter

The affinity of cocaine for the dopamine transporter in primate brain is relatively low (Madras et al. 1989*a),* its dissociation from these sites occurs within seconds, and approximately 25 to 30 percent of the [^{3}H]cocaine binding is associated with targets unrelated to the dopamine transporter. In recent years, a number of dopamine transport inhibitors structurally dissimilar to cocaine, including GBR 12935 and nomifensine, were proposed as probes for the dopamine transporter (Kuhar et al. 1990). Their suitability as probes for the dopamine transporter, however, is limited by their association with sites in addition to the dopamine transporter (Andersen et al. 1987, 1989; Seeman and Niznik 1990). This limitation, combined with the possibility that cocaine and its congeners may bind differently to the dopamine transporter than compounds of other chemical classes (Fahey et al. 1989; Rothman 1990), suggested the need for novel approaches to this problem. In 1989, the high-affinity cocaine congener WIN 35,428 (Clarke et al. 1973) was proposed as a probe for the dopamine transporter (Madras et al. 1989*a*).

[^{3}H]WIN 35,428, also designated [^{3}H]CFT, offers several advantages over [^{3}H]cocaine as a probe (Madras et al. 1989*b*, table 1). The sites labeled by [3H]CFT are of similar density and have virtually the same pharmacological specificity as [^{3}H]cocaine. Furthermore, the binding isotherms of [^{3}H]CFT model to two affinity components, a property

TABLE 1. *Comparison of the binding properties of [^{3}H]cocaine and [^{3}H]CFT ([^{3}H]WIN 35,428, Madras et al. 1989a, 1989b)*

SIMILARITIES

	[^{3}H]Cocaine	[3H]CFT
Site density	431 pmol/g	388 pmol/g
High/Low affinity	yes	yes
NaCl requirement	yes	yes

DIFFERENCES

	[^{3}H]Cocaine	[^{3}H]CFT
Affinity	283 nM	16 nM
Dissociation time	seconds	23 min
Nonspecific binding	20 to 30 percent	3 to 9 percent

characteristic of [^{3}H]cocaine binding. However, [^{3}H]CFT is superior to [^{3}H]cocaine inasmuch as its affinity is higher and its dissociation from these sites is slower (> 20 min versus seconds), which results in highly reproducible binding data. Most significantly for brain imaging, nonspecific binding of [^{3}H]CFT is less than 10 percent, and frequently less than 5 percent, a value considerably lower than that of [^{3}H]cocaine (20 to 30 percent). The markedly low level of nonspecific binding observed in homogenates was the authors' initial impetus to develop radiolabeled CFT and similar congeners as imaging agents.

Brain Distribution of [^{3}H]CFT (WIN 35,428)

Subsequent experimental findings with [^{3}H]CFT supported the authors' initial proposal and the progressive development of [^{3}H]CFT for this application. [^{3}H]CFT distributed primarily to dopamine-rich regions of primate brain (Canfield et al. 1990; Kaufman et al. 1991; Kaufman and Madras 1992). [^{3}H]CFT binding sites in the caudate-putamen and nucleus accumbus were relevant to the behavioral effects of cocaine (Madras 1989*c*). The sites were localized presynaptically (Kaufman and Madras 1991). In this regard, earlier studies reported a severe depletion of [^{3}H]CFT binding in post-mortem human Parkinson's diseased caudate and putamen compared with controls (Madras et al.

1990; Kaufman and Madras 1991). These brain regions undergo a marked loss of dopamine fibers in the course of Parkinson's disease. An additional advantage of [^{3}H]CFT was the high striatum:cerebellum ratio (3.3:5.6) observed by ex vivo autoradiography between 30 and 90 min, a period of time corresponding to a serviceable timeframe for a PET imaging procedure (Kaufman and Madras 1992, 1993). Finally, whereas a number of cocaine congeners bind to both the dopamine and serotonin transporter (Boja et al. 1992; Kaufman and Madras 1992; Laruelle et al. 1993), CFT demonstrated the highest selectivity, fifteenfold, for the dopamine compared with the serotonin transporter of compounds available during this period (Meltzer et al. 1993).

[^{11}C]CFT as a PET Ligand

A project was initiated to evaluate [^{11}C]CFT as a PET imaging probe for cocaine recognition sites associated with the dopamine transporter. Adult male and female cynomolgus monkeys *(Macacafascicularis)* were used for the imaging studies. PET imaging was conducted with a high-resolution positron emission tomograph (PCR-1, Brownell et al. 1985). The resolution of PCR-1 for a point source at the center is 4.5 mm, and the sensitivity is 46,000 counts per s for a source 20 cm in diameter with a concentration of 1 uCi/ml and a plane thickness of 1 cm. The plane thickness, 5 mm, used in these studies were obtained by the use of cylindrical collimators, which limited the effective height of the detectors. Each monkey was anesthetized, and PET imaging was conducted as described previously (Hantraye et al. 1992). Indwelling venous and arterial catheters were used for drug injections and for monitoring blood levels of [^{11}C]CFT. Sequential dynamic imaging for 90 min was carried out at earbar levels corresponding to 30 mm, 25 mm, 20 mm, 15 mm, 10 mm, -5 mm, and - 10 mm. Data were corrected for sensitivity and attenuation using a mathematical correction. For image reconstruction, a Hanning windowed filter convolution backprojection was used. Calibration of the camera was performed using a cylindrical plastic phantom (0 = 6 cm) and ^{18}F-solution, and cross calibration with the same solution was conducted using a gamma counter. Regions of interest (ROI) were drawn over the caudate, putamen, cortex, and cerebellum, and subsequently striatal:cerebellar and cortical:cerebellar ratios were calculated.

RESULTS

[^{11}C]CFT Accumulation in the Striatum

The accumulation of [^{11}C]CFT in the brain was evident within 2.5 min, and it was observed initially in the cortex, striatum, and additional brain regions. Within 40 min, regions other than the striatum were cleared of the radioligand, and dynamic images showed high uptake of [^{11}C]CFT in the caudate and putamen, which increased as a function of time for at least 100 min (figure 1). The ratio of specific to non-specific binding was determined by comparing the uptake in the caudate nucleus and putamen with the uptake in the cerebellum. At 90 min, the striatum:cerebellum ratio was 4.21±0.02 and 4.88±0.25 for the caudate nucleus and putamen, respectively. The ratio for the putamen was consistently 15 percent higher, a finding that corresponded with an earlier report using [^{3}H]CFT (Kaufman et al. 1991).

Pharmacological Specificity of [^{11}C]CFT Binding Sites

In order to determine whether binding was principally to the dopamine transporter, the effects of a number of selective and nonselective dopamine transport inhibitors on [^{11}C]CFT accumulation was determined. The dopamine transport inhibitors (-)-cocaine, GBR 12909, and mazindol, at doses that produce behavioral stimulation (Spealman et al. 1989), attenuated the accumulation of [^{11}C]CFT (Madras et al. 1991). In contrast, the selective and high-affinity serotonin transport inhibitor citalopram did not appreciably alter the accumulation of [^{11}C]CFT in striatum at low doses, but it did so at higher doses.

The present results clearly indicate that [^{11}C]CFT is a promising ligand for monitoring behaviorally relevant cocaine binding sites in striatum and for monitoring dopamine terminals. Its striatum:cerebellum ratio is higher than other PET ligands targeted to the dopamine transporter, its pharmacokinetic properties are suitable for imaging, and its initial metabolism is minimal (Kaufman and Madras 1992). Consequently, PET imaging of the dopamine transporter may expedite research in cocaine abuse. Equally important, it may serve as a powerful method for measuring the onset time and length of occupancy of cocaine therapeutic agents targeted to the dopamine transporter.

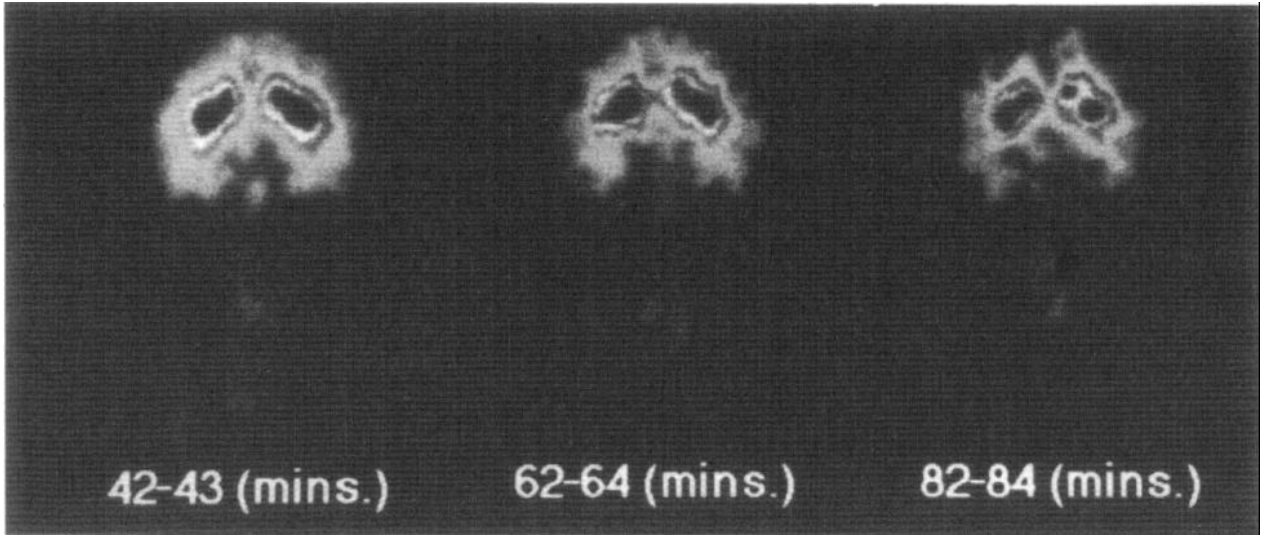

FIGURE 1. *Accumulation of [^{11}C]CFT in monkey striatum as a function of time*

The low level of nonspecific binding also suggested that radiolabeled CFT may be a marker for Parkinson's disease. This application for both [^{11}H]CFT and [^{11}C]CFT has been documented (Madras et al. 1990; Kaufman and Madras 1991; Hantraye et al. 1992), and it demonstrates an unanticipated benefit of cocaine research.

IMPLICATIONS

Applications of [^{11}C]CPT for Medications Development

The mounting evidence that dopamine contributes significantly to mediating the effects of cocaine offers several avenues for medications development. Among classes of drugs to be considered are compounds that target the dopamine transporter or dopamine receptors, including potential cocaine antagonists (Kitayama et al. 1992). Drug substitutes are the most frequently prescribed and effective medications used in the treatment of drug abuse. Cocaine substitutes require a careful consideration of the potential benefits of candidate compounds. In addition to efficacy, factors to be considered are comparisons between candidate compounds and cocaine with regard to abuse liability; behavioral, physiological, neurochemical, and toxic sequelae; and oral efficacy. Such information is needed to weigh carefully the risks and benefits of such an approach. Although a number of dopamine transport inhibitors are thought to exhibit less abuse liability than cocaine, this assumption should be validated by comparing the effects of candidate compounds when administered by the same routes as cocaine.

Criteria for therapeutic agents that target the dopamine transporter have not been clearly established. A candidate therapeutic agent that demonstrates a longer onset time and prolonged duration of action may offer some advantages. In this regard, the slow onset may result in diminished euphoric effects compared with cocaine, and the long duration of action may minimize frequent dosing, thereby reducing the risk of acquiring AIDS by the intravenous route. One example of such a drug is indantraline (Lu 19-005), which has a relatively slow onset and long duration of action (> 2 d) in primates (Rosenzweig-Lipson et al. 1992).

The authors administered indantraline (0.2 mg/kg) 24 h prior to onset of a PET imaging procedure. At this low dose, equivalent to one-fifth the dose that generated behavioral stimulation for longer than 2 d, uptake of [^{11}C]CFT was reduced in two of three animals. At 60 min into the PET imaging procedure, [^{11}C]CFT accumulation was reduced by 31 percent in the caudate nucleus and by 25 percent in the putamen. These results suggest that prolonged stimulation by indantraline may be related directly to occupancy of the dopamine transporter. Furthermore, the results demonstrate the feasibility of using PET imaging to identify whether candidate compounds occupy the dopamine transporter in the brain and to measure the occupancy period.

The long duration of action of indantraline may be related to its high affinity (0.081 pM) for the dopamine transporter in monkey brain and possibly to its occupancy of the serotonin transporter in the periphery (Madras et al. 1993). In this regard, another high-affinity serotonin transport inhibitor, RTI-55 (Boja et al. 1992), was shown to accumulate in high concentrations in lung, a potential depot for drugs that are potent inhibitors of serotonin transport (Kaufman and Madras 1992).

PET Imaging of the D_1 Dopamine Receptor

Because they are the indirect targets of cocaine, dopamine receptors represent another potential target for therapeutic agents. Although two families of dopamine receptors are found in the brain, D_1 and D_2, the majority of drugs currently available are of the D_2 type. D_2 agonists and antagonists have received attention as possible therapeutic agents (Preston et al. 1992). The adverse side effects of agonists (dyskinesias) and antagonists (extrapyramidal signs) has focused interest on antagonists with reduced extrapyramidal signs. Recently, researchers have focused more attention on drugs that target the D_1 dopamine receptor. The authors have initiated studies to determine whether D_1 agonists occupy D_1 dopamine receptors in vivo. The D_1 receptor was imaged with [^{11}C]SCH 39166, a selective D_1 receptor antagonist that accumulates in high concentrations in the striatum. A preliminary study using an MPTP-treated monkey has demonstrated D_1 receptor occupancy by the selective D_1 agonist, SKF 81297 (Madras et al. 1992).

CONCLUSION

These preliminary studies demonstrate the potential utility of PET as a technique for imaging the dopamine transporter, a principal target of cocaine in the brain. Furthermore, they illustrate a potential application of PET imaging in medications development. PET imaging appears to be useful for identifying the receptor targets of candidate compounds. PET also may be useful for assessing whether a compound, which produces prolonged stimulant effects, occupies the dopamine transporter during the timeframe that behavioral effects are measurable. Thus, combined with other strategies, PET imaging studies can accelerate preclinical evaluation of potential cocaine therapeutic agents.

REFERENCES

Andersen, P.H. The dopamine uptake inhibitor GBR 12909: Selectivity and molecular mechanism of action. *Eur J Pharmacol* 166:493-504, 1989.

Andersen, P.H.; Jansen, J.A.; and Nielsen, E.B. [^{3}H]GBR 12935 binding in vivo in mouse brain: Labelling of a piperazine acceptor site. *Eur J Pharmacol* 144:1-6, 1987.

Bergman, J.; Madras, B.K.; Johnson, S.E.; and Spealman, R.D. Effects of cocaine and related drugs in nonhuman primates: III. Self-administration by squirrel monkeys. *J Pharmacol Exp Ther* 251:150-155, 1989.

Boja, J.W.; Mitchell, W.M.; Patel, A.; Kopajtic, T.A.; Carroll, F.I.; Lewin, A.H.; Abraham, P.; and Kuhar, M.J. High-affinity binding of [^{125}I]RTI-55 to dopamine and serotonin transporters in rat brain. *Synapse* 12:27-36, 1992.

Brownell, G.L.; Bumham, C.A.; and Chesler, D.A. High resolution tomograph using analog coding. In: Greitz, T.; Ingvar, D.H.; and Widen, L., eds. *The Metabolism of the Human Brain Studied With Positron Emission Tomography.* New York: Raven Press, 1985.

Canfield, D.R.; Spealman, R.D.; Kaufman, M.J.; and Madras, B.K. Autoradiographic localization of cocaine receptors by [^{3}H]CFT in monkey brain. *Synapse* 5:189-195, 1990.

Clarke, R.L.; Daum, S.J.; Gambino, A.J.; Aceto, M.D.; Pearl, J.; Levitt, M.; Cumisky, W.R.; and Bogado, E.F. Compounds affecting the central nervous system: IV. 2-ß-phenyltropane-2-carboxylic esters and analogs. *J Med Chem* 16:1260-1267, 1973.

Fahey, M.A.; Canfield, D.R.; Spealman, R.D.; and Madras, B.K. Comparison of [^{3}H]GBR 12935 and [^{3}H]cocaine binding sites in monkey brain. *Soc Neurosci Abst* 15:1090, 1989.

Hantraye, P.; Brownell, A.-L.; Elmaleh, D.; Spealman, R.D.; Wullner, U.; Brownell, G.L.; Madras, B.K.; and Isacson, O. Dopamine fiber detection by ^{11}C-CFT and PET in a primate model of Parkinsonism. *Neuroreport* 3:265-268, 1992.

Kaufman, M.J., and Madras, B.K. Severe depletion of cocaine recognition sites associated with the dopamine transporter in Parkinson's diseased striatum. *Synapse* 9:43-49, 1991.

Kaufman, M.J., and Madras, B.K. Cocaine recognition sites labeled by [^{3}H]CFT and [^{125}I]RTI-55 in monkey brain: II. Ex vivo autoradiographic distribution. *Synapse* 12:99-111, 1992.

Kaufman, M.J., and Madras, B.K. [^{3}H]CFT ([^{3}H]WIN 35,428) accumulation in dopamine regions of monkey brain: Comparison of a mature and an aged monkey. *Brain Res* 611:322-325, 1993.

Kaufman, M.J.; Spealman, R.D.; and Madras, B.K. Distribution of cocaine recognition sites in monkey brain: I. In vitro autoradiography with [^{3}H]CFT. *Synapse* 9:177-187, 1991.

Kitayama, S.; Shimada, S.; Xu, H.; Markham, L.; Donovan, D.M.; and Uhl, G.R. Dopamine transporter site-directed mutations differentially alter substrate transport and cocaine binding. *Proc Natl Acad Sci U S A* 89:7782-7785, 1992.

Kuhar, M.J.; Sanchez-Roa, P.M.; Wong, D.F.; Dannals, R.F.; Grigoriadis, D.E.; Lew, R.; and Milberger, M. Dopamine transporter: Biochemistry, pharmacology, and imaging. *Eur Neurol* 30:15-20, 1990.

Laruelle, M.; Baldwin, R.M.; Malison, R.T.; Zea-Ponce, Y.; Zoghbi, S.S.; Al-Tikriti, M.S.; Sybirska, E.H.; Zimmermann, R.C.; Wisniewski, G.; Milius, R.A.; Wang, S.; Smith, E.O.; Roth, R.H.; Chamey, D.S.; Hoffer, P.B.; and Innis, R.B. SPECT imaging of dopamine and serotonin transporters with [^{125}I]ß-CIT: Pharmacological characterization of brain uptake in nonhuman primates. *Synapse* 13:295-309, 1993.

Madras, B.K. "Cocaine Recognition Sites in Primate Nucleus Accumbens and Medial Prefrontal Cortex: Relationship to the Behavioral Effects of Cocaine-like Drugs." Paper presented at the annual meeting of the American College of Neuropsychopharmacology, Maui, Hawaii, 1989*c*.

Madras, B.K.; Elmaleh, D.; Meltzer, P.; Lee-Parritz, D.E.; Hantraye, P.; Isacson, O.; Brownell, G.L.; and Brownell, A.-L. Parkinsonian signs in MPTP-treated monkeys are alleviated by the high efficacy D_1 dopamine receptor agonist SKF 81297. *Soc Neuosci Abstr* 18:935, 1992.

Madras, B.K.; Fahey, M.A.; Bergman, J.; Canfield, D.R.; and Spealman, R.D. Effects of cocaine and related drugs in nonhuman primates: I. [^{3}H]Cocaine binding sites in caudate-putamen. *J Pharmacol Exp Ther* 251:131-141, 1989*a*.

Madras, B.K.; Fahey, M.A.; and Kaufman, M.J. [^{3}H]CFT and [^{3}H]Lu 19-005: Markers for cocaine receptors/dopamine nerve terminals in Parkinson's disease. *Soc Neurosci Abstr* 16:14, 1990.

Madras, B.K.; Fahey, M.A.; Kaufman, M.J.; Spealman, R.D.; Schumacher, J.; Isacson, O.; Brownell, A.-L.; Brownell, G.L.; and Elmaleh, D.R. Cocaine receptor probes in nonhuman and human brain: In vitro characterization and in vivo imaging. *Soc Neurosci Abstr* 17:190, 1991.

Madras, B.K.; Spealman, R.D.; Fahey, M.A.; Neumeyer, J.L.; Saha, J.K.; and Milius, R.A. Cocaine receptors labeled by [^{3}H]2ß-carbomethoxy-3ß-(4-fluorophenyl)tropane. *Mol Pharmacol* 36:518-524, 1989*b*.

Meltzer, P.C.; Liang, A.Y.; Brownell, A.-L.; Elmaleh, D.R.; and Madras, B.K. Substituted 3-phenyltropane analogs of cocaine: Synthesis, inhibition of binding at cocaine recognition sites, and positron emission tomography. *J Med Chem* 36:855-862, 1993.

Preston, K.L.; Sullivan, J.T.; Strain, E.C.; and Bigelow, G.E. Effects of cocaine alone and in combination with bromocriptine in human cocaine abusers. *J Pharmacol Exp Ther* 262:279-291, 1992.

Ritz, M.C.; Lamb, R.J.; Goldberg, S.R.; and Kuhar, M.J. Cocaine receptors on dopamine transporters are related to self-administration of cocaine. *Science* 237:1219-1223, 1987.

Rosenzweig-Lipson, S.J.; Bergman, J.; Spealman, R.D.; and Madras, B.K. Stereoselective behavioral effects of Lu 19-005 in monkeys: Relation to binding at cocaine recognition sites. *Psychopharmacology* 107:186-194, 1992.

Rothman, R.B. High affinity dopamine reuptake inhibitors as potential cocaine antagonists: A strategy for drug development. *Life Sci* 46:PL-17-PL-21, 1990.

Seeman, P., and Niznik, H.B. Dopamine receptors and transporters in Parkinson's disease and schizophrenia. *FASEB J* 4:2737-2744, 1990.

Spealman, R.D.; Madras, B.K.; and Bergman J. Effects of cocaine and related drugs in nonhuman primates: II. Stimulant effects on schedule-controlled behavior. *J Pharmacol Exp Ther* 251:142-149, 1989.

ACKNOWLEDGMENTS

This research has been supported by United States Public Health Service grants DA06303 and RR00168. Dr. D. Lee-Parritz for advice on anesthesia, and Dr. J. Amt (Lundbeck A/S) for indantraline. The animals were maintained in accordance with the guidelines of the Committee on Animals of the Harvard Medical School and according to DHHS publication No. (NIH)85-23.

AUTHOR

Bertha K. Madras, Ph.D.
Associate Professor
Harvard Medical School
New England Regional Primate Research Center
One Pine Hill Drive
Southborough, MA 01772

David R. Elmaleh, Ph.D.
Associate Professor

Gordon L. Brownell, Ph.D.
Professor

Anna-Liisa Brownell, Ph.D.
Nuclear Physicist
Department of Radiology
Massachusetts General Hospital
Boston, MA 02115

Peter C. Meltzer, Ph.D.
Chemist

Anna Y. Liang, Ph.D.
Chemist
Organix, Inc.
Wobum, MA 01801

Metabolic Mapping Methods for the Identification of the Neural Substrates of the Effects of Novel Tropane Analogs

Linda J. Porrino, Lisa Williams-Hemby, and Huw M.L. Davies

INTRODUCTION

The administration of any psychoactive drug to an organism produces a variety of pharmacological actions that may include both central and peripheral effects. These physiological and behavioral responses are unlikely to result from a single action in a single brain region; they are more likely to be the product of multiple processes at a number of distinct anatomical sites. In addition, most drugs, particularly when administered over a broad range of doses, may not act on only one neurotransmitter system or receptor subtype but on some combination thereof. These issues are particularly pertinent when new compounds are to be investigated. Such compounds may have actions in vivo not necessarily predictable from in vitro characterizations.

In order, then, to determine the neural substrates of the actions of a drug, especially when the actions of the drug are not completely specified (as is the case when drugs are in development), it is necessary to identify neural events in circuits and pathways throughout the brain, not just at one location. This requires either that researchers investigate small portions of the brain one at a time, as with electrophysiological or in vivo microdialysis methods, or that they use methods capable of surveying the entire brain simultaneously. The development of the 2-[^{14}C]deoxyglucose (2-DG) method by Sokoloff and colleagues (1977) has provided the means to accomplish the latter approach. The 2-DG method is a means with which functional events in the brain related to various physiological, pharmacological, and behavioral states can be investigated. It has been used extensively in neuropharmacology to identify the neural circuits that mediate the effects of a wide variety of pharmacological agents (for reviews cf.

McCulloch 1982; Porrino and Pontieri 1993). This chapter will describe the 2-DG method and its application to the study of a series of novel tropane analogs recently synthesized by Davies and colleagues (1991, 1993).

MEASUREMENT OF RATES OF GLUCOSE UTILIZATION

The 2-DG method measures rates of local cerebral glucose utilization (LCGU) throughout all portions of the central nervous system (CNS). It is a biochemical method that measures a biological process-glucose utilization or the rate at which energy is consumed in neuro-anatomically defined regions in the CNS of conscious animals. The value of the measurement of rates of glucose utilization stems from the fact that in the brain, as in other tissues that do physicochemical work, the amount of energy used is correlated with the amount of work done in that tissue. Glucose utilization in the brain is a measure of energy use under normal physiological conditions because glucose is virtually the exclusive substrate for energy metabolism. The basic rationale of the 2-DG method is that functional activity in any given brain region is related directly to energy metabolism in that region. It is possible, therefore, through the measurement of changes in rates of glucose utilization to identify brain regions in which functional activity is altered during various experimental manipulations.

Although there are a number of energy-requiring processes in the brain that contribute to basal rates of glucose utilization, transmitter synthesis, release and reuptake, and protein synthesis, the largest portion of energy in the CNS, however, is used to maintain and restore ionic gradients. It has been estimated that 80 percent of the energy generated in the brain is used for this purpose (Kurumaji et al. 1993). It is important to appreciate that the changes in rates of glucose utilization that are evoked by an experimental manipulation are thought to result mainly from increases or decreases in electrical activity or synaptic activity in the CNS. These changes in electrical activity in turn produce corresponding increases or decreases in the activity of Na+, K^+,ATPase, the energy consuming enzyme involved in the restoration of neuronal ionic gradients to their resting state. Experi-ments with 2-DG have shown that the coupling of glucose utilization to functional activity is dependent on Na^+, K^+-ATPase activity in that ouabain, an

ATPase inhibitor, can block the increases in glucose utilization that accompany electrical stimulation (Mata et al. 1980).

The measurement of rates of glucose utilization follows the basic principles for the measurement of rates of any reaction with radioactive tracers. The amount of product formed over an interval of time is determined, related to the integrated specific activity (i.e., the ratio of the labeled precursor to the total precursor pool integrated over the time of measurement), and corrected for kinetic differences between the labeled and unlabeled compounds. Rates of LCGU are measured with a radioactively labeled analog of glucose, 2-DG, that, like glucose, is transported into cerebral tissue by the same carrier and phosphorylated by hexokinase but, unlike glucose, is not metabolized further and is, therefore, trapped within cells. It is this sequestration within cells that allows quantitative autoradiography to be used to measure actual rates of glucose utilization in individual brain regions.

The details of the derivation of the 2-DG method and an extensive discussion of its theoretical basis are beyond the scope of this chapter, but for further discussion see Sokoloff and colleagues (1977, 1982) and Sokoloff and Porrino (1986). The techniques used for the application of the 2-DG method have also been described in detail elsewhere (Porrino and Crane 1990).

ADVANTAGES AND DISADVANTAGES OF THE 2-DG METHOD

Advantages

One of the principal advantages of the 2-DG method is the use of autoradiography, which permits the visualization of individual structures within the brain as well as anatomical subdivisions within a given structure. The resolution of the 2-DG method is approximately 100μ. The limiting factors are the energy of the isotope and the diffusion and migration of the labeled compound in the tissue during freezing and cutting of the brain. Even in the rat, though, it is possible to distinguish subdivisions of a structure as small as the lateral habenula. For example, glucose utilization in the lateral portion of the lateral habenula is decreased significantly following the administration of

dopaminergic agonists (McCulloch et al. 1982; Wechsler et al. 1979; Porrino et al. 1984, 1988). With many other neurochemical methods, such as in vivo microdialysis or neurotransmitter turnover determinations, it is not possible to ascribe effects to particular divisions or subdivisions of brain regions because the areas sampled are by necessity rather large. In 2-DG studies, the use of quantitative autoradiography makes it possible to evaluate changes in functional activity in highly circumscribed brain regions.

Another advantage is that a broad survey of effects at all levels of the brain is possible. This means that investigations are not limited to those sites in which effects are expected, a particularly important factor when a drug has not been characterized completely. If the whole brain is examined, effects of a pharmacological agent may be seen that otherwise would have gone unnoticed. In a study of the effects of lesions of the substantia nigra of primates induced by the infusion of 1-methyl-4-phenyl-1,2,3,6-tetrahydropyridine, alterations in cerebral glucose utilization rates were evident not just within the basal ganglia as expected but also in circuits mediating eye movements (Porrino et al. 1987). Using this kind of an approach, it is possible to survey effects in a number of systems without using different sets of animals.

Although earlier experiments with the 2-DG method were conducted in restrained or partially restrained animals, methods have been developed that permit the use of the 2-DG method in freely moving, conscious animals (Crane and Porrino 1989). This approach allows the application of the method to the study of behavior. In pharmacological studies, behavioral effects produced by drug administration can be related directly to changes in functional activity in specific brain regions.

One problem with the 2-DG method is that the uptake of 2-deoxyglucose is dependent on variables such as blood pressure, cardiac output, and plasma glucose levels. Overall differences in uptake based on these variables could obscure differences between groups that are the result of changes in functional activity, particularly if non- or semiquantitative methods are used. Because the calculation of absolute rates of glucose utilization with the 2-DG method takes these variables into account, however, valid comparisons can be made between groups, allowing both the identification of brain areas with altered

functional activity and the magnitude of these changes. This is clearly an advantage in pharmacological studies in which the physiological status of the animal frequently is altered by drug administration.

Disadvantages

Despite its advantages, the 2-DG method has a number of limitations. Foremost among these is the inability to differentiate between direct and indirect effects of a given stimulus. An entire pathway or circuit may be activated metabolically, even though the direct action of the stimulus may occur only at the origin of or at some point along the pathway. The 2-DG method, therefore, cannot identify the sites at which a drug binds or the sites at which a drug initiates its actions. This is illustrated by the results of a study in which the effects of diazepam on cerebral metabolism were measured (Ableitner et al. 1985). Little overlap was evident between regions in which significant changes in rates of metabolism were found and those areas identified as having high benzodiazepine binding. More specifically, glucose utilization was increased in the lateral thalamus, an area low in binding sites, and not altered in areas such as the ventromedial hypothalamus and medial amygdala, both rich in binding sites. It is important to consider that glucose utilization changes reflect only a corresponding change in afferent input to that region and not a change in the functional activity of cell bodies in that structure. An entire pathway may be activated, even though the direct action of the drug occurred only at the origin of the circuit. Although this lack of specificity may be a limitation in some instances, as in the case of determining the primary site of action of a drug, it is an advantage when the goal is to identify the neural circuits or pathways that mediate a specific behavioral response.

Other disadvantages include the fact that it is not possible to identify the specific neurotransmitters, neuromodulators, or receptor types that are responsible for changes in functional activity and the inability to distinguish between inhibitory and excitatory processes on the basis of increases or decreases in 2-DG uptake. Both excitation and inhibition at the neuronal level involve similar metabolic processes in that maintenance and restoration of ionic gradients have similar energy requirements, regardless of whether excitatory or inhibitory neurotransmitters are secreted at synaptic terminals.

The 2-DG method also has poor time resolution. The rather long experimental time period can be a significant limitation in drug studies because steady state or constant conditions need to be maintained for accurate measurement of rates of glucose utilization. Physiological and behavioral responses to drug administration can vary significantly across the 45 minutes required for the application of the 2-DG method. For example, although the total experimental time is 45 minutes, the uptake and phosphorylation of 2-DG in the brain reflect predominantly its metabolism in the first 5 to 10 minutes of this period. This is because the tissue concentrations of free 2-DG available for metabolism are highest during the first 5 to 10 minutes after its injection (Sokoloff et al. 1977). Correct choice of the optimal time for drug administration in relation to the time of injection of 2-DG is, then, important to ensure maximal sensitivity of the method as well as to ensure that data will be comparable across treatments. Drug administration should be timed so that the maximum drug response coincides with the time of maximum incorporation of 2-DG.

A final disadvantage that should be noted is that repeated measurements are not possible in the same animal. Groups of separate animals must be used to determine the effects of each experimental condition, which increases variability as well as the number of animals necessary.

Despite these constraints, the 2-DG method has been applied effectively in many neuropharmacological studies. The method can provide novel information about the identity of brain regions functionally involved in mediating the effects of a given drug. It can be particularly useful when the actions of the drug in question have not been described completely. An example of such an application is discussed in the next section.

NOVEL TROPANE ANALOGS

One approach to the study of the neurobiological actions of cocaine has been through the use of cocaine analogs. Because many of the important behavioral and physiological effects of cocaine, in particular its euphorogenic properties, have been attributed to its actions at dopaminergic synapses, tropane analogs that mimic or are more potent than cocaine at these sites can be useful tools. A variety of tropane

analogs have been synthesized by a number of investigators to date (Abraham et al. 1992; Lewin et al. 1992; Carroll et al. 1992*a*; 1992*b*; Davies et al. 1991; Kozikowski et al. 1991).

One such series of novel tropane analogs was reported recently by Davies and colleagues (1991, 1993). These analogs are synthesized with a novel strategy utilizing vinylcarbenoid precursors instead of more traditional methods in which cocaine is used as the starting material. Characterization of these compounds in vitro has shown that several of the compounds are as much as 900 to 1300 times more potent than cocaine in displacing [^{125}I]RTI-55 binding in rat striatal membrane preparations (Davies et al. 1993). In addition to being more potent than cocaine at dopamine transporters, some analogs in this series also were significantly more potent than cocaine in binding to serotonin transporters in rat frontal cortex. As with cocaine, many of the analogs tended to be comparatively nonselective with respect to dopamine and serotonin (Childers, Bennett, Sexton, Saikali, and Davies, unpublished observations). Several of the analogs, however, demonstrated a relative selectivity for dopamine, including 2ß-propanoyl-3ß-(4-toluyl) tropane (PTT), which displayed at least a twentyfold selectivity for dopamine in binding assays. Results from uptake studies have confirmed both the potencies and specificities of these tropanes as well (Bennett, Hyde, Saikali, and Davies, unpublished observations).

To date, PTT has been the only analog that has undergone a thorough evaluation in vivo. These studies have verified that, like cocaine, PTT acts as a stimulant in many respects (Porrino et al., submitted). These studies, however, also show that PTT differs from cocaine qualitatively in other aspects, as might be expected from an analog with a different specificity than cocaine. For example, PTT produced significant dose-dependent behavioral activating effects when administered to rats intraperitoneally. Within the range of doses tested in these comparison studies, PTT was approximately 10 to 30 times more potent than cocaine in stimulating locomotor activity (Porrino et al., submitted). This corresponds closely to the relative potency of this novel tropane analog at binding to the dopamine transporter as well as its potency at inhibiting dopamine uptake (Davies et al. 1993). There is, then, good agreement between the relative potencies of PTT and cocaine in in vitro and in vivo behavioral studies,

The behavioral effects of PTT, however, did not always coincide with those of cocaine when examined more closely (Porrino et al., submitted). Animals treated with low doses of PTT, for example, exhibited little movement. These rats remained awake and alert but relatively motionless for long periods. In contrast, at moderate doses PTT produced cocaine-like behavioral effects in the form of increases in exploratory behaviors such as sniffing, rearing, and forward locomotion, and the administration of higher doses of PTT were accompanied by intense patterns of stereotypic head movements. PTT elicited a far greater degree of stereotypic movements than cocaine, and the character of these behaviors also was quite different. Even at the highest dose tested in this assay, cocaine treatment was associated mainly with forward locomotion and rearing with few stereotyped behaviors evident, whereas PTT administration produced focused, circular head bobbing restricted to one comer of the test chamber. The differences in the behavioral effects elicited by cocaine and PTT support the view that they are qualitatively different in vivo.

METABOLIC MAPPING OF PTT

To investigate the differences between PTT and cocaine further and to determine the neuroanatomical substrates of these differences, metabolic mapping with the quantitative autoradiographic 2-DG method was utilized (Porrino, unpublished observations). The purpose of this study was to identify the effects of PTT on functional activity and to compare these effects to those of cocaine. The effects of the acute intravenous (IV) administration of low (0.1 mg/kg), moderate (0.5 mg/kg), and high (1.0 mg/kg) doses of PTT on rates of LCGU were measured in portions of the dopaminergic mesocorticolimbic and nigrostriatal systems as well as in limbic, cortical, and thalamic regions.

At moderate and high doses, widespread increases in LCGU were seen in all portions of the nigrostriatal motor system (see figure 1 for example) and throughout the thalamus and cortex. PTT at these doses also elevated rates of cerebral metabolism in all portions of the mesocorticolimbic system with the largest increases in medial prefrontal cortex, olfactory tubercle, and nucleus accumbens (see figure 2 for example). This distribution of LCGU changes closely parallels the

dose-dependent metabolic changes observed following cocaine administration (Porrino et al. 1988). The similarities between PTT and other psychostimulants are depicted in figures 3 and 4 in which the effects of high, medium, and low doses of PTT, cocaine, and methamphetamine on rates of cerebral metabolism in portions of the nigrostriatal and mesocorticolimbic systems are compared. The similarities are consistent with increased activity that accompany treatment with these drugs.

In contrast, at low doses, PTT had few effects on LCGU in most brain regions but significantly decreased metabolism in the mesocorticolimbic system (figure 2). These metabolic changes may reflect the behavioral suppression seen at low doses in the activity studies previously described. The depression of metabolic activity in the nucleus accumbens, olfactory tubercle, and medial prefrontal cortex following PTT administration clearly is different from the pattern of changes produced by cocaine, which at low doses produces selective increases in metabolism in these same brain regions (Porrino et al. 1988). Figure 4 compares the effects of high, medium, and low doses of PTT, cocaine, and methamphetamine on cerebral metabolism in the olfactory tubercle and nucleus accumbens. The decreases in metabolism evident following PTT administration are not seen following acute treatment with other psychostimulants or other dopaminergic drugs, regardless of the dose range tested. PTT, then, is unique in its effects at low doses, although at higher doses its effects strongly resemble those of other psychostimulants.

CONCLUSIONS

The 2-DG method has provided a comprehensive view of the functional involvement of various brain areas in response to the administration of a novel tropane analog and has furnished information about the specific neural substrates responsible for the behavioral and physiological effects of PTT. As demonstrated here, this method can reveal unexpected actions of a drug not immediately obvious with either behavioral testing or in vitro pharmacological assays. The significance of the 2-DG method for medication development, then, is that it can provide a powerful tool for investigating the nature, specificity,

anatomical substrates, and potential neurotoxicity of medications developed for treatment of substance abuse or other diseases.

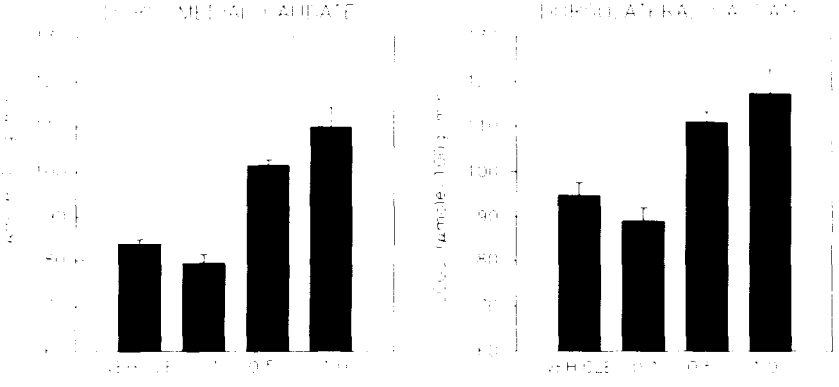

FIGURE 1. *Effects of various doses of PTT on rates of LCGU in the dorsomedial caudate (left) and dorsolateral caudate (right). Values represent means and standard errors of rates of glucose utilization (μmol/100 g/min), n = 4 in each group.*

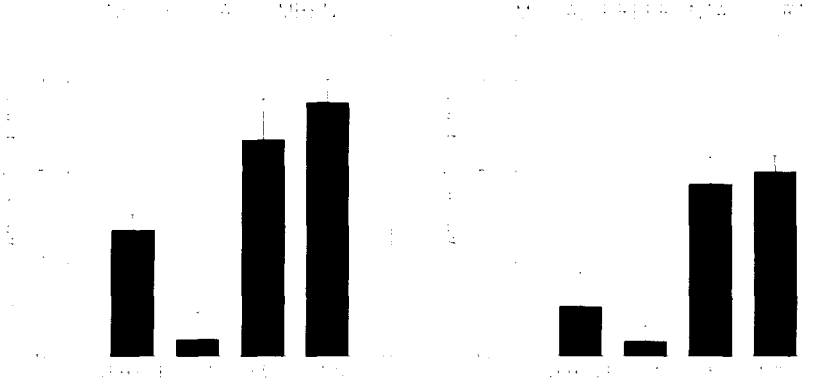

FIGURE 2. *Effects of various doses of PTT on rates of LCGU in the nucleus accumbens (left) and medial prefrontal cortex (right). Values represent means and standard errors of rates of glucose utilization (μmol/100 g/min), n = 4 in each group.*

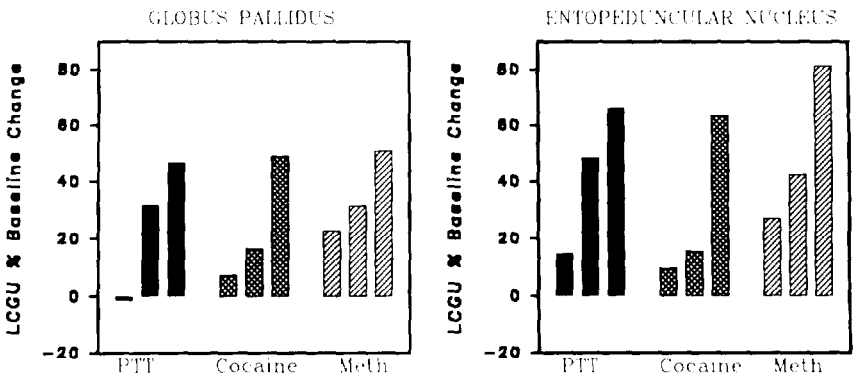

FIGURE 3. *Comparison of the alterations in LCGU accompanying the administration of PTT and other psychostimulants in the globus pallidus (left) and the entopeduncular nucleus (right). Values are percent change from control for low, medium, and high doses of PTT = 2ß-propanoyl-3ß-(4-toluyl)-tropane (0.1, 0.5, and 1.0 mg/kg, IV; Porrino et al. in preparation); Cocaine (0.25, 1.0, and 5.0 mg/kg, IV, Porrino et al. 1988); and Meth = methamphetamine (0.5, 1.0, and 2.5 mg/kg, IV; Pontieri et al. 1990). Note the similarities in the pattern of changes across the three drugs.*

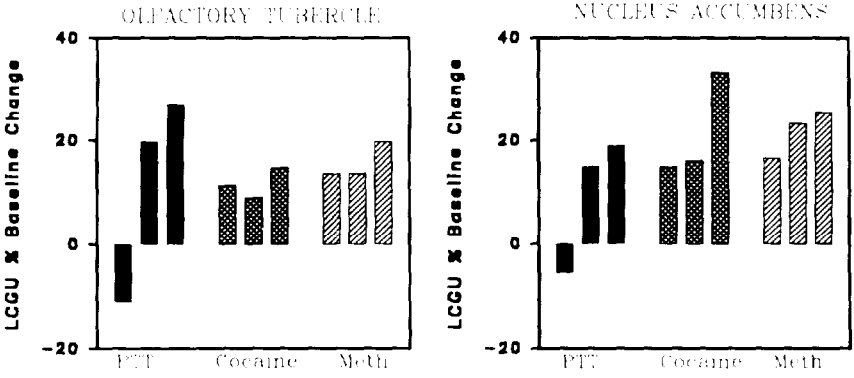

FIGURE 4. *Comparison of the alterations in LCGU accompanying the administration of PTT and other psychostimulants in the olfactory tubercle (left) and the nucleus accumbens (right). Values are percent change from control for low, medium, and high doses of PTT = 2ß-propanoyl-3ß-(4-toluyl)-tropane (0.1, 0.5, and 1.0 mg/kg,* IV; *Porrino et al., in preparation); Cocaine = (0.25, 1.0, and 5.0 mg/kg, IV; Porrino et al. 1988); and Meth = methamphetamine (0.5, 1.0, and 2.5 mg/kg, IV; Pontieri et al. 1990). Note the differences in the patterns of glucose utilization changes between PTT and cocaine and methamphetamine. Low doses of PTT produce depressions in glucose utilization in these structures not seen with cocaine or methamphetamine.*

REFERENCES

Ableitner, A.; Wuster, M.; and Herz, A. Specific changes in local cerebral glucose utilization in the rat brain induced by acute and chronic diazepam. *Brain Res* 359:49-56, 1985.

Abraham, P.; Pitner, J.B.; Lewin, A.H.; Boja, J.W.; Kuhar, M.J.; and Carroll, F.I. N-Modified analogues of cocaine. Synthesis and inhibition of binding to the cocaine receptor. *J Med Chem* 35:141, 1992.

Carroll, F.I.; Gao, Y.; Abraham, P.; Lewin, A.H.; Parham, K.A.; Boja, J.W., and Kuhar, M.J. Isopropyl and phenyl esters of 3ß-(4-substituted phenyl)tropane-2ß-carboxylic acids. Potent and selective compounds for the dopamine transporter. *J Med Chem* 35:1813, 1992*b*.

Carroll, F.I.; Lewin, A.H.; Boja, J.W.; and Kuhar, M.J. Cocaine receptor: Biochemical characterization and structure-activity relationships of cocaine analogues at the dopamine transporter. *J Med Chem* 35:969, 1992*a*.

Crane, A.M., and Porrino, L.J. Adaptation of the quantitative 2-[^{14}C]deoxyglucose method for use in freely-moving rats. *Brain Res* 499:87-92, 1989.

Davies, H.M.L.; Saikali, E.; and Sexton, T.; Childers, S.R. Novel 2-substituted cocaine analogs: Binding properties at dopamine transport sites in rat striatum. *Eur J Pharmacol* 244:93-97, 1993.

Davies, H.M.L.; Saikali, E.; and Young, W.B. Synthesis of (±)-ferruginine and (±)-anhydroecgonine methyl ester by a tandem cyclopropanation/Cope rearrangement. *J Org Chem* 56:5696, 1991.

Kozikowski, A.P.; Xiang, L.; Tanaka, J.; Bergmann, J.S.; and Johnson, K.M. Use of nitrile oxide cycloaddition (NOC) chemistry in the synthesis of cocaine analogs; mazindol binding and dopamine uptake studies. *Med Chem Res* 1:312, 1991.

Kurumaji, A.; Dewar, D.; and McCulloch, J. Metabolic mapping with deoxyglucose autoradiography as an approach for assessing drug action in the central nervous system. In: London, E.D., ed. *Imaging Drug Action in the Brain.* Boca Raton, FL: CRC Press, 1993. pp. 219-245.

Lewin, A.H.; Gao, Y.; Abraham, J.W.; Boja, J.W.; Kuhar, M.J.; and Carroll, F.I. 2ß-Substituted analogues of cocaine. Synthesis and inhibition of binding to the cocaine receptor. *J Med Chem* 35:135, 1992.

Mata, M.; Fink, D.J.; Gainer, H.; Smith, C.B.; Davidsen, L.; Savaki, H.E.; Schwartz, W.J.; and Sokoloff, L. Activity-dependent energy metabolism in rat posterior pituitary primarily reflects sodium pump activity. *J Neurochem* 34:213-215, 1980.

McCulloch, J. Mapping functional alterations in the CNS with [^{14}C]deoxyglucose. In: Iverson, L.; Iverson, S.; and Snyder, S., eds. *Handbook of Psychopharmacology.* Vol. 15. New York: Plenum, 1982. pp. 321-410.

McCulloch, J.; Savaki, H.E.; and Sokoloff, L. The distribution of alterations in energy metabolism in the rat brain produced by apomorphine. *Brain Res* 243:67-80, 1982.

Pontieri, F.E.; Crane, A.M.; Seiden, L.S.; Kleven, M.S.; and Porrino, L.J. Metabolic mapping of the effects of intravenous methamphetamine administration in freely-moving rats. *Psychopharmacology* 102:175- 182, 1990.

Porrino, L.J.; Bums, R.S.; Crane, A.M.; Palombo, E.; Kopin, I.J.; and Sokoloff, L. Changes in local cerebral glucose utilization associated with Parkinson's syndrome induced by 1-methyl-4-phenyl-1,2,3,6-tetrahydropyridine (MPTP) in the primate. *Life Sci* 40: 1657-1664, 1987.

Porrino, L.J., and Crane, A.M. Metabolic mapping of the effects of drugs of abuse with the 2-[^{14}C]deoxyglucose method. In: Adler, M.W., and Cowan, A., eds. *Modem Methods in Pharmacology: Testing and Evaluation of Drugs of Abuse.* New York: Alan R. Liss, 1990. pp. 147-164.

Porrino, L.J.; Domer, F.R.; Crane, A.M.; and Sokoloff, L. Selective alterations in cerebral metabolism within the mesocorticolimbic dopaminergic system produced by acute cocaine administration in rats. *Neuropsychopharmacology* 1:109-118, 1988.

Porrino, L.J.; Lucignani, G.; Dow-Edwards, D.L.; and Sokoloff, L. Correlation of dose-dependent effects of acute amphetamine administration on behavior and local cerebral metabolism in rats. *Brain Res* 307:311-320, 1984.

Porrino, L.J.; Migliarese, K.; Davies, H.M.L.; Saikali, E.; and Childers, S.R. Behavioral effects of the novel tropane analog, 2ß-propanoyl-3ß-(4-toluyl)-tropane (PTT). *Neuropharmacology.* Submitted for publication.

Porrino, L.J., and Pontieri, F.E. Metabolic mapping of the effects of psychomotor stimulants in rats. In: London, E.D., ed. *Imaging Drug Action in the Brain.* Boca Raton, FL: CRC Press, 1993. pp. 247-263.

Sokoloff, L. The radioactive deoxyglucose method: Theory, procedure, and applications for the measurement of local glucose utilization in the central nervous system. In: Agranoff, B.W., and Aprison, M.H., eds. *Advances in Neurochemistry.* Vol. 4. New York: Plenum, 1982. pp. 7-36.

Sokoloff, L., and Porrino, L.J. Some fundamental considerations in the application of the deoxyglucose method to pharmacological studies. In: Kriegelstein, I. ed. *Pharmacology of Cerebral Ischemia.* Amsterdam: Elsevier, 1986. pp. 65-76.

Sokoloff, L.; Reivich, M.; Kennedy, C.; DesRosiers, M.H.; Patlak, C.S.; Pettigrew, K.D.; Sakurada, O.; and Shinohara, M. The [^{14}C]deoxyglucose method for the measurement of local cerebral glucose utilization: theory, procedure and normal values in the conscious and anesthetized albino rat. *J Neurochem* 28:897-916, 1977.

Wechsler, L.R.; Savaki, H.E.; and Sokoloff, L. Effects of d- and l-amphetamine on local cerebral glucose utilization in the conscious rat. *J Neurochem* 32:15, 1979.

ACKNOWLEDGMENTS

This work was supported by United States Public Health Service grants P50 DA06634, DA07522 (LJP), and DA06301 (HMLD) and Training Grant DA07246 (LWH) from NIDA.

AUTHORS

Linda J. Porrino, Ph.D.
Associate Professor

Lisa Williams-Hemby, B.S.
Graduate Student

Department of Physiology and Pharmacology
Bowman Gray School of Medicine
Medical Center Boulevard
Winston-Salem, NC 27157-1083

Huw M.L. Davies, Ph.D.
Associate Professor
Department of Chemistry
Wake Forest University
Winston-Salem, NC 27 104

Noninvasive Evaluation of the Sympathetic Nervous System of the Heart by Nuclear Imaging Procedures

Markus Schwaiger, James C. Sisson, and Donald Wieland

INTRODUCTION

The autonomic nervous system plays an important role in the regulation of cardiovascular performance under physiologic and pathophysiologic conditions. The sympathetic and parasympathetic innervations of the heart facilitate the electrophysiologic and hemodynamic adaptations to changing cardiovascular demands. Both sympathetic and parasympathetic tones control the rate of electrophysiologic stimulation, whereas the contractile performance of the heart is modulated primarily by sympathetic neurotransmission. The evaluation of the sympathetic nervous system has been limited in the past to catheterization of the coronary sinus vein and measurement of plasma levels of norepinephrine (NE) and its metabolites in arterial and venous blood across the heart (Goldstein et al. 1988). These procedures are invasive and do not provide regional assessment of neuronal integrity within the heart. More recently, radiolabeled pharmaceuticals have been introduced for the noninvasive assessment of the sympathetic nervous system using nuclear medicine imaging approaches (Wieland et al. 1983). Improvement in radiochemistry and imaging technology allows the specific visualization of sympathetic nerve terminals and adrenergic receptors of the living heart. Iodinated compounds have been used with planar and tomographic gamma camera imaging for the delineation of sympathetic nerve terminals. Recently, positron emission tomography (PET) has been employed to assess more specifically uptake as well as synthesis of neurotransmitters in the heart. This new imaging modality, in combination with short-lived isotopes, permits the quantitative definition of regional myocardial tracer distribution, which may be useful for the quantification of regional neuronal function in the living human heart.

This chapter addresses the emerging role of nuclear imaging procedures in the noninvasive characterization of the cardiac sympathetic nervous system. It addresses the physiology of the sympathetic nervous system and discusses radiochemical approaches to tracing sympathetic neurotransmission. Finally, it describes initial experimental and clinical experience with these radiopharmaceuticals in the animal model and in human patients with various cardiac diseases.

PHYSIOLOGY OF THE SYMPATHETIC NERVOUS SYSTEM

Presynaptic Nerve Terminal

The postganglionic sympathetic fibers travel along vascular structures on the surface of the heart. On entering the myocardial wall, the fibers branch into multiple sympathetic nerve terminals. These terminals include vesicles, which are the storage pools for neurotransmitters, enzymes, and other proteins. NE, the dominant neurotransmitter in cardiac sympathetic nerve terminals, is synthesized from the amino acid tyrosine by several enzymatic steps (figure 1). Synthesis of dopa from tyrosine is the rate-limiting step in the biosynthesis of catecholamines. Dopamine, converted from dopa, is transported into storage vesicles by an active transport mechanism. Within the storage vesicles, NE is synthesized, stored, and released on nerve stimulation by exocytosis (Levitt et al. 1965). The regulation of neuronal NE release is complex. Alpha-2-receptors have been postulated to exist on the membrane of the presynaptic nerve terminal. Activation of these receptors by NE leads to a negative feedback of the exocytotic process. In addition to the presynaptic α-2-receptors, the presence of other inhibitory presynaptic receptors suggests that multiple control mechanisms modulate the NE release from sympathetic nerve terminals (Francis 1988).

The reuptake of released NE by the nerve terminal from the synaptic cleft is an important and efficient mechanism to maintain the stores of neurotransmitters. As much as 80 percent of the NE that is released from the nerve terminal is taken up through this mechanism (uptake-I mechanism). Following reuptake, NE recycles into the storage vesicles by active transport (Goldstein et al. 1988).

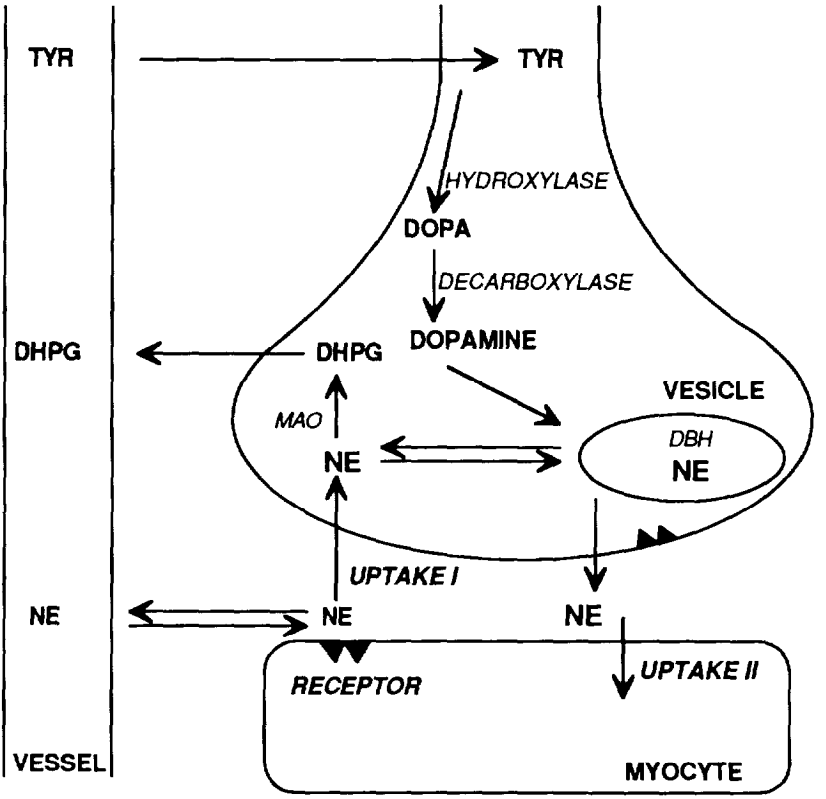

FIGURE 1. *Schematic display of the sympathetic nerve terminal. NE is synthesized from dopamine by the dopamine-beta-hydroxylase and stored in vesicles. Released NE undergoes reuptake by the nerve terminal (uptake I). Only a small amount of NE binds to the adrenergic receptors or is taken up by nonneuronal tissue (uptake II).*

A fraction of the released NE diffuses back into the vascular space where it can be measured as NE spillover in the coronary sinus venous blood (Goldstein 1981). Only a small amount of NE in the synaptic cleft is actually available to activate receptors on the surface of the myocyte or to enter the cardiac cell directly (uptake-II mechanism).

NE undergoes rapid metabolism in neuronal and extraneuronal tissue. Metabolism of the neurotransmitter in the neuronal cytosol is by monoamine oxidase (MAO), whereas extraneuronal NE is metabolized by the catechol-o-methyltransferase (COMT) enzyme system (Axelrod 1960; Hertting et al. 1961).

Adrenergic Receptors

General classes of postsynaptic adrenergic receptors are designated as α- or ß-receptors. This distinction is based on pharmacological studies describing specific functional responses of each receptor system (Lefkowitz and Caron 1988). A positive inotropic response to catecholamine stimulation is mediated primarily by ß-receptors. In the normal left and right ventricular myocardium, the subset of receptors, ß1, makes up about 80 percent of the total pool of ß-receptors (Stiles et al. 1983). It has been speculated that ß2-receptors are most prevalent in the atria and that ß2-selective agonists elicit a more chronotropic response than do ß1-selective drugs (Carlsson et al. 1977). Recent investigations indicate that functional ß-receptors of the heart exist on the surface of cell membranes, but other nonfunctional ß-receptors are within the cells. Internalization of the receptors may be in response to homologous desensitization (a method of regulation) of ß-receptors under various physiologic and pathophysiologic conditions (Lefkowitz and Caron 1988; Bristow et al. 1982).

RADIOPHARMACEUTICALS

The complex neurophysiology of cardiac innervation makes it apparent that the noninvasive characterization of neuronal function by a single tracer is difficult. Physiologic function of the sympathetic nerve terminal includes the synthesis and release of NE as well as reuptake and metabolism of neurotransmitters. The characterization of this complex physiologic system by radiopharmaceuticals requires detailed understanding of their physiologic behavior. Several approaches of tracer design that can be pursued for the evaluation of the sympathetic nervous system include the use of analogs, neurotransmitter precursors, and receptor antagonists. Table 1 lists radiopharmaceuticals currently used for the characterization of the sympathetic nervous system by nuclear medicine procedures.

TABLE 1. *Currently available tracers for the noninvasive characterization of presynaptic and postsynaptic sympathetic nervous system*

Radiopharmaceuticals for the Noninvasive Evaluation of the Sympathetic Nervous System	
Presynaptic	Postsynaptic
[^{123}I]metaiodobenzylguanidine (MIBG)	[^{123}I]iodocyanopindolol (ICYP)
[^{11}C]hydroxyephedrine (HED)	[^{11}C]practolol
[^{18}F]metaraminol	[^{11}C]propanolol
[^{18}F]fluorodopamine	[^{11}C]CGP12177

NE Analogs

Radiopharmaceutical research efforts have focused initially on the design of radiotracers that serve as markers for the presynaptic neuron. An obvious tracer for the delineation of adrenergic nerve terminal is NE. The first in vivo image of the heart based on adrenergic nerve accumulation of a radiotracer was accomplished, appropriately, with [^{11}C]NE in 1975 (Fowler et al. 1975). In the early 1980s, MIBG was developed at the University of Michigan for selective mapping of the heart's sympathetic nerve endings using conventional nuclear medicine procedures (figure 2) (Wieland et al. 1981*a*).

Recently, radiopharmaceuticals have been developed at the University of Michigan for the PET characterization of the autonomic nervous system. Development of these radiopharmaceuticals centered around the false neurotransmitter metaraminol, which is a close structural analog of NE (figure 2). Metaraminol has been used extensively in animal models as a tool to study the transport characteristic of the neuronal uptake (Anton and Berk 1977). This tracer has high affinity for the catecholamine uptake mechanism, and its retention in tissue is not complicated by neuronal metabolism. The metabolic refractoriness

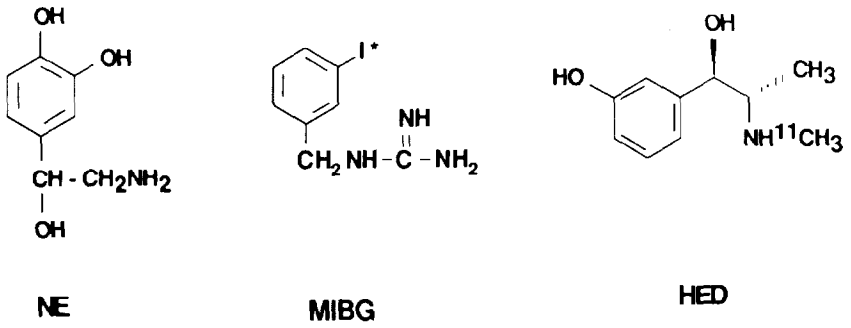

FIGURE 2. *Chemical structure of NE, MIBG, and [^{11}C]HED*

of metaraminol relative to NE is caused by the presence of the α-methyl group that effectively blocks the action of MAO and the absence of a catechol group that confers resistance to COMT. Following the initial validation of titrated metaraminol as a suitable presynaptic tracer of the heart, [^{18}F]metaraminol was synthesized using the electrophilic fluorination method (Wieland et al. 1990). However, the specific activity of [^{18}F]metaraminol achievable with this synthetic method was not high enough to avoid pharmacological effects if injected intravenously.

Another analog of metaraminol subsequently has been synthesized at the authors' laboratory (Rosenspire et al. 1990). HED is structurally very similar to metaraminol, but it can be labeled with [^{11}C] to yield a radiopharmaceutical with very high specific activity (figure 2). This radiopharmaceutical behaves very similarly to [^{11}F]metaraminol, but, because of a short physical half-life, it can be administered in large doses and in combination with other PET tracers such as flow and metabolic markers.

NE Precursors

A biochemical parameter that can be used to assess sympathetic function is the rate of endogenous NE synthesis. [^{18}F]Fluorodopamine allows imaging of sympathetic nerve terminals as demonstrated in animal experiments (Eisenhofer et al. 1989; Goldstein et al. 1990). Because this tracer is converted to [^{18}F]NE within the sympathetic

nerve terminals, synthesis and release can be studied using this radiopharmaceutical. However, the tracer kinetics are expected to be complicated, and sophisticated tracer kinetic modeling will be necessary to deconvolute synthesis and neuronal release of this radiotracer in the living heart. Because secreted NE is taken up by the neuron terminal, pharmacological interventions to inhibit the uptake-I pathway are needed to quantify the neuronal release rate of NE using [^{18}F]fluorodopamine.

Adrenergic-Receptor Ligands

A number of receptor sites or uptake carriers in the adrenergic neuron could be targeted with labeled ligands. Numerous reports exist on the subject of radiolabeled adrenergic-receptor antagonists. [^{11}C]Propanolol and [^{11}C]practolol have been synthesized and evaluated for PET imaging (Syrota 1990). [^{123}I]ICYP has been proposed as a marker for the assessment of myocardial ß-receptor density using γ-camera imaging techniques. However, these tracers are lipophilic and exhibit considerable binding to lung tissue, limiting the accurate quantification of regional receptor binding by imaging approaches. Recently, a hydrophilic ß-receptor antagonist (CGP12177) was labeled with [^{11}C] for use in combination with PET (Syrota 1990). Initial results in the animal model are promising for the noninvasive quantification of myocardial ß-receptor density. However, such radiopharmaceuticals are still considered experimental.

EXPERIMENTAL AND CLINICAL IMAGING OF THE SYMPATHETIC NERVOUS SYSTEM

Radiolabeled MIBG

Labeled with [^{131}I], MIBG concentrates in adrenergic tumors, and the radiopharmaceutical has become popular to portray scintigraphically the locations of pheochromocytomas (Shapiro et al. 1985; Sisson et al. 1981) and neuroblastomas (Geatti et al. 1985; Hoefnagel et al. 1987). MIBG also can be labeled with [^{123}I], a radionuclide that, relative to [^{131}I], is safer in larger doses and exhibits more favorable imaging characteristics. Thus, [^{123}I]MIBG was selected to depict the adrenergic neurons in the heart (Kline et al. 1981).

Studies in Cell Cultures and Animals. The pharmacology of MIBG largely has been delineated. The agent enters adrenergic cells, including neuron terminals, through the uptake-I pathway (Jaques et al. 1984). Some MIBG may enter the adrenergic tissues by diffusion (Jaques et al. 1984), but, under ordinary conditions, it seems likely that this route carries only a small fraction of the radiopharmaceutical. Within an adrenergic cell, MIBG is retained in specialized storage vesicles (Gasnier et al. 1986; Wieland et al. 1981*b*). These characteristics enable the uptake and retention of MIBG to represent the integrity of adrenergic neurons, particularly those in the heart. Pretreatment with the neurotoxin 6-hydroxydopamine (De Champlain and Nadeau 1971) caused a generalized decrease in the MIBG uptake retention in the hearts of rats, indicating the specificity of this tracer for nerve terminals (Sisson et al. 1987*a*). Regional denervation can be produced by the application of phenol to localized areas of pericardium (Barber et al. 1984). This type of treatment produced, within the region of neuronal injury, decreases in MIBG concentrations that were easily detectable by scintigraphic imaging procedures (Dae et al. 1989; Minardo et al. 1988; Sisson et al. 1988).

Thus, images of the heart made with [^{123}I]MIBG are capable of demonstrating neuronal injuries (i.e., denervation) that are either global or regional in extent. Minardo and coworkers (1988) employed this approach for the delineation of denervated, viable myocardium following an ischemic injury. Regions of infarction can be identified by flow tracers such as thallium-201(^{201}TI) and subtracted from the defect appearing on the [^{123}I]MIBG image, which includes both denervated and infarcted myocardium. However, the effects of reduced blood flow on the delivery of the MIBG to the peri-infarct myocardium must be taken into account (Sisson et al. 1990*a*). Large regions of peri-infarct denervation can be visualized readily (Minardo et al. 1988), but the identification of smaller regions and the quantification of denervation will require new and sophisticated approaches to the analysis of neuron integrity and regional myocardial perfusion.

In images of the heart made soon after injection of MIBG, the non-neuronal uptake of the radiopharmaceutical appeared to be as much as 20 percent. However, after several hours, the vast majority of MIBG probably resides within neurons (Sisson et al. 1987*a*). The physiologic function of adrenergic neurons leads to secretion of NE by exocytosis,

and MIBG exits the neuron terminals by this same mechanism (Jaques and Tobes 1985). The rate of loss of NE from the neurons in an organ such as the heart appears to be proportional to the functional activity of these nerves (Hasking et al. 1986); the NE "spills over" into the circulation. The rate of loss of MIBG from the rat heart followed a pattern similar to that of NE, but the rate for MIBG was more rapid (Sisson et al. 1987*a*). MIBG possibly exits more rapidly from neurons because a greater fraction of MIBG than of NE is extravesicular, where leakage from a neuron may be independent of functional activity in the nerve. Nevertheless, changes in neuron activity are reflected in changes in the rates of loss of MIBG from the heart. This was true when nerve traffic was increased by eating (Sisson et al. 1987*b*) or stimulated by the pharmacologic action of yohimbine (Sisson et al. 1990*b*) and when the nerve function was decreased by inhibition with clonidine (Sisson et al. 1990*b*).

The animal studies indicate that scintigraphic portrayal of uptake and retention (over hours) of [^{123}I]MIBG will identify healthy neurons in the heart, and injured or destroyed neurons will be depicted by diminished or absent uptake and retention. In addition, quantified changes in rates of loss of the radiopharmaceutical may provide an index of changes in nerve activity within that organ.

Studies in Human Subjects. As in dog hearts, [^{123}I]MIBG in the normal human myocardium appears to be homogeneously distributed throughout the walls of the left ventricle (Sisson et al. 1987*b*) (figure 3); the apical segments contain lesser quantities because there is less myocardium and diminished innervation (Pierpont et al. 1985). The nonneuronal component of MIBG in the human heart probably is reduced to low levels by 2 hours after injection (Sisson et al. 1987*b*).

Transplanted hearts are denervated, at least for many months, and, hence, represent a model in which neuronal function is absent. In such hearts, the uptake of MIBG, even at 1 hour, was virtually undetectable (Glowniak et al. 1989). Accordingly, generalized adrenergic neuropathies affecting the heart are associated with diminished concentrations of MIBG throughout most of the heart. However, the neuronal injuries may not be uniform (Sisson et al. 1987*b*). Uneven patterns of MIBG conceivably may define the heterogenous nature of neuronal injury and detect patterns that predict serious arrhythmias (Kahn et al.

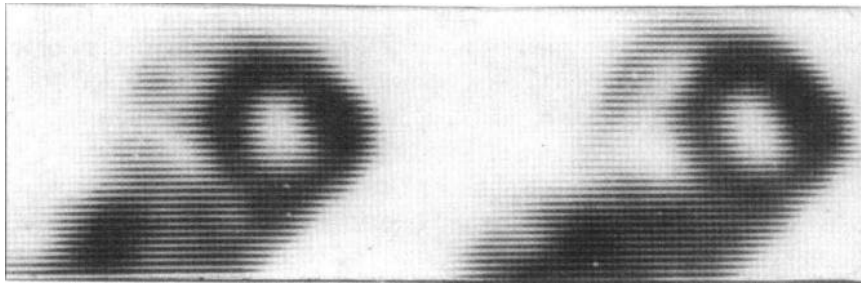

FIGURE 3. *Tomographic images of a normal volunteer 20 hours after injection of [^{123}I] MIBG. Left: short axis (oblique) slice through midheart; the left ventricle wall is most prominent, but activity can be seen in the right ventricle (to the left). Activity below is in the liver. Mid-oblique coronal slice showing left ventricle walls and apex; right ventricle is again seen. Right: oblique sagittal slice showing only left ventricle.*

1988). The rapid early egress of MIBG from the hearts of patients with autonomic neuropathy (Nakajo et al. 1985) may be the consequence of a greater proportion of the more transient, nonneuronal MIBG, or from neurons with a lesser capacity to retain MIBG, or both.

During heart failure, the adrenergic nervous system becomes dysfunctional, a state associated with diminished levels of NE in the myocardium (Chidsey et al. 1966; DeQuattro et al. 1973). However, the increase (Hasking et al. 1986) and decrease (DeQuattro et al. 1973) of the synthesis of NE in failing myocardium suggest that the identified abnormalities of neurons vary and possibly change during the course of the disease. Reports of cardiac uptake and retention of [^{123}I]MIBG in patients with heart failure caused by congestive cardiomyopathy have recorded differing results. When the concen-trations of MIBG were measured between 15 and 85 minutes after injection, the hearts of normal subjects showed no change, but those of patients with cardiomyopathy exhibited a significant loss of 25 percent (Henderson et al. 1988). In contrast, other investigators observed, by visual assessment of images, that patients with subnormal ejection fractions had low or absent levels of cardiac MIBG at 2 hours, but there was no appreciable

change over the next 4 hours (Schofer et al. 1988). Another group found, by quantifying the radiopharmaceutical in the heart, a sustained decline in concentrations of MIBG over a time period of from 1 to 16 hours and a more rapid loss in the patients with cardiomyopathy (Glowniak et al. 1989). Summarizing these reports indicates the probability that the rates of loss of MIBG from the cardiomyopathic heart are increased. This more rapid exit of MIBG possibly signifies an increased rate of loss of NE as well, but the concentrations of NE are low in these hearts (Schofer et al. 1988); thus, the total adrenergic nerve function, measured as the total NE secretion, may not be elevated. Moreover, it is possible that some of the effects occur because of neuron injury (perhaps ischemia), and the increase in rate of escape of MIBG and of NE loss occurs through a pathway unrelated to the physiologic activity of the nerves.

It is important to remember that generalized decreases in the uptake and retention of MIBG may be caused by a number of factors, some of which are not related directly to heart and nerve function. For example, elevated levels of catecholamines (Nakajo et al. 1983) and a variety of drugs (Sisson et al. 1987*b*; Khafagi et al. 1989) will diminish the uptake of MIBG by the heart.

[^{18}F]Metaraminol and [^{11}C]HED

Animal Validation. Extensive testing with [^{18}F]metaraminol and [^{11}C]HED has been carried out in animal models. To determine whether [^{18}F]metaraminol or [^{11}C]HED is actually stored in the vesicles of sympathetic nerve terminals, the retention of both tracers was assessed in the myocardial tissue of a second group of animals that had been pretreated with reserpine to inhibit vesicular storage. Reset-pine reduced the retention of [^{18}F]metaraminol and [^{11}C]HED by more than 70 percent, suggesting that the majority of the tracer is retained in the vesicles of the sympathetic nerve terminals. Furthermore, the tracer retention was reduced following treatment with 6-hydroxydopamine, which destroys sympathetic neurons in the heart (Wieland et al. 1990). The results of these pharmacological interventions confirmed that the nonneuronal binding of both tracers in myocardial tissue is very low.

An animal model with a short period of regional ischemia and subsequent reperfusion was used to demonstrate the sensitivity

of sympathetic neurons to ischemia (Schwaiger et al. 1990*a*). [^{18}F]Metaraminol was injected into an open-chest dog model, following a 30-minute occlusion of the left anterior descending artery, and tissue activity was determined 30 minutes after intravenous injection. Despite restoration of blood flow, [^{18}F]metaraminol retention in the reperfused myocardium was reduced significantly as compared with the control myocardium. These data confirmed previous observations that neuronal dysfunction can occur without myocardial necrosis. Tracers such as [^{18}F]metaraminol and [^{11}C]HED can be used to delineate the integrity of the neuronal uptake mechanism of catecholamines. Because NE is stored in the vesicles with a high concentration gradient, it is expected that this storage mechanism is sensitive to deprivation of oxygen and high-energy phosphates. Further longitudinal studies are needed to define the possible recovery of neuronal function following an ischemic injury.

Clinical Application. The only PET radiopharmaceutical available for the evaluation of the sympathetic nervous system in humans at the present time is [^{11}C]HED (Schwaiger et al. 1990*b*). Figure 4 shows [^{11}C]HED images obtained in a normal volunteer following intravenous injection of the tracer. These cross-sectional images through the left ventricle were obtained 40 minutes after injection and demonstrate the high image quality achievable with this tracer. Although [^{11}C]HED clears rapidly from blood, levels of the agent remain stable in the myocardium. The heart-to-blood ratio increases rapidly and averages at 5 minutes after injection more than 5:l. The retention of [^{11}C]HED is homogeneous throughout the left ventricle, reflecting the distribution of sympathetic nerve terminals in this organ. The findings in normal volunteers were compared with those obtained in patients with cardiac transplantation, which provides a unique clinical model of sympathetic denervation. [^{11}C]HED uptake in the left ventricle was reduced markedly in the transplant patients (figure 5). The relative retention of [^{11}C]HED was reduced by 76 percent in five patients with recent cardiac transplantation as compared with the control population. This indicates a relatively high specificity of [^{11}C]HED for the sympathetic nervous system in the human heart.

It is interesting to note that regional [^{11}C]HED uptake in patients with remote cardiac transplant showed a heterogeneous pattern. In particular, the basal aspects of the left ventricle appeared to extract [^{11}C]HED

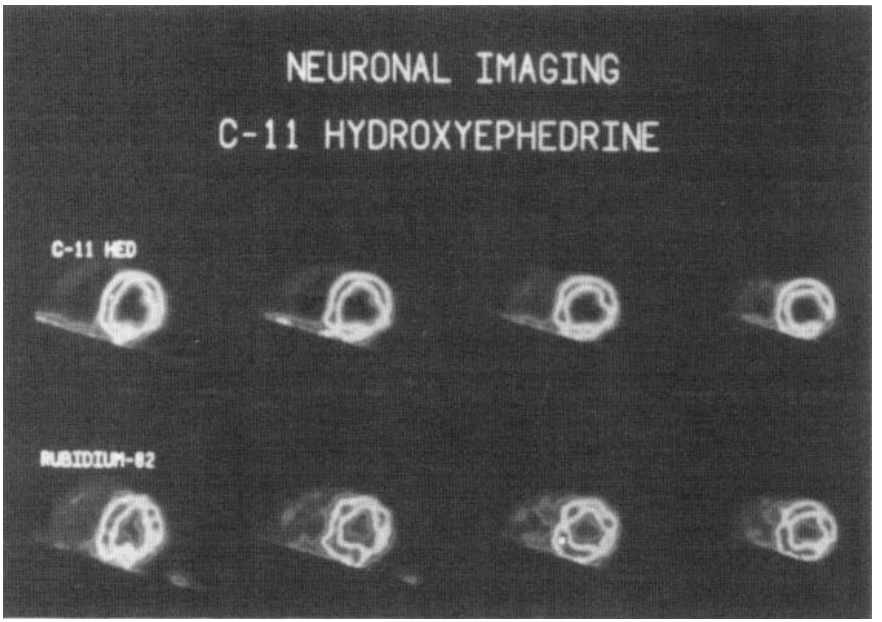

FIGURE 4. *Cross-sectional PET images obtained in normal volunteer 40 minutes following injection of [^{11}C]HED (above). Note the high contrast between myocardial and blood pool activity. For comparison, blood flow images with (^{82}Rb) are displayed below.*

to a greater extent than early after surgery. These data offered the first direct evidence of sympathetic reinnervation of the human cardiac transplant. Such reinnervation has been documented extensively in the animal model, but there is ongoing controversy about reinnervation in the human transplant (Schwaiger et al. 1990*c*).

Figure 6 shows a [^{11}C]HED study obtained in a patient with acute anterior myocardial infarction. This patient underwent thrombolytic therapy, and the [^{11}C]HED PET study was obtained within 3 days after the therapy. The blood flow images (^{82}Rb) indicate reduced blood flow in the anteroapical regions of the left ventricle. The [^{11}C]HED study clearly indicates a larger defect of tracer retention. The combined tracer approach using a blood flow tracer in [^{11}C]HED

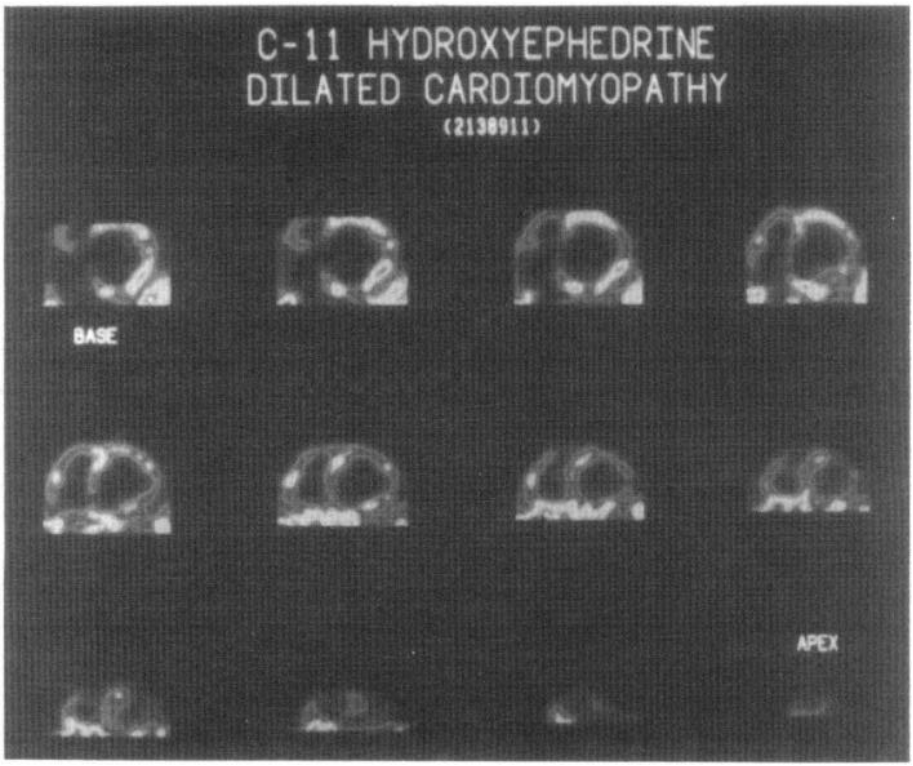

FIGURE 5. *[^{11}C]HED PET images obtained in a patient with dilated cardiomyopathy. Short-axis images from base (left upper row) to apex (right lower row) are displayed. The tracer distribution is heterogenous with an uptake gradient from base to apex of the left ventricle indicating nonuniform neuronal damage in patients with dilated cardiomyopathy.*

allows accurate delineation of neuronal dysfunction in relation to the infarct territory. Thus, [^{11}C]HED may be useful in the evaluation of neuronal integrity in patients with ischemic heart disease. Since heterogeneity of sympathetic tone has been linked to dysrhythmias in patients with ischemic heart disease, such an imaging approach may provide prognostic information for the identification of high-risk patients.

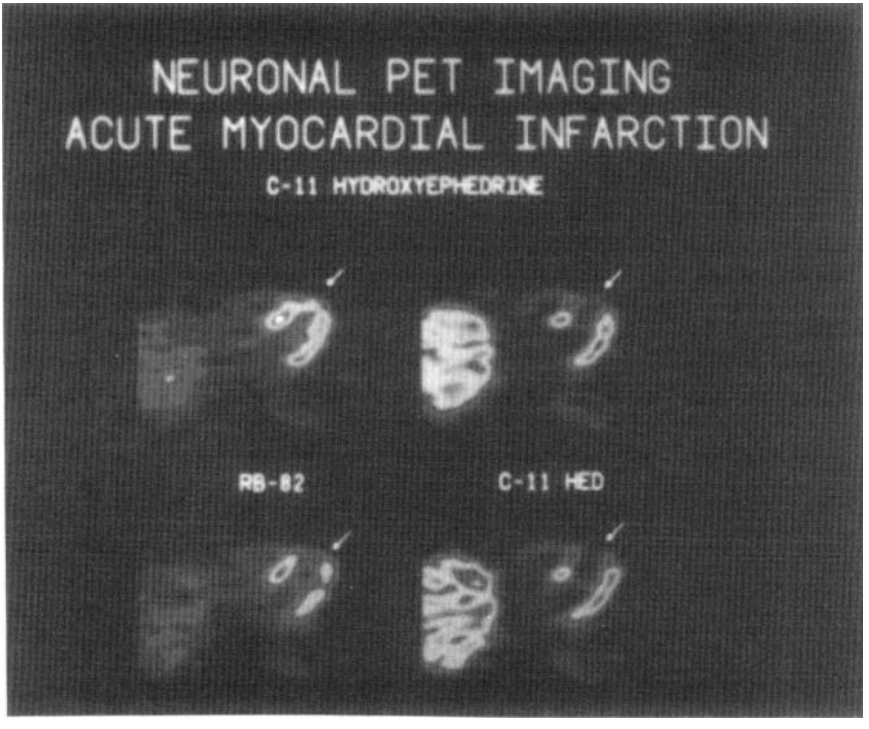

FIGURE 6. *[^{11}C]HED (right) and ^{82}Rb (left) images obtained in a patient with recent anterior myocardial infraction. The arrows indicate the flow and neuronal defect within the anterior wall. Please note the larger [^{11}C]HED defect suggesting neuronal dysfunction beyond the infarct area depicted by the flow tracer.*

As discussed above, alterations of the sympathetic system have been observed in patients with heart failure. Reduced cardiac-pump function leads to increased sympathetic tone involving high plasma NE levels and increased central stimulation of the cardiac sympathetic nerves. Because the reuptake and storage of NE in the presynaptic nerve terminals are important mechanisms to regulate NE content, the dysfunction of the nerve terminals may be an important pathophysiologic factor of the overexposure of the postsynaptic receptor sites to catecholamines. [^{11}C]HED allows assessment of the integrity of

presynaptic nerve terminals in these patients. Myocardial retention of [^{11}C]HED was quantified in patients with dilated cardiomyopathy. Figure 6 displays the [^{11}C]HED images in a patient with dilated cardiomyopathy. [^{11}C]HED retention is heterogeneously reduced with gradient from base to apex of left ventricle. The neuronal catecholamine storage capacity as assessed by quantitation of [^{11}C]HED tissue retention was reduced markedly in patients with cardiomyopathy, approaching values found in the denervated transplanted heart (Schwaiger et al. 1990*d*). The relatively large standard deviation of the measurements in patients with cardiomyopathy indicates a large variability of findings. These quantitative data obtainable by PET indicate that the presynaptic uptake of catecholamines is altered severely in patients with cardiomyopathy; this may affect the reuptake of extraneuronal NE by sympathetic nerve terminals and, hence, result in an overexposure of myocytes to NE. This hypothesis is supported by recent findings that indicate a beneficial effect of ß-receptor blockade in patients with congestive heart failure (Waagstein et al. 1989). Thus, the quantitative delineation of the sympathetic nervous function in such patients by PET may aid in the selection of individuals for therapy with ß-receptor blockers and enhance understanding of the cardiac sympathetic nervous system in patients with dilated cardiomyopathy.

The Effect of Cocaine on [^{11}C]HED Kinetics

Cocaine has well-documented cardiotoxicity. Acute exposure to this drug results in coronary vasoconstriction, which together with increased oxygen demand may lead to myocardial ischemia. Although the pharmacology of cocaine is well described, little is known about its direct effect on cardiac neurons. Imaging approaches using [^{11}C]HED allow the investigation of the pharmacokinetics of cocaine on the uptake of catecholamines in the sympathetic nerve terminal. Preliminary results by Melon and colleagues from the authors' institution demonstrate the marked reduction of [^{11}C]HED uptake in the canine heart following intravenous injection. The effect of one injection is sustained for several hours (Melon et al. 1992). These studies suggest that PET may be uniquely suited to define the time course and intensity of drug effects on cardiac sympathetic neurons. Future studies in human drug abuse may define possible alterations of sympathetic innervation following chronic drug abuse.

REFERENCES

Anton, A., and Berk, A. Distribution of metaraminol and its relation to norepinephrine. *Eur J Pharmacol* 44:161-167, 1977.

Axelrod, J. The fate of adrenaline and noradrenaline. In: Vane, J.; Wolstenholme, G.; and O'Connor, M., eds. *Adrenergic Mechanisms.* Boston: Little, Brown, 1960. pp. 28-39.

Barber, M.; Mueller, T.; Davies, B.; and Zipes, D. Phenol topically applied to canine left ventricular epicardium interrupts sympathetic but not vagal afferents. *Circ Res* 55:532-544, 1984.

Bristow, M.; Ginsburg, R.; Minobe, W.; Cubicciotti, R.S.; Sageman, W.S.; Lurie, K.; Billingham, M.E.; Harrison, D.C.; and Stinson, E.B. Decreased catecholamine sensitivity and beta-adrenergic receptor density in failing human hearts. *N Engl J Med* 307: 205-211, 1982.

Carlsson, E.; Dahof, C.; and Hedberg, A. Differentiation of cardiac chronotropic and inotropic effects of beta-adreno-ceptor angonists. *Naunyn Schmiedebergs Arch Pharmacol* 300:101-106, 1977.

Chidsey, C.; Sonnenblick, E.; Morrow, A.; and Braunwald, E. Norepinephrine stores and contractile force of papillary muscle from failing human heart. *Circulation* 33:43-51, 1966.

Dae, M.; O'Connell, J.; Botvinick, E.; Aheam, T.; Yee, E.; Huberty, J.; Mori, H.; Chin, M.; Hattner, R.; Herre, J.; and Munoz, L. Scintigraphic assessment of regional cardiac adrenergic innervation. *Circulation* 79:634-644, 1989.

De Champlain, J., and Nadeau, R. 6-Hydroxydopamine, 6-hydroxy-dopa, and degeneration of adrenergic nerves. *Fed Proc* 30:877-885, 1971.

DeQuattro, V.; Nagatsu, T.; Mendez, A.; and Verska, J. Determinants of cardiac noradrenaline depletion in human congestive failure. *Cardiovasc Res* 7:344-350, 1973.

Eisenhofer, G.; Hovevey-Sion, D.; Kopin, I.; Miletich, R.; Kirk, K.; Finn, R.; and Goldstein, D. Neuronal uptake and metabolism of 2- and 6-fluorodopamine: False neurotransmitters for positron emission tomographic imaging of sympathetically innervated tissues. *J Pharmacol Exp Ther* 248:419-427, 1989.

Fowler, J.; Wolf, A.; Cristman, R.; MacGregor, R.; Ansari, A.; and Atkins, H. Carrier-free 11C-labeled catecholamines. In: Subramanian, G.; Rhodes, B.; Cooper, J.; and Sodd, V., eds. *Radiopharmaceuticals.* New York: Society of Nuclear Medicine, *1975.* pp. 196-204.

Francis, G. Modulation of peripheral sympathetic nerve transmission. *J Am Coll Cardiol* 12:250-254, 1988.

Gasnier, B.; Roisin, M.; Scherman, D.; Coornaert, S.; Desplanches, G.; and Henry, J. Uptake of metaiodobenzylguanidine by bovin chromaffin granule memberances. *Mol Pharmacol* 29:275-280, 1986.

Geatti, O.; Shapiro, B.; Sisson, J.; Hutchinson, R.; Mallette, S.; Eyre, P.; and Beierwaltes, W. 131-Metaiodobenzylguanidine (131-I-MIBG) scintigraphy for the location of neuroblastoma: Preliminary experience in 10 cases. *J Nucl Med* 26:736-742, 1985.

Glowniak, J.; Turner, F.; Gray, L.; Palac, R.; Lagunas-Solar, M.; and Woodward, W. Iodine- 123 metaiodobenzylguanidine imaging of the heart in idiopathic congestive cardiomyopathy and cardiac transplants. *J Nucl Med* 30:1182-1191, 1989.

Goldstein, D. Plasma norepinephrine as an indicator of sympathetic neural activity in clinical cardiology. *Am J Cardiol* 48:1147, 1981.

Goldstein, D.; Brush, J., Jr.; Eisenhofer, G.; Stull, R.; and Esler, M. In vivo measurement of neuronal uptake of norepinephrine in the human heart. *Circulation* 78:41-48, 1988.

Goldstein, D.; Chang, P.; Eisenhofer, G.; Miletich, R.; Finn, R.; Bather, J.; Kirk, K.; Bacharach, S.; and Kopin, I. Positron emission tomographic imaging of cardiac sympathetic innervation and function. *Circulation* 81:1606-1621, 1990.

Hasking, G.; Esler, M.; Jennings, G.; Burton, D.; and Korner, P. Norepinephrine spillover to plasma in patients with congestive heart failure: Evidence of increased overall and cardiorenal sympathetic nervous activity. *Circulation* 73:615-621, 1986.

Henderson, E.; Kahn, J.; Corbett, J.; Jansen, D.; Pippin, J.; Kulkami, P.; Ugolini, V.; Akers, M.; Hansen, C.; Buja, L.; Parkey, R.; and Willerson, J. Abnormal I-123 metaiodobenzylguanidine myocardial washout and distribution may reflect myocardial adrenergic derangement in patients with congestive cardiomyopathy. *Circulation* 78:1192-1199, 1988.

Hertting, G.; Axelrod, J.; Kopin, J.; and Whitby, L. Effect of drugs on the uptake and metabolism of H3-norepinephrine. *J Pharmacol Exp Ther* 134:146-153, 1961.

Hoefnagel, C.; Voute, P.; de Kraker, J.; and Marcuse, H. Radionuclide diagnosis and therapy of neural crest tumors using iodine-131 metaiodobenzylguanidine. *J Nucl Med* 28:308-314, 1987.

Jaques, S., Jr., and Tobes, M. Comparison of the secretory mechanisms of metaiodobenzylguanidine (MIBG) and norepinephrine (NE) from cultured bovin adrenomedullary cells. *J Nucl Med* 26:17, 1985.

Jaques, S., Jr.; Tobes, M.; Sisson, J.; Baker, J.; and Wieland, D. Comparison of the sodium dependency of uptake of meta-iodobenzylguanidine and norepinephrine into cultured bovin adrenomedullary cells. *Mol Pharmacol* 26:539-546, 1984.

Kahn, J.; Sisson, J.; and Vinik, A. Prediction of sudden cardiac death in diabetic autonomic neuropathy. *J Nucl Med* 29:1605-1606, 1988.

Khafagi, F.; Shapiro, B.; Fig, L.; Mallette, S.; and Sisson, J. Labetalol reduces iodine-131 MIBG uptake by pheochromocytoma and normal tissues. *J Nucl Med* 30:481-489, 1989.

Kline, R.; Swanson, D.; and Wieland, D. Myocardial imaging in man with I- 123 meta-iodobenzylguanidine. *J Nucl Med* 22:129-132, 1981.

Lefkowitz, R., and Caron, M. Adrenergic receptors. *J Biol Chem* 263:4993-4996, 1988.

Levitt, M.; Spector, S.; Sjoerdsma, A.; and Udenfriend, S. Elucidation of the rate-limiting step in norepinephrine biosynthesis in the perfused guinea-pig heart. *J Pharmacol Exp Ther* 148:1, 1965.

Melon, P.; DeGrado, T.; Nguyen, N.; Tooronigian, S.; Hutchins, G.; and Schwaiger, M. Noninvasive assessment of regional myocardial sympathetic neuronal function following intravenous cocaine injection in dogs. *J Nucl Med* 33:994, 1992.

Minardo, J.; Tuli, M.; Mock, B.; Weiner, R.; Pride, H.; Wellman, H.; and Zipes, D. Scintigraphic and electrophysiological evidence of canine myocardial sympathetic denervation and reinnervation produced by myocardial infarction or phenol application. *Circulation* 78:1008-1019, 1988.

Nakajo, M.; Shapiro, B.; and Glowniak, J. Inverse relationship between cardiac accumulation of meta-[131I]-iodobenzylguanidine (I-131-MIBG) and circulating catecholamines in suspected pheochromocytoma. *J Nucl Med* 24:1127-1134, 1983.

Nakajo, M.; Shimabukuro, K.; Miyaji, N.; Shimada, J.; Shirono, K.; Sakata, H.; Yoshimura, H.; Yonekura, R.; and Shinohara, S. Rapid clearance of iodine- 13 1 MIBG from the heart and liver of patients with adrenergic dysfunction and pheochromocytoma. *J Nucl Med* 26:357-365, 1985.

Pierpont, G.; DeMaster, E.; Reynolds, S.; Pederson, J.; and Cohn, J. Ventricular myocardial catecholamines in primates. *J Lab Clin Med* 106:205-210, 1985.

Rosenspire, K.; Kaka, M.; Jewett, D.; Van Dort, M.; Gildersleeve, D.; Schwaiger, M.; and Wieland, D. Synthesis and preliminary evaluation of [11C]meta-hydroxyephedrine: A false transmitter agent for heart neuronal imaging. *J Nucl Med* 31:163-167, 1990.

Schafer, J.; Speilmann, R.; Schuchert, A.; Weber, K.; and Schlüter, M. Iodine-123 meta-iodobenzylguanidine scintigraphy: A noninvasive method to demonstrate myocardial adrenergic nervous system disintegrity in patients with idiopathic dilated cardiomyopathy. *J Am Cull Cardiol* 12:1252-1258, 1988.

Schwaiger, M.; Guibourg, H.; Rosenspire, K.; McClanahan, T.; Gallagher, K.; Hutchins, G; and Wieland, D. Effect of regional myocardial ischemia on sympathetic nervous system as assessed by F-18 metaraminol. *J Nucl Med* 31(8):1352-1357, 1990*a*.

Schwaiger, M.; Hutchins, G.; Kalff, V.; Molina, E.; Rosenspire, K.; Haka, M.; Deeb, M.; and Wieland, D. Evidence of regional reinnervation of cardiac transplants by neuronal PET imaging. *J Am Coll Cardiol* 15:224, 1990*c*.

Schwaiger, M.; Hutchins, G.; Rosenspire, K.; Haka, M.; and Wieland, D. Quantitative evaluation of the sympathetic nervous system by PET in patients with cardiomyopathy. *J Nucl Med* 31:792, 1990*d*.

Schwaiger, M.; Kalff, V.; Rosenspire, K.; Haka, M.; Molina, E.; Hutchins, G.; Deeb, M.; Wolfe, E., Jr.; and Wieland, D. The noninvasive evaluation of the sympathetic nervous system in the human heart by PET. *Circulation* 82:457-464, 1990*b*.

Shapiro, B.; Copp, J.; Sisson, I.; Eyre, P.; Wallis, J.; and Beierwaltes, W. Iodine-131 metaiodobenzylguanidine for the locating of suspected pheochromocytoma: Experience in 400 cases. *J Nucl Med* 26:576-585, 1985.

Sisson, J.; Bolgos, G.; and Johnson, I. Measuring acute changes in adrenergic nerve activity in the living animal. *Am Heart J* 121:1119-1123, 1990*b*.

Sisson, J.; Frager, M.; Valk, T.; Gross, M.; Swanson, D.; Wieland, D.; Tobes, M.; Beierwaltes, W.; and Thompson, N. Scintigraphic localization of pheochromocytoma. *N Engl J Med* 305:12-17, 1981.

Sisson, J.; Johnson, J.; Bolgos, G.; Lynch, J.; Uprichard, A.; Driscoll, E.; Wieland, D.; and Lucchesi, B. Portrayal of adrenergic denervation in the presence of myocardial infarction: A feasibility study. *Am J Physiol Imaging* 5:151-166, 1990*a*

Sisson, J.; Lynch, J.; Johnson, J.; Jaques, S., Jr.; Wu, J.-L.; Bolgos, G.; Lucchesi, B.; and Wieland, D. Scintigraphic detection of regional disruption of adrenergic neurons in the heart. *Am Heart J* 116:67-76, 1988.

Sisson, J.; Shapiro, B.; Meyers, L.; Mallette, S.; Mangner, T.; Wieland, D.; Glowniak, J.; Sherman, P.; and Beierwaltes, W. Metaiodo-benzylguanidine to map scintigraphically the adrenergic nervous system in man. *J Nucl Med* 28:1625-1636, 19876.

Sisson, J.; Wieland, D.; Sherman, P.; Mangner, T.; Tobes, M.; and Jaques, S., Jr. Metaiodobenzylguanidine as an index of the adrenergic nervous system integrity and function. *J Nucl Med* 28:1620-1624, 1987*a.*

Stiles, G.; Taylor, S.; and Lefkowitz, R. Human cardiac beta-adrenergic receptors: Subtype heterogeneity delineated by direct radioligand binding. *Life Sci* 33:467-473, 1983.

Syrota, A. Positron emission tomography: Evaluation of cardiac receptors. In: Marcus, M.L.; Skorton, D.J.; Schelbert, H.R.; and Wolf, G.L., eds. Braunwald, E., consulting ed. *Cardiac Imaging: A Companion of Braunwald's Heart Disease.* Philadelphia: W.B. Sanders, 1990. pp. 1256-1270.

Waagstein, F.; Caidahl, K.; Wallentin, I.; Bergh, C-H.; and Hjalmarson, A. Long-term B-blockade in dilated cardiomyopathy: Effects of short- and long-term metoprolol treatment followed by withdrawal and readministration of metoprolol. *Circulation* 80:551-563, 1989.

Wieland, D.; Brown, L.; Rogers, W.; Worthington, K.; Wu, J.-L.; Clinthorne, N.; Otto, C.; Swanson, D; and Beierwaltes, W. Myocardial imaging with a radioiodinated norepinephrine storage analog. *J Nucl Med* 22:22-31, 1981*a*.

Wieland, D.; Brown, L.; Rogers, W.; Worthington, K.; Wu, J.-L.; Clinthome, N.; Otto, C.; Swanson, D.; and Beierwaltes, W. Myocardial imaging with a radioiodinated norepinephrine storage analog. *J Nucl Med* 24:1127-1134, 1983.

Wieland, D.; Brown, L.; Tobes, M.; Rogers, W.; Marsh, D.; Mangner, T.; Swanson, D.; and Beierwaltes, W. Imaging the primate adrenal medulla with [123] and [131] metaiodobenzylguanidine: Concise communication. *J Nucl Med* 22:358-364, 1981*b*.

Wieland, D.; Rosenspire, K.; Hutchins, G.; Van Dort, M.; Rothley, J.; Mislankar, S.; Lee, H.; Massin, C.; Gildersleeve, D.; Sherman, P.; and Schwaiger, M. Neuronal mapping of the heart with 6-[18F]fluorometaraminol. *J Med Chem* 33:956-964, 1990.

Wolpers, H.; Nguyen, N.; Rosenspire, K.; Haka, M.; Wieland, D.; and Schwaiger, M. C-11 hydroxyephedrine as marker for neuronal dysfunction in reperfused canine myocardium. *Coronary Artery Dis* 2:923-929, 1990.

ACKNOWLEDGMENTS

This work was done during the tenure of an established investigatorship from the American Heart Association and also was supported in part by National Institutes of Health grants R01 HL41047-01 and R01 HL27555-06.

AUTHORS

Markus Schwaiger, M.D.
Professor of Internal Medicine
and
Director
Cardiovascular Nuclear Imaging
University of Michigan Medical Center
UH B1G505, Box 0028
1500 East Medical Center Drive
Ann Arbor, MI 48109-0028

James C. Sisson, M.D.
Professor of Internal Medicine
and
Associate Chief
Clinical Nuclear Medicine

Donald Wieland, M.D.
Professor of Internal Medicine and Research Scientist
and
Director
Radiopharmaceutical Chemistry

Division of Nuclear Medicine
Department of Internal Medicine
University of Michigan Medical Center
Ann Arbor, MI 48109

Development of PET/SPECT Ligands for the Serotonin Transporter

Ursula Scheffel, Robert F. Dannals, Makiko Suehiro, George A. Ricaurte, F. Ivy Carroll, Michael J. Kuhar, and Henry N. Wagner, Jr.

INTRODUCTION

There is clear evidence in rodents and nonhuman primates that the widely abused "designer" drug, 3,4-methylenedioxymethamphetamine (MDMA, "ecstasy"), causes loss of central serotonergic (5-hydroxytryptamine [5-HTJ]) neurons (Commins et al. 1986; Ricaurte et al. 1988*a*). Doses of MDMA that approximate those typically taken by humans have been shown to be toxic to serotonergic nerve fibers in the monkey brain (Ricaurte et al. 1988*b*; Slikker et al. 1988). Of similar or greater concern are neurochemical studies showing that the anorectic agent fenfluramine causes serotonergic damage in rodents as well as in primates (Harvey et al. 1975; Schuster et al. 1986). Currently, fenfluramine is a clinically prescribed drug in both the United States and Europe. It is used to treat obesity with doses that closely approach those that produce neurotoxic effects in animals (0.2 to 2.0 mg/kg). At this time, it is not known whether regeneration of 5-HT neurons occurs in nonhuman primates and, if so, what the timeframe for recovery is.

Long-term neurotoxic damage caused by MDMA and fenfluramine appears to be restricted to the presynaptic element of the serotonergic nerve fiber. Recent investigations on the effect of MDMA on postsynaptic 5-HT_2 receptors in the rat brain have shown that, although there is an initial down-regulation of these postsynaptic receptors, it is of short duration. Approximately 1 week after administration of MDMA (eight subcutaneous injections [20 mg/kg], twice daily for 4 days), the number of 5-HT_2-ligand binding sites returns to control levels (Scheffel et al. 1992*a*). In contrast, 5-HT uptake sites, located

on presynaptic nerve endings in the rat brain, recover very slowly after MDMA treatment: their number remains decreased for up to 12 months (Battaglia et al. 1988*a*).

Several methods have been employed to test for serotonin neurotoxicity in humans, including measurement of the serotonin metabolite 5-hydroxyindoleacetic acid in cerebrospinal fluid (Moir et al. 1970) and endocrine challenge using intravenously administered L-tryptophane (Heninger et al. 1984). All these tests are indirect and cannot accurately reflect the state of the central serotonergic neuron. Therefore, a presynaptic marker is needed to indicate serotonergic neurotoxicity in the living human brain.

This chapter describes work performed in the authors' laboratories in the development and in vivo testing of radiolabeled ligands for the serotonin uptake site suitable for single photon emission computed tomography (SPECT) or positron emission tomography (PET) imaging. Several compounds with known in vitro affinity for the 5-HT uptake site were labeled with [^{123}I] for SPECT studies or with either [^{11}C] or [^{18}F] for investigations using PET. The radiotracers were characterized in rodents for their in vivo kinetics, distribution, and specificity of binding to the 5-HT uptake site.

PAROXETINE, N-[^{11}C]METHYL PAROXETINE, AND [^{18}F]FLUOROALKYLATED PAROXETINE ANALOGS

Paroxetine, first described in the late 1970s (Petersen et al. 1977; Buus Lassen 1978), is an antidepressant drug with high affinity and selectivity for the 5-HT uptake site in platelets and presynaptic neurons in the central nervous system (CNS) (Habert et al. 1985; Marcusson et al. 1988). In its tritiated form, paroxetine has been used to characterize the binding to the 5-HT uptake site (Mellerup et al. 1983; Mellerup and Plenge 1986) and to determine the density and distribution of 5-HT uptake sites in the rat and human brain (Battaglia et al. 19886; Cortes et al. 1988).

Studies by Scheffel and Hartig (1989) indicated that [^{3}H]paroxetine is a potent and selective agent for in vivo labeling of cerebral serotonin uptake sites. Furthermore, Scheffel and Ricaurte (1990) demonstrated

that paroxetine can serve as an in vivo indicator of MDMA neurotoxicity. They concluded that labeling paroxetine with [^{11}C] ($t_{1/2}$ = 20 min) or [^{18}F] ($t_{1/2}$ = 110 min) would yield a useful PET tracer for imaging and quantitating 5-HT uptake sites in the CNS of living mammals and humans, However, introduction of a positron emitter label into the authentic paroxetine molecule has not been accomplished yet.

Several analogs of paroxetine that could be labeled more easily with [^{11}C] or [^{18}F] than authentic paroxetine were prepared (Villemagne et al. 1989; Suehiro et al. 1991). However, in vitro binding assays demonstrated a considerable loss of affinity of these analogs: N-(methyl) paroxetine displaced [^{3}H]paroxetine binding to 5-HT uptake sites 25 times less potently than authentic paroxetine; N-(3-fluoroethyl) and N-(3-fluoropropyl) paroxetine had 424 and 1,220 times lower potencies, respectively (table 1).

TABLE 1. *Potencies of paroxetine and analogs in inhibiting [^{3}H]paroxetine binding to 5-HT uptake sites in rat cortical homogenates. K_i values are means of four assays performed in triplicate.*

Inhibitor	K_i(M)
Paroxetine*	5.9×10^{-11}
N-(methyl) paroxetine†	1.5×10^{-9}
N-(2-fluoroethyl) paroxetine*	2.5×10^{-8}
N-(3-fluoropropyl) paroxetine*	7.2×10^{-8}

SOURCE: *Suehiro et al. 1991; †Plenge et al. 1987

Similar results were obtained in in vivo studies using N-([^{11}C]methyl) paroxetine and N-(3-[^{18}F]fluoropropyl) paroxetine (figure 1). After intravenous (IV) injection of these high specific activity tracers into mice, the radioactivity concentrations in different areas of the brain were measured by dissecting the brain regions and weighing and counting the tissue samples. Ratios of the radioactivities in the hypothalamus, an area known to contain high densities of 5-HT uptake

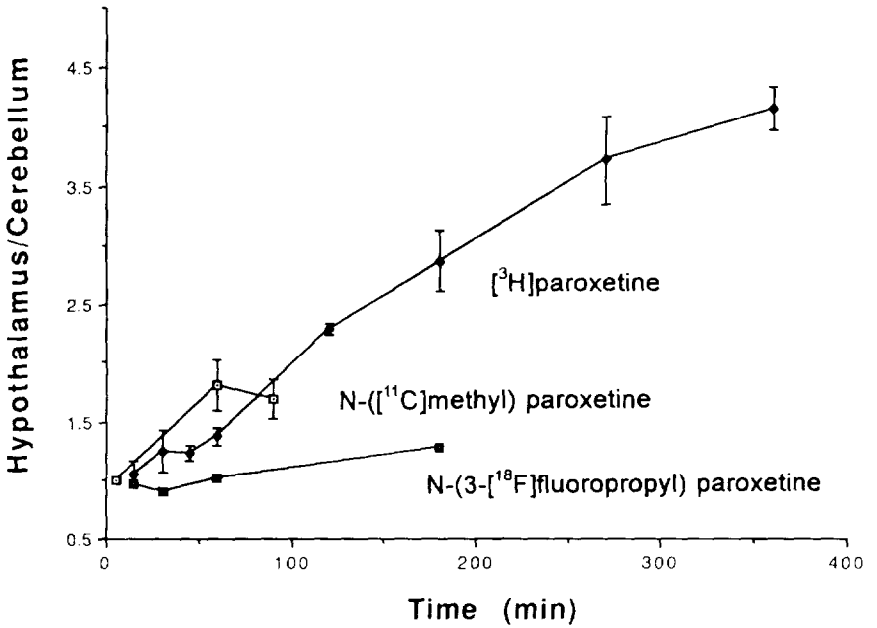

FIGURE 1. *Comparison of the in vivo binding of [^{3}H]paroxetine with that of its analogs, N-([^{11}C]methyl) paroxetine and N-(3-[^{18}F]fluoropropyl) paroxetine. Time course of hypothalamus to cerebellar radioactivity ratios in the mouse brain.*

KEY: ♦ = [^{3}H]paroxetine; ❑ =N-([^{11}C]methyl) paroxetine; ■ = N-(3-[^{18}F]fluoropropyl) paroxetine

sites, and in the cerebellum, a region relatively devoid of binding sites, were calculated to estimate total/nonspecific binding. With N-([^{11}C]methyl) paroxetine, the highest hypothalamus-to-cerebellar ratio was 1.8:1 at 60 min after administration. For N-(3-[^{18}F]fluoropropyl) paroxetine, the hypothalamus-to-cerebellar ratio climbed to only 1.3:1 at 3 hours after injection. Ratios for [^{3}H]paroxetine (Scheffel and Hartig 1989) were plotted for comparison.

Attempts to derivatize paroxetine for SPECT have been made. Mathis and coworkers (1991) recently reported on several iodinated paroxetine

analogs, of which (±)-2'-[^{125}I]iodo paroxetine appeared to be the most promising. However, subsequent in vivo experiments showed that this tracer penetrated the blood-brain barrier rather poorly, and nonspecific binding was too high for the tracer to be useful for SPECT studies.

[^{11}C]CITALOPRAM, [^{11}C]FLUOXETINE, AND CIS-[^{11}C]DDPI

Citalopram, fluoxetine, and cis-N,N,-dimethyl-3-(2',4'-dichlorophenyl)-indanamine (cis-DDPI) are known to be potent and selective serotonin uptake site blockers (Hyttel 1982; Fuller and Wong 1977; Bogeso et al. 1985). These compounds were radiolabeled with [^{11}C] to assess their potential use as PET ligands.

[^{11}C]Citalopram, [^{11}C]fluoxetine, and cis-[^{11}C]DDPI were synthesized from their respective precursors and [^{11}C]iodomethane (Dannals et al. 1990; Kilboum 1988; Suehiro et al. 1992*a)*. The biological activity of these compounds was studied in mice (Scheffel et al. 1990; Suehiro et al. 1992*a*). [^{11}C]Citalopram, [^{11}C]fluoxetine, and cis-[^{11}C]DDPI penetrated the blood-brain barrier well with 1.3, 3.1, and 3.6 percent of the injected dose (%D), respectively, in the whole mouse brain at 15 min after IV injection.

As shown in figure 2, [^{11}C]fluoxetine did not exhibit any specific binding to 5-HT uptake sites during the time of observation (15 to 90 min after injection). At no time after administration did [^{11}C]fluoxetine distribution agree with that of 5-HT uptake site densities, nor did preinjection of the high-affinity uptake site blocker paroxetine (1 mg/kg) cause any inhibition of the accumulation of the tracer. The reasons for the failure of [^{11}C]fluoxetine to bind to 5-HT uptake sites in vivo are unknown. However, it is possible that metabolism of the radioligand occurred before specific binding in the CNS could take place. Conversely, cis-[^{11}C]DDPI showed specific accumulation in areas rich in 5HT uptake sites (e.g., the hypo-thalamus, olfactory tubercles, and prefrontal cortex). This binding could be blocked 60 to 80 percent by preinjection of 1 mg paroxetine/ kg bodyweight. However, because nonspecific binding was high and the clearance of this nonspecifically bound fraction was slow, the ratio between total to nonspecific binding reached only 1.4:1 at 60 to 90 min after injection (figure 2).

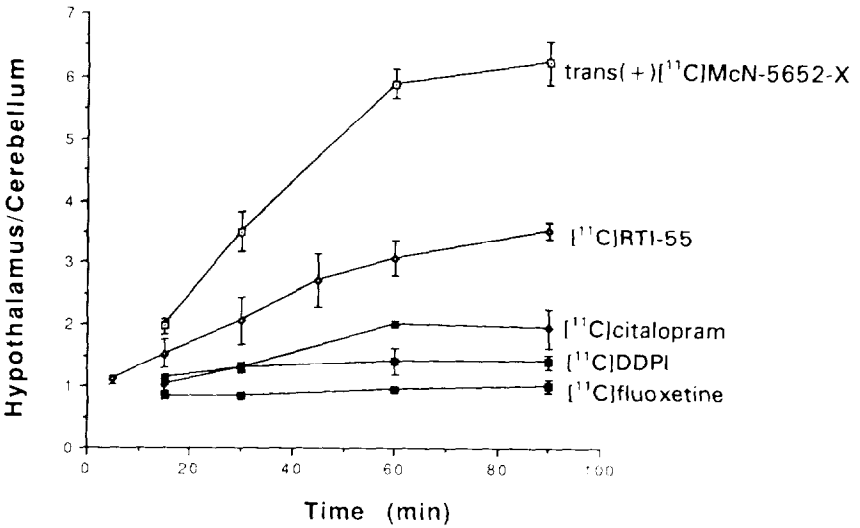

FIGURE 2. *Hypothalamus-to-cerebellar ratios of [^{11}C] concentrations at different times afer IV injection of 300 to 500 μCi of either [^{11}C]fluoxetine, cis-[^{11}C]DDPI, [^{11}C]citalopram, [^{11}C]RTI-SS, or trans(+)[^{11}C]McN-5652-X into mice weighing 25 to 35 g. The specific activity at time of injection of each of the tracers was approximately 3,000 mCi/μmol. Data are means ±1 standard deviation, and n = 3 to 4 mice for each time point.*

[^{11}C]Citalopram was the most promising of the three candidate ligands. Hypothalamus-to-cerebellar ratios rose to 2.0:1 at 60 min (figure 2). Regional [^{11}C]citalopram distribution at this time was in agreement with 5-HT uptake site densities, and preadministration of a blocking dose of paroxetine did significantly inhibit tracer binding. Although these results were encouraging, the ratios between specific and nonspecific binding were not high enough to guarantee successful imaging of 5-HT uptake sites by PET.

TRANS(±)[^{11}C]McN-5652-Z AND (+)[^{11}C]McN-5652-X

Trans(±)McN-5652-Z was described by Shank and colleagues (1968) as a highly potent serotonin uptake inhibitor. In addition, several stereoisomers of this compound were isolated and tested for their binding to presynaptic monoaminergic neurotransmitter uptake sites (Shank et al. 1968). Trans(±)McN-5652-X was shown to exhibit the highest affinity toward the 5-HT uptake site (K_i for inhibition of [^{3}H]5-HT = 0.4 nM), followed by trans(±)McN-5652-X (K_i = 0.6 nM) and cis McN-5655 (K_i = 16.6 nM); the trans(-)McN-5652-W isomer was approximately 150 times less potent (K_i = 58.4 nM) than the corresponding (+) isomer. All these compounds showed moderate in vitro affinity for the norepinephrine (NE) uptake site (i.e., five times lower than for the 5-HT uptake site) and little or no affinity for the dopamine (DA) uptake site.

Trans(±)McN-5652-Z trans(+)McN-5652-X, trans(-)McN-5652-W, and cis McN-5655-Z were labeled recently with [^{11}C] (Suehiro et al. 1992*b,* in press). The synthesis of these tracers was performed by S-methylation of the respective precursors with [^{11}C]iodomethane. The specific activity determined at the end of synthesis ranged from 3,300 to 4,250 mCi/μmol.

As shown in figure 2, [^{11}C]McN-5652-X, the trans(+) isomer, far exceeded all previously tested radioligands in specific binding to the 5-HT transporter in the mouse brain. Ratios between hypothalamus and cerebellar radioactivity concentrations reached 5.9:1 and 6.2:1, respectively, at 60 and 90 min after IV injection of the tracer. In contrast, [^{11}C]McN-5652-W, the trans(-) isomer, displayed little specific binding. For this compound, the ratio of the radioactivity concentration in the hypothalamus to the nonspecifically bound radioactivity concentration in the cerebellum was 1.3:l at 60 min and 1.9:1 at 90 min after administration.

[^{11}C]McN-5652-Z, the racemic (±) mixture of the optical isomers (+) and (-) [^{11}C]McN-5652, was prepared to study the selectivity of in vivo binding to the 5-HT uptake site in the mouse model. Blocking doses of drugs known to bind to specific monoamine neurotransmitter sites were injected intravenously 5 min before tracer injection. Tissue-to-cerebellar radioactivity ratios in different brain regions were deter-

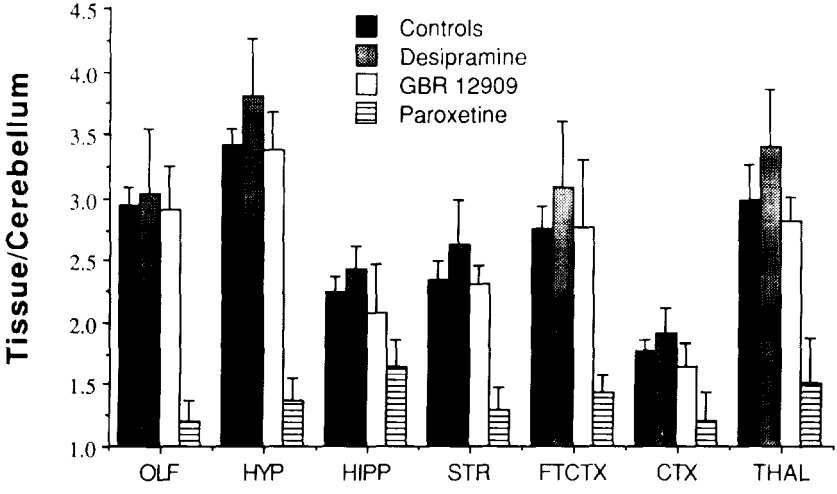

FIGURE 3. *Effect of blocking doses (5 mg/kg) of paroxetine (specific for the 5-HT uptake site), GBR 12909 (DA uptake site), and desipramine (NE uptake site) on [^{11}C]McN-5652-Z binding. The drugs were injected intravenously 5 minutes before administration of the tracer. Tissue-to-cerebellar ratios were determined 60 minutes after tracer injection. Data are means ±1 standard deviation (n = 4).*

KEY: OLF = olfactory tubercles; HYP = hypothalamus; HIPP = hippocampus; STR = striatum; FTCTX = prefrontal cortex; CTX = cortex; THAL = thalamus

SOURCE: Suehiro et al. 1993. Copyright 1993 by Society of Nuclear Medicine.

mined 60 min after tracer injection and compared with those of saline-injected controls. The results of these studies are shown in figure 3.

Paroxetine (5 mg/kg) significantly decreased the specific binding of [^{11}C]McN-5652-Z in all areas examined. In contrast, GBR 12909, a DA uptake site-specific drug, and desipramine, which blocks the NE

uptake sites, had no effect. The results indicate that [^{11}C]McN-5652-Z is a highly selective in vivo label for the serotonin transporter.

The ability of [^{11}C]McN-5652-Z to detect serotonergic damage in the CNS was shown in rats lesioned with the known 5-HT neurotoxin 5,7-dihydroxytryptamine (5,7-DHT) (200 µg 5,7-DHT in 10 µL 0.01 percent ascorbic acid, injected intracerebroventricularly after NE uptake sites were blocked by pretreatment of the animals with desipramine [25 mg/kg, IV]) 13 days before the tracer study. [^{11}C]McN-5652-Z was injected intravenously 60 min before sacrifice of the animals. As shown in figure 4, specific [^{11}C]McN-5652-Z binding (expressed as %D/g tissue minus %D/g in cerebellum) was reduced by 50 to 90 percent in different brain regions of the 5,7-DHT lesioned rats. Moreover, the regional decreases in [^{11}C]McN-5652-Z binding after 5,7-DHT treatment corresponded with those observed using [^{3}H]paroxetine as the in vivo indicator. These results indicate that [^{11}C]McN-5652-Z can be used to quantify the extent of serotonergic damage.

[^{125}I]-RTI-55 AND [^{11}C]-RTI-55

Recently, several cocaine analogs have been synthesized, radiolabeled, and tested for their in vitro and in vivo affinities for monoaminergic neurotransmitter uptake sites. (For a recent overview of this work, see Boja et al. 1992*a*). Of these compounds, [$^{123/125}$I] 2ß-carbomethoxy-3ß-(4-iodophenyl)tropane ([$^{123/125}$I]RTI-55) (Carroll et al. 1991; Neumeyer et al. 1991) was found to bind to both the DA and 5-HT transporters in homogenate binding assays (Boja et al. 1992*b)* as well as after IV injection in the brain of rodents and baboons (Cline et al. 1992; Innis et al. 1991; Scheffel et al. 1992*b*). The affinity of RTI-55 was approximately 100 times greater than that of (-) cocaine for both the DA and the 5-HT transporters (Boja et al. 1992*b*).

Studies in rats demonstrated that the in vivo distribution of [^{123}I]RTI-55 in CNS areas rich in serotonin uptake sites correlated well with regional densities of [^{3}H]serotonin uptake sites (figure 5). Maximal target-to-nontarget ratios (up to 7.4) in 5-HT uptake site-rich areas in the rat brain were reached 5 hours after IV injection (figure 6). However, as mentioned before, [^{123}I]RTI-55 labels not only 5-HT but

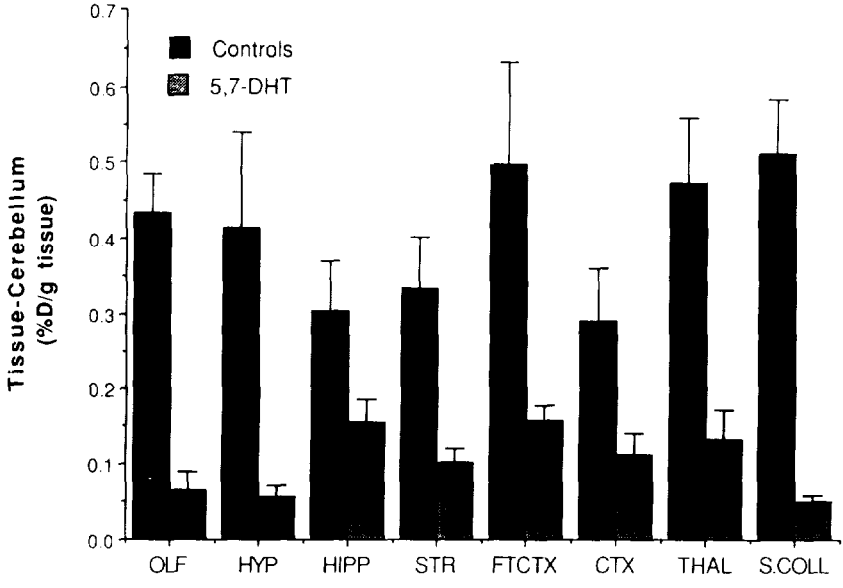

FIGURE 4. *Effect of 5,7-DHT lesioning on the specific binding (%D/g tissue-%D/g cerebellum) of [^{11}C]McN-5652-Z at 60 minutes after tracer injection. Rat brains were lesioned by intracerebroventricular injection of 5,7-DHT 13 days before the trucer study. Data are means ±1 standard deviation, n = 3.*

KEY: OLF = olfactory tubercles; HYP = hypothalamus; HIPP = hippocampus; STR = striatum; FTCTX = prefrontal cortex; CTX = cortex; THAL = thalamus; S.COLL = superior colliculi

SOURCE: Suehiro et al. 1993. Copyright 1993 by Society of Nuclear Medicine.

DA transporters as well. At the time when [^{123}I]RTI-55 specific binding in 5-HT uptake site-rich areas was highest (the hypothalamus-to-cerebellar ratio was 7.4:1), the striatal-to-cerebellar ratio was 22.7:1.

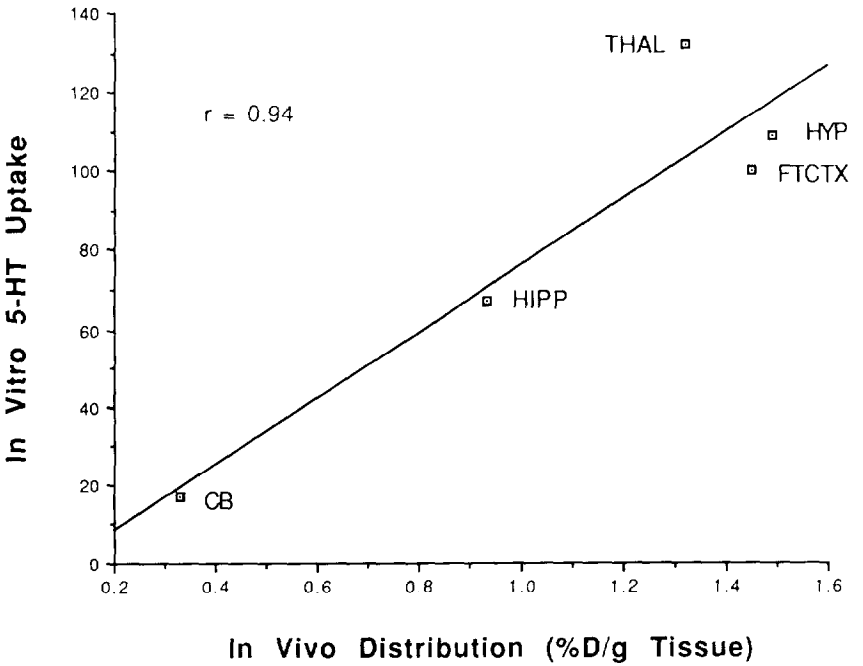

FIGURE 5. *Comparison between [^{123}I]RTI-55 concentrations (%D/g tissue) in various regions of the rat brain at 2 hours after IV injection and the proportional distribution of [^{3}H]serotonin uptake in synaptosomal preparations of these regions as published by Leysen (1985), where [^{3}H]serotonin uptake in the frontal cortex is set at 100 percent.*

KEY: CB = cerebellum, HIPP = hippocampus, THAL = thalamus, FTCTX = prefrontal cortex, HYP = hypothalamus

Despite the fact that [^{123}I]RTI-55 is not selective for the serotonin uptake site, it is anticipated that the tracer will be useful for quantitating 5-HT uptake sites in vivo by SPECT. In rats, neurotoxic doses of fenfluramine caused decreases of 66 percent (in the hypothalamus) to 83 percent (in the superior colliculi) of specific [^{123}I]RTI-55 binding in all areas except in the striatum and the olfactory tubercles (regions rich in DA transporters) (Scheffel et al. 1992*b*). In baboons, Innis and colleagues (1991) and Laruelle and coworkers (1992) observed specific

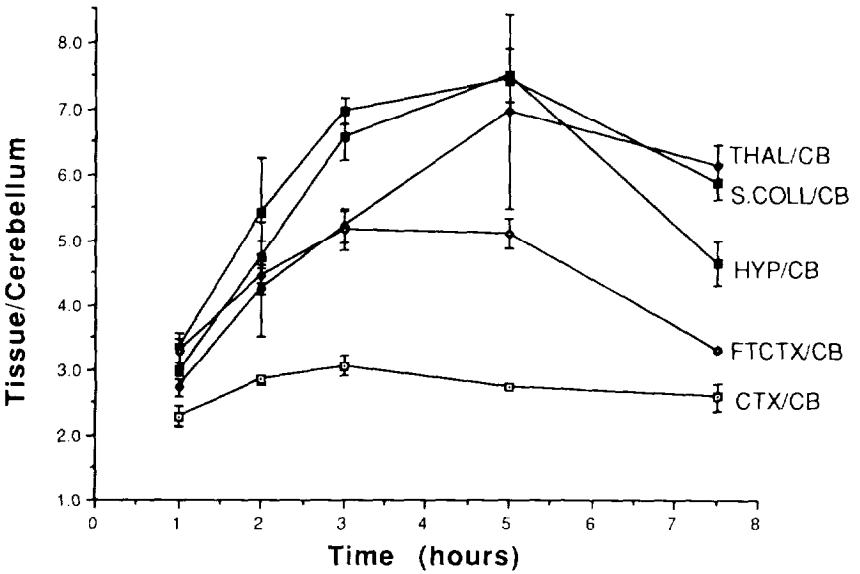

FIGURE 6. *Time course of tissue-to-cerebellar radioactivity ratios in selected areas of the rat brain after IV injection of ([123I]RTI-55. Data are means ± SEM; n = 2 to 4 rats/time point.*

KEY: THAL = thalamus; CB = cerebellum; S.COLL = superior colliculi; HYP = hypothalamus; FTCTX = prefrontal cortex; CTX = cortex

SOURCE: Scheffel et al. 1992*b*. Copyright 1992 by Wiley-Liss.

binding of [^{123}I]RTI-55 in the midbrain that was associated primarily with 5HT transporters. A more selective SPECT agent for the serotonin transporter has recently been described by Mathis and colleagues (1992). Studies with [^{125}I]-iodo-6-nitroquipazine showed excellent target-to-nontarget ratios in 5-HT transporter-rich regions of the rat brain; a hypothalamus-to-cerebellar ratio of 6.3:1 at 6 hours after injection was reported.

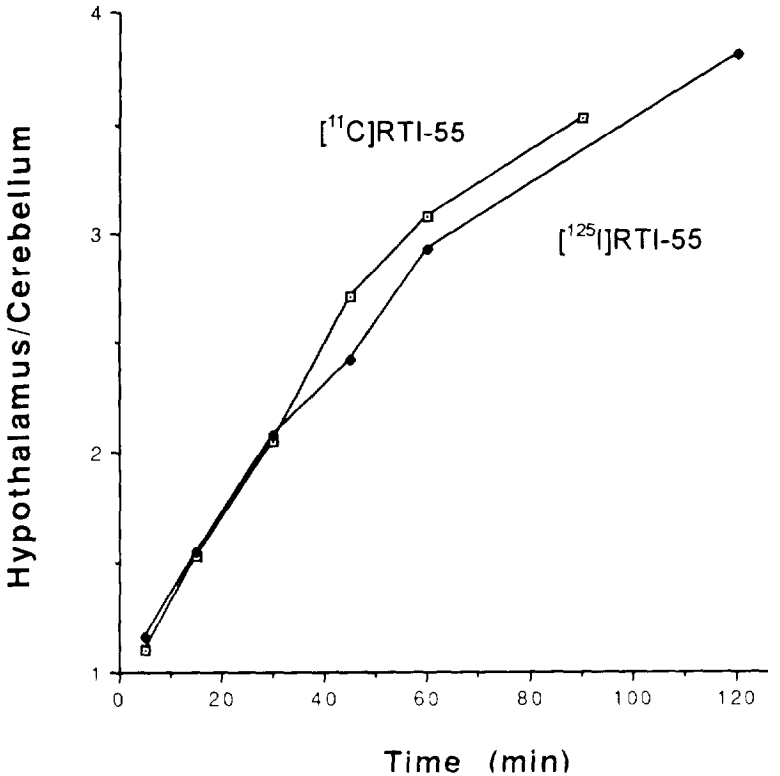

FIGURE 7. *Time course for hypothalamus-to-cerebellar ratios in the mouse brain after injection of either [^{125}I]RTI-5.5 or [^{11}C]RTI-55*

SOURCE: [^{125}]RTI-55 data are from Cline and colleagues (1992).

RTI-55 recently was labeled with [^{11}C] (Dannals, unpublished results), and studies in mice were performed to compare the specificity and selectivity of [^{11}C]RTI-55 binding to 5-HT uptake sites with that of [^{123}I]RTI-55. Similar results were obtained with both tracers (figure 7) [^{11}C]RTI-55 is being evaluated in nonhuman primates as a PET tracer for 5-HT and DA uptake sites.

SUMMARY

There is a great need for PET and SPECT ligands with high affinity and selectivity for the serotonin uptake site. These imaging agents would be useful in screening human populations at risk (e.g., individuals exposed to neurotoxic amphetamines such as MDMA and fenfluramine). Moreover, these radioligands would allow the study of serotonergic function in the normal living human brain, and they also would be useful in the examination of altered serotonergic neurotransmission in diseases such as depression and obsessive-compulsive and other neuropsychiatric disorders.

Over the past several years, a number of radioligands have been studied in several laboratories for their in vivo binding to 5-HT uptake sites. Although [^{3}H]paroxetine showed promising binding characteristics, conversion of authentic paroxetine into a PET or SPECT tracer turned out to be difficult and has not been achieved yet. Analogs of paroxetine displayed considerable loss of binding affinity and were, therefore, not useful for imaging purposes. For [^{11}C]fluoxetine, [^{11}C]citalopram, and cis-[^{11}C]DDPI, target-to-nontarget (hypothalamus-to-cerebellar) ratios remained less than 2.0:1 over a 90-min period after injection. The most promising PET agents identified today are [^{11}C]RTI-55 and [^{11}C]McN-5652-X. [^{11}C]RTI-55 labels both 5-HT and DA uptake sites. [^{11}C]McN-5652-X is highly selective for 5-HT uptake sites, and its distribution is consistent with the neuroanatomical distribution of the 5-HT uptake site. Because [^{11}C]McN-5652-Z is a racemic mixture of two stereoisomers, of which the (+) isomer (McN-5652-X) binds to the 5-HT uptake site in vivo and the (-) isomer (McN-5652-W) does not, the possibility exists that regional-specific binding can be determined by subtracting nonspecific binding of the (-) isomer from total radioactivity counts obtained with the (+) isomer. [^{11}C]McN-5652-X is the best PET radioligand for the 5-HT uptake site described thus far. This tracer warrants further testing in nonhuman primates. Efforts are underway to obtain an investigational new drug application for use of the tracer in humans.

Promising candidates as SPECT imaging agents for the 5-HT uptake site are [^{123}I]RTI-55 and [^{123}I]-iodo-6-nitroquipazine. Both agents are under intense investigation in different laboratories in the United States.

REFERENCES

Battaglia, G.; Yeh, S.Y.; and DeSouza, E.B. MDMA-induced neurotoxicity: Parameters of degeneration and recovery of brain serotonin neurons. *Pharmacol Biochem Behav* 29:269-274, 1988*a*.

Battaglia, G.; Yeh, S.Y.; O'Hearn, E.; Molliver, M.E.; Kuhar, M.J.; and DeSouza, E.B. 3,4-Methylenedioxymethamphetamine and 3,4-methylenedioxyamphetamine destroy serotonin terminals in rat brain: Quantification of neurodegeneration by measurement of [^{3}H]paroxetine-labeled serotonin uptake sites. *J Pharmacol Exp Ther* 242:911-916, 1988*b*.

Bogeso, K.P.; Christensen, A.V.; Hyttel, J.; and Liljefors, T. 3-Phenyl-1-indanamines. Potential antidepressant activity and potent inhibition of dopamine, norepinephrine and serotonin uptake. *J Med Chem* 28:1817-1828, 1985.

Boja, J.W.; Cline, E.J.; Carroll, F.I.; Lewin, A.H.; Philip, A.; Dannals, R.; Wong, D.; Scheffel, U.; and Kuhar, M.J. High potency cocaine analogs: Neurochemical, imaging, and behavioral studies. In: Kalivas, P.W., and Samson, H.H., eds. *The Neurobiology of Drug and Alcohol Addiction.* Vol. 654, *Annuals of the New York Academy* of *Sciences.* New York: The New York Academy of Sciences, 1992*a*.

Boja, J.W.; Mitchell, W.M.; Patel, A.; Kopajtic, T.A.; Carroll, F.I.; Lewin, A.H.; Abraham, P.; and Kuhar, M.J. High affinity binding of [^{125}I]RTI-55 to dopamine and serotonin transporters in the rat brain. Synapse 12:27-36, 1992*b*.

Buus Lassen, J. Potent and long-lasting potentiation of two 5-hydroxytryptophan-induced effects in mice by three selective 5-HT uptake inhibitors. *Eur J Pharmacol* 47:351-358, 1978.

Carroll, F.I.; Rahman, M.A.; Abraham, P.; Parham, K.; Lewin, A.H.; Dannals, R.F.; Shaya, E.; Scheffel, U.; Wong, D.F.; Boja, J.W.; and Kuhar, M.J. [^{123}I]313-(4-Iodophenyl)tropan-2ß-carboxylic acid methyl ester (RTI-55), a unique cocaine receptor ligand for imaging the dopamine and serotonin transporters in vivo. *Med Chem Res* 1:289-294, 1991.

Cline, E.J.; Scheffel, U.; Boja, J.W.; Mitchell, W.M.; Carroll, F.I.; Rahman, A.; Lewin, A.H.; and Kuhar, M.J. In vivo binding of [^{125}I]RTI-55 to dopamine transporters: Pharmacology and regional distribution with autoradiography. *Synapse* 12:37-46, 1992.

Commins, D.L.; Vosmer, G.; Virus, R.M.; Woolverton, W.L.; Schuster, C.R.; and Seiden, L.S. Biochemical and histological evidence that methylenedioxymethamphetamine (MDMA) is toxic to neurons in the rat brain. *J Pharmocol Exp Ther* 241:338-345, 1986.

Cortes, R.; Soriano, E.; Pazos, A.; Probst, A.; and Palacios, J.M. Autoradiography of antidepressant binding sites in the human brain: Localization using [^{3}H]imipramine and [^{3}H]paroxetine. *Neuroscience* 27:473-496, 1988.

Dannals, R.F.; Ravert, H.T.; Wilson, A.A.; and Wagner, H.N., Jr. Synthesis of a selective serotonin uptake inhibitor: [^{11}C]Citalopram. *Appl Radiat Isot* 41:541-543, 1990.

Fuller, R.W., and Wong, D.T. Inhibition of serotonin reuptake. *Fed Proc* 36:2154-2158, 1977.

Habert, E.; Graham, G.; Tahraoui, L.; Claustre, U.; and Langer, S.Z. Characterization of [^{3}H]paroxetine binding in rat cortical membranes. *Eur J Pharmacol* 118:107-114, 1985.

Harvey, J.; McMaster, S.; and Yunger, L. p-Chloroamphetamine: Selective neurotoxic action in brain. *Science* 187:841-843, 1975.

Heninger, G.; Chamey, D.S.; and Stemberg, D.E. Serotonergic function in depression: Prolactin response to intravenous tryptophan in depressed patients and healthy subjects. *Arch Gen Psychiatry* 41:398-402, 1984.

Hyttel, J. Citalopram; basic and clinical studies. *Pros Neuropsycho-pharmacology Biol Psychiatry* 6:275-295, 1982.

Innis, R.; Baldwin, R.; Sybirska, E.; Zea, Y.; Laruelle, M.; Al-Tikriti, M.; Chamey, D.; Zoghbi, S.; Smith, E.; Wisniewski, G.; Hoffer, P.; Wang, S.; Milius, R.; and Neumeyer, J. Single photon emission computed tomography imaging of monoamine reuptake sites in primate brain with [^{123}I]CIT. *Eur J Pharmacol* 200:369-370, 1991.

Kilboum, M.R. Synthesis of carbon-11 labelled nisoxetine and fluoxetine, monoamine reuptake inhibitors. (Abstract.) *J Nucl Med* 29:932, 1988.

Laruelle, M.; Baldwin, R.M.; Zea-Ponce, Y.; Zoghbi, S.S.; Al-Tikriti, M.S.; Sybirska, E.H.; Malison, R.T.; Neumeyer, J.L.; Milius, R.; Wong, S.; Smith, E.O.; Wisniewski, G.; Chamey, D.S.; Hoffer, P.B.; and Innis, R.B. SPECT imaging of monoamine transporter sites with 123I-CIT in nonhuman primates brain. Abstract. *J Nucl Med* 33:945-946, 1992.

Leysen, J.L. Characterization of serotonin receptor binding sites. In: Green, A.R., ed. *Neuropharmacology of Serotonin.* New York: Oxford University Press, 1985. pp. 79-116.

Marcusson, J.O.; Bergstrom, M.; Eriksson, K.; and Ross, S.B. Characterization of [^{3}H]paroxetine binding in rat brain. *J Neurochem* 50: 1783-1790, 1988.

Mathis, C.; Biegon, A.; Taylor, S.; Enas, J.; Hanrahan, S.; and Jagust, W. I-125-5-iodo-6-nitro-2-piperazinylquinoline: A potent and selective ligand for the serotonin uptake complex. *Eur J Pharmacol* 210:103-104, 1992.

Mathis, C.A.; Gerdes, J.M.; Enas, J.D.; Havlik, S.; and Peroutka, S.J. (±)-2^{11}-[I-125]iodoparoxetine: Synthesis and preliminary evaluation of a presynaptic serotonin ligand. Abstract. *J Nucl Med* 32:965, 1991.

Mellerup, E.T., and Plenge, P. High affinity binding of [^{3}H]paroxetine and [^{3}H]imipramine to rat neuronal membranes, *Psychopharmacology* 89:436-439, 1986.

Mellerup, E.T.; Plenge, P.; and Engelstoft, M. High affinity binding of [^{3}H]paroxetine and [^{3}H]imipramine to human platelet membranes. *Eur J Pharmacol* 96:303-309, 1983.

Moir, A.T.; Ashcroft, G.W.; Crawford, T.B.; Eccleston, D.; and Guldbert, H.C. Cerebral metabolites in cerebrospinal fluid as a biochemical approach to the brain. *Brain* 93:357-368, 1970.

Neumeyer, J.L.; Wang, S.; Milius, R.A.; Baldwin, R.M.; Zea-Ponce, Y.; Hoffer, P.B.; Chamey, D.S.; Malison, R.T.; Laruelle, M.; and Innis, R.B. [^{123}I] 2ß-Carbomethoxy-3ß-(4-iodophenyl)tropane: High affinity SPECT radiotracer of monoamine reuptake sites in brain. *J Med Chem* 34:3144-3146, 1991.

Petersen, E.N.; Olsson, S.O.; and Squires, R.F. Effects of 5-HT uptake inhibitors on the pressor response to 5-HT in the pithed rat. The significance of the 5-HT blocking property. *Eur J Pharmacol* 43:209-215, 1977.

Plenge, P.; Mellerup, E.T.; Honore, T.; and LeFevre-Honore, P. The activity of 25 paroxetine/femoxetine structure variants in various reactions, assumed to be important for the effect of antidepressants. *J Pharm Pharmacol* 38:877-882, 1987.

Ricaurte, G.A.; DeLanney, D.E.; Irwin, I.; and Langston, J.W. Toxic effects of MDMA on central serotonergic neurons in the primate: Importance of route and frequency of drug administration. *Brain Res* 446:165-168, 1988*a*.

Ricaurte, G.A.; Forno, L.S.; Wilson, M.A.; and DeLanney, L.E. (±)3,4-Methylenedioxymethamphetamine (MDMA) selectively damages central serotonergic neurons in non-human primates. *JAMA* 260:51-55, 1988*b*.

Scheffel, U.; Dannals, R.F.; Cline, E.J.; Ricaurte, G.A.; Carroll, F.I.; Abraham, P.; Lewis, A.H.; and Kuhar, M.J. [$^{123/125}$I]RTI-55, an in vivo label for the serotonin transporter. Synapse 11:134-139, 19926.

Scheffel, U.; Dannals, R.F.; Suehiro, M.; Ravert, H.T.; Stathis, M.; and Wagner, H.N., Jr. Evaluation of ^{11}C-citalopram and ^{11}C-fluoxetine as in vivo ligands for the serotonin uptake site. Abstract. *J Nucl Med* 31:883, 1990.

Scheffel, U., and Hartig, P.R. In vivo labeling of serotonin uptake sites with [^{3}H]paroxetine. *J Neurochem* 52:1605-1612, 1989.

Scheffel, U.; Lever, J.R.; Stathis, M.; and Ricaurte, G.A. Repeated administration of MDMA causes transient down-regulation of 5-HT$_2$ receptors: In vitro and in vivo studies using the ligand Nl-methyl-2-[^{125}I]-LSD. *Neuropharmacology* 31:881-893, 1992*a*.

Scheffel, U., and Ricaurte, G.A. Paroxetine as an in vivo indicator of 3,4-methylenedioxymethamphetamine neurotoxicity: A presynaptic serotonergic positron emission tomography ligand? *Brain Res* 527:89-95, 1990.

Schuster, C.R.; Lewis, M.; and Seiden, L.S. Fenfluramine neurotoxicity . *Psychopharmacol Bull* 22:148-151, 1986.

Shank, R.P.; Vaught, J.L.; Pelley, K.A.; Settler, P.E.; McComsey, D.F.; and Maryanoff, B.E. McN-5652: A highly potent inhibitor of serotonin uptake. *J Phannacol Exp Ther* 247:1032-1038, 1968.

Slikker, W.; Ali, SF.; Scallet, A.C.; Frith, C.H.; Newport, G.D.; and Bailey, J.R. Neurochemical and neurohistological alterations in the rat and monkey produced by orally administered methylene-dioxymethamphetamine (MDMA). *Toxicol Appl Pharmacol* 94:448-457, 1988.

Suehiro, M.; Ravert, H.T.; Dannals, R.F.; Scheffel, U.; and Wagner, H.N., Jr. Synthesis of a radiotracer for studying serotonin uptake sites with positron emission tomography: [^{11}C]McN-5652. *J Labelled Comp Radiopharm* 31:841-848, 1992*b*.

Suehiro, M.; Scheffel, U.; Dannals, R.F.; Ravert, H.T.; and Wagner, H.N., Jr. [^{11}C](+)McN5652 as a radiotracer for imaging serotonin uptake sites with PET. *Life Sci,* in press.

Suehiro, M.; Scheffel, U.; Dannals, R.F.; Ricaurte, G.A.; Ravert, H.T.; and Wagner, H.N., Jr. A PET radiotracer for studying serotonin uptake sites: [^{11}C]McN-5652-Z. *J Nucl Med* 34:120-127, 1993.

Suehiro, M.; Scheffel, U.; Dannals, R.F.; Wilson, A.A.; Ravert, H.T.; and Wagner, H.N., Jr. A new radiotracer for in vivo labeling of serotonin uptake sites by PET, cis-N,N[^{11}C]dimethyl-3-(2',4'-dichlorophenyl)-indanamine, cis-[^{11}C]DDPI. *Nucl Med Biol* 19:549-553, 1992*a*.

Suehiro, M.; Wilson, A.A.; Scheffel, U.; Dannals, R.F.; Ravert, H.T.; and Wagner, H.N., Jr. Radiosynthesis and evaluation of N-(3-[^{18}F]fluoropropyl) paroxetine as a radiotracer for in vivo labeling of serotonin uptake sites by PET. *Nucl Med Biol* 18:791-796, 1991.

Villemagne, V.L.; Dannals, R.F.; Sanchez-Roa, P.M.; Scheffel, U.; Ravert, H.T.; Wilson, A.A.; Natarajan, T.K.; Frost, J.J.; and Wagner, H.N., Jr. PET imaging of central serotonin re-uptake sites in the baboon brain with [^{11}C]-N-Me-Paroxetine. Abstract. Paper presented at the Society of Nuclear Medicine, St. Louis, MO, June *13-16,* 1989.

ACKNOWLEDGMENTS

This work was supported by U.S. Public Health Service grants DA-05477, NS-15080, and CA-32845. Marigo Stathis and Christine Steinert provided work in biodistribution studies in rodents and assistance with baboon studies. Robert Smoot assisted with the operation of the cyclotron. Dr. Hayden T. Ravert helped to prepare the [^{11}C] and [^{18}F] tracers.

AUTHORS

Ursula Scheffel, Sc.D.
Assistant Professor

Robert F. Dannals, Ph.D.
Associate Professor

Makiko Suehiro, Ph.D.
Research Associate

Henry N. Wagner, Jr., M.D.
Professor
Division of Nuclear Medicine
Department of Radiology
The Johns Hopkins Medical Institutions
615 North Wolfe Street
Baltimore, MD 21205

George A. Ricaurte, M.D., Ph.D.
Assistant Professor
Department of Neurology
The Johns Hopkins Medical Institutions
Baltimore, MD 21224

F. Ivy Carroll, Ph.D.
Director for Organic and Medicinal Chemistry
Research Triangle Institute
Research Triangle Park, NC 27709

Michael J. Kuhar, Ph.D.
Professor
Neuroscience Branch
National Institute on Drug Abuse
Addiction Research Center
Baltimore, MD 21224

SPECT Imaging of Dopamine and Serotonin Transporters in Nonhuman Primate Brain

Marc Laruelle, Ronald M. Baldwin, and Robert B. Innis

INTRODUCTION

Since the recent introduction of high affinity iodinated ligands and high-resolution, brain-dedicated, single photon emission computerized tomography (SPECT) devices, SPECT has been used to visualize various neuroreceptors, including the acetylcholine muscarinic receptor (Eckelman et al. 1985), the dopamine D_2 receptor (Kung et al. 1989, 1990), and the benzodiazepine receptor (Innis et al. 1991*a*).

The ability to visualize and quantify dopamine (DA) and serotonin (5-HT) transporters presumably would lead to several clinical applications. Alteration of these transporters has been described in Parkinson's disease (Cash et al. 1985; Raisman et al. 1986; Janowsky et al. 1987; Hirai et al. 1988; Maloteaux et al. 1988; Kaufman and Madras 1991; Niznik et al. 1991), Alzheimer's disease (Allard et al. 1990), suicide victims (Stanley et al. 1982), patients with major affective disorders (Perry et al. 1983; Crow et al. 1984; Paul et al. 1984), and schizophrenia (Joyce et al. 1993; Laruelle et al., in press-a). In addition to their association with pathophysiological processes, DA and 5-HT transporters are implicated in the mechanism of some antidepressant drugs (Glowinsky and Axelrod 1964) and addictive substances like cocaine (Kuhar et al. 1991). Therefore, radiolabeled tracers suitable for visualization and quantification of these sites may provide valuable tools for the diagnosis and treatment of several neuropsychiatric disorders.

Multiple saturable binding sites for [^{3}H]cocaine have been identified in the central nervous system, the majority of which being associated with DA, 5-HT, and norepinephrine (NE) transporters (Reith et al. 1980, 1983). Some of the cocaine phenyltropane congeners are more potent than cocaine itself in behavioral stimulation, monoamine uptake

inhibition, and affinity for the monoamine transporters (Clarke et al. 1973; Madras et al. 1989*a*; Ritz et al. 1990; Balster et al. 1991). For example, the radiolabeled phenyltropane fluoro derivative [^{3}H]2P-carbomethoxy-3ß-(4-fluorophenyl)tropane (WIN 35, 428, also designated CFT, figure 1) is used as a potent in vitro ligand for the DA transporter (Madras et al. 1989*a*).

The search for an iodinated analog of CFT led to the development of methyl 3ß-(4-iodophenyl)tropane-2ß-carboxylate (figure 1), designated as ß-CIT in analogy to CFT (Neumeyer et al. 1991) and by the code number RTI-55 (Carroll et al. 1991). This chapter presents the major steps in the development of radiolabeled ß-CIT as a SPECT tracer for visualization of the DA and 5-HT transporters in nonhuman primates: in vitro binding studies, radiolabeling, pharmacokinetics, metabolites analysis, brain uptake kinetics, and in vivo pharmacology. This work has been published previously in a series of articles by the authors and others (Boja et al. 1991, 1992; Carroll et al. 1991; Innis et al. 1991*b*; Neumeyer et al. 1991; Cline et al. 1992; Scheffel et al. 1992; Shaya et al. 1992; Baldwin et al. 1993; Laruelle et al. 1993*a)*.

METHODS

Binding Studies

Binding studies were performed with unlabeled ß-CIT. The affinity of ß-CIT for DA and 5-HT transporters was evaluated by measuring the IC_{50} of ß-CIT for displacing [^{3}H]CFT from DA transporters and [^{3}H]paroxetine from 5-HT transporters in baboon striatum and rat cortex, respectively. Assays were performed according to previously published methods (Laruelle et al. 1988; Madras et al. 1989*b*). ß-CIT was compared with cocaine, CFT, and α-CIT (the C-2 epimer of ß-CIT).

Radiolabeling

[^{123}I]ß-CIT was prepared by oxidative iododestannylation of the corresponding tributylstannyl precursor (Neumeyer et al. 1991; Baldwin et al. 1993), and, in turn, was synthesized from ß-CIT by palladium catalyzed reaction with the bis(trialkyl)distannane

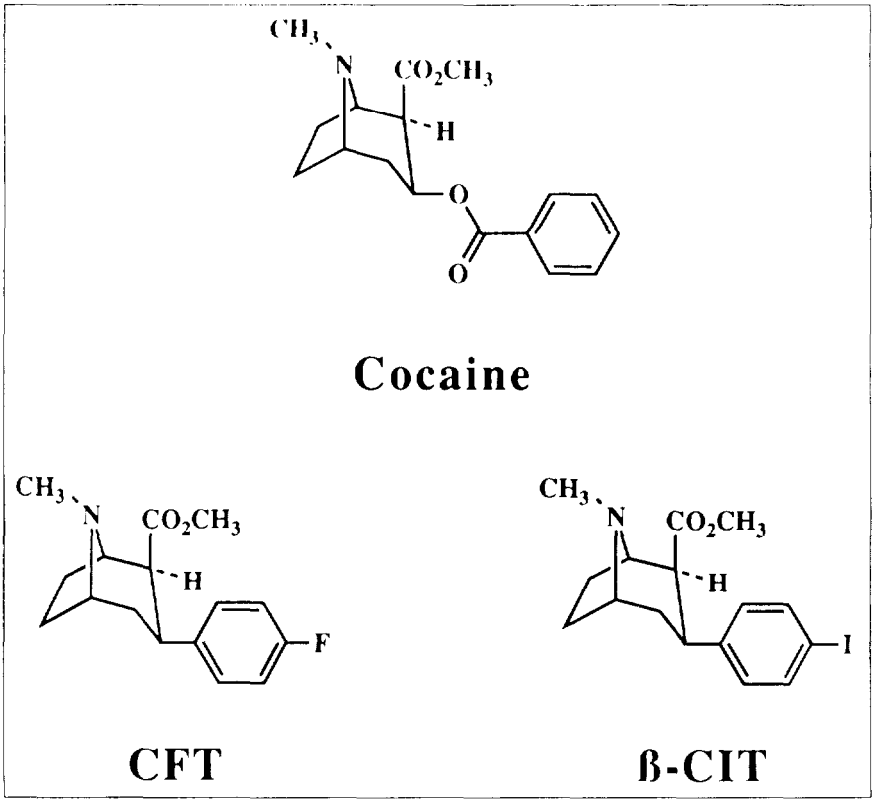

FIGURE 1. *Chemical formula of cocaine and its phenyltropane congeners, CFT and ß-CIT*

(Azizian et al. 1981). The radiolabeling of the precursor with ^{123}I was performed using the following method: To a vial containing 50 µg (0.094 µmol) methyl 3ß-(4-tributylstannylphenyl)tropane-2ß-carboxylate was added, in the following order, 50 µL ethanol, 150 µL 0.5 M H_3PO_4, 125-500 µL (20-30 mCi) $Na^{123}I$ solution, and 100 µL (4.2 µmol) 0.32 percent peracetic acid (freshly prepared from 32 percent CH_3CO^3H). After 20-30 min at room temperature, 50 µL (5 mg) 100 mg/mL aqueous $NaHSO_3$ solution was added, and the vial headspace was purged into charcoal with a stream of N_2 or Ar for 10 min. Saturated $NaHCO_3$ solution (1 mL) was added, and the mixture was extracted with 3x1 mL ethyl acetate; the combined extracts were passed through a small column of anhydrous Na_2SO_4 and

evaporated on a rotary evaporator with a stream of N_2 at a bath temperature of 37 °C. The residue was dissolved in 50 µL CH_3OH, mixed with 100 µL mobile phase, and injected into the High Performance Liquid Chromatography (HPLC). The fraction eluting at the retention time of ß-CIT was collected in a 50 mL pear-shaped flask containing 100 µL (100 µg; 5.7 µmol) 1 mg/mL L-ascorbic acid. The solvent was evaporated as above, and the residue was dissolved in 400 µL ethanol and diluted with 6-8 ml 0.9 percent NaCl. The final solution (approximately 5 percent ethanol and 0.1 mM ascorbic acid at a pH of 5-5.5) was filtered through a 0.2 µ membrane filter into a sterile 10 mL serum vial or 10 mL syringe. The radiochemical purity was measured by HPLC immediately after preparation and again after storage at room temperature for 15-28 h. Specific activity was measured by comparing the UV response of the sample with that of known concentrations of ß-CIT. Radiolabeling yield was calculated as the fraction extracted by ethyl acetate times the fraction of product in the extract measured by HPLC. Radiochemical yield was calculated by dividing the radioactivity in the final purified product, corrected for decay ($T_{1/2}$ 13.2 h) by the amount of starting [^{123}I]NaI. Radioactivities were measured in a gamma ionization chamber calibrated for each geometry and vessel configuration.

Anesthesia Procedure

Pharmacokinetic and SPECT brain imaging experiments were performed with 11-14 kg baboons (Papio anubis) and 6-7 kg vervet monkeys (Cercopiftzecus aethiops). Fasted animals were immobilized with ketamine (10 mg/kg intramuscular [i.m.]) and anesthetized with 2.5 percent isoflurane through an endotracheal tube. Glycopyrrolate (10 µg/kg i.m.), a long-acting peripheral anticholinergic drug, was administered at the beginning of the study to decrease respiratory and digestive secretions. Vital signs were monitored every 30 min, and the temperature was kept constant at 36.5-37.5 °C with heated water blankets. An IV perfusion line with 0.9 percent NaCl was maintained during the experiment and used for the injection of radiotracer and nonradioactive drugs. The animal's head was immobilized within the camera gantry with a "bean bag" that hardens on evacuation.

Pharmacokinetics and Plasma Metabolites Analysis

Plasma pharmacokinetics were studied in one baboon and two vervet monkeys, with each animal studied in two separate experiments 28-33 days apart. [^{123}I]ß-CIT (9.8-13.5 mCi for the baboon and 3.2-6.5 mCi for the vervets) was injected intravenously. Arterial blood samples were collected every 10 s up to 2 min and at longer intervals thereafter, up to 300-360 min after administration of the tracer. Selected venous samples were taken from the contralateral vein.

Plasma was extracted with ethyl acetate, and selected samples were analyzed by HPLC, estimating intermediate values by linear interpolation. Control samples incubated with whole blood and treated in the same way were used to calculate the recovery coefficient for [^{123}I]ß-CIT and to verify stability of the compound in blood under the storage conditions (18-22 h at 4 °C). Extraction values for plasma samples were corrected by dividing by the recovery coefficient. The precision of the extraction method, measured by extracting five repeated aliquots of a single large plasma sample from one baboon experiment, was 0.5 percent expressed as the coefficient of variation. Control experiments in which [^{123}I]ß-CIT was added to whole blood and subjected to the metabolite extraction procedure produced a recovery of 92.0±0.6 percent (n = 6). The stability of the compound in blood was demonstrated in each experiment by adding one aliquot to a sample of blood at the time of administration to the animal and comparing the result after overnight storage with that of a fresh sample added at the time of metabolite analysis. The content of parent [^{123}I]ß-CIT was similar in both samples, averaging 92.6±0.5 percent versus 91.3±0.6 percent (n = 6) at an average time interval of 20.3± 0.5 h between the first and second incubation. Plasma protein binding was measured by ultrafiltration with membranes having a 30,000 mol wt cutoff. A control sample consisting of tracer diluted with 0.9 percent NaCl was run concurrently.

Plasma total parent concentrations were fitted to a three exponential function with a weighted least squares program. The half-life $T_{1/2}$ derived from the relation $T_{1/2} = (\ln 2)/\lambda i$ with λi as the rate constant of each exponential.

SPECT Data Acquisition and Analysis

Data were acquired with two brain-dedicated SPECT cameras: the multislice CERASPECT device (Digital Scintigraphics, Cambridge; Holman et al. 1990) and the single slice 810X Brain Imager (Strichman Medical Equipment, Medfield, MA; Stoddart and Stoddart 1979). The injected dose of [^{123}I]ß-CIT was 6.52±.5 mCi, with these and subsequent data expressed as mean ± SEM.

Scans were acquired in continuous mode for 3 min throughout the experiments. Scanning experiments (n = 39) lasted 329±8 min yielding 94±3 acquisitions per experiment. Tomographic backprojection and image reconstruction were performed as previously described (Laruelle et al. 1993*a*). Attenuation correction was performed assuming uniform attenuation equal to that of water (attenuation coefficient μ = 0.150 cm^2/g) within an ellipse drawn around the brain (Chang 1987). Four regions of interest (ROIs) were examined on both Strichman and CERASPECT scans (striatum, occipital, hypothalamic/midbrain area, and cerebellum). In addition, frontal pole was examined on the CERASPECT scans. The ROIs were positioned by reference to the activity distribution, using a baboon brain atlas (Riche et al. 1988) and magnetic resonance imaging (MRI) scans, performed in three of the animals and coregistered to the SPECT images (Malison et al., in press). ROI activities were decay corrected to the time of injection.

Pharmacological Selectivity

The pharmacological nature of in vivo [^{123}I]ß-CIT binding was investigated by displacement studies, achieved by IV injections of pharmacological doses of nonradioactive compounds with known pharmacological properties.

[^{123}I]ß-CIT binding to DA, 5-HT, and NE transporters was evaluated with four non-cocaine-related monoamine uptake inhibitors: LU 19-005, a nonspecific monoamine uptake inhibitor (Hyttel and Larsen 1985); GBR 12909, a specific DA uptake inhibitor (Andersen 1989); citalopram, a specific 5-HT uptake inhibitor (Hyttel 1982); and maprotiline, a specific NE uptake inhibitor (Hyttel 1982). Displacement experiments were analyzed by comparing the ROI activity after

injection of the displacing agent to the projected ROI activity in the absence of its injection, estimated using the kinetic parameters derived from the control scans.

In Vivo Potencies of Cocaine Analogs

The authors investigated the ability of [^{123}I]ß-CIT SPECT imaging to provide quantitative information about the level of in vivo site occupancy reached by IV injection of cocaine (n = 5), CFT (n = 4), and ß-CIT (n = 8). The level of site occupancy induced by the injection of a given dose of the drug was estimated as the difference between the level of [^{123}I]ß-CIT specific uptake before injection and the level at which the uptake curve stabilized after injection. The percentage displacements (P) were logit transformed as ln[P/(100-P)] and plotted versus 1n dose or 1n cumulative dose in case of multiple injections. The dose inducing 50 percent site occupancy (ED_{50}) was calculated as the x-axis intercept and expressed in µmol/kg. The Hill coefficient was calculated as the slope of the regression line divided by 2.303. The relationship between the in vivo ED_{50} and the in vitro IC_{50} was investigated by linear regression analysis (IC_{50}-3.8 nM), where IC_{50} is the concentration of drug required to displace 50 percent of the specifically bound radiotracer.

RESULTS

Binding Studies

ß-CIT showed high potency for displacing both [^{3}H]CFT (IC_{50} = 1.6 nM) from DA transporter sites and [^{3}H]paroxetine from 5-HT transporter sites (IC_{50} = 3.8 nM; table 1). The binding was stereoselective: the affinity of the isomer a-CIT was much lower (IC_{50} of 87.6 nM and 210 nM for DA and 5-HT transporters, respectively). ß-CIT was 10 times and 100 times more potent than CFT for DA transporters (IC_{50} = 15.3 nM) and 5-HT transporters (IC_{50} = 479 nM), respectively. ß-CIT also displayed greater potency than cocaine at each of these sites (IC_{50} of 221 nM and 207 nM for DA and 5-HT transporters, respectively).

TABLE 1. *ß-CIT, CFT, and Cocaine: Comparison between in vitro ID_{50} for DA and 5-HT transporters and in vivo ED_{50} for displacing striatal [^{123}I]ß-CIT specific binding*

	In vitro [^{3}H]CFT IC_{50}[a]	In vitro [^{3}H]paroxetine IC_{50}[b]	In vivo [^{123}I]ß-CIT ED_{50}[c]
	nM	nM	µmol/kg
ß-CIT	1.6 ± 0.15	3.8 ± 0.53	0.11
CFT	15.3 ± 1.2	479 ± 59	0.40
Cocaine	221 ± 14	207 ± 66	9.6

[a]Measured in baboon caudate homogenates membranes, according to Madras et al. (1989*b*); n = 4.

[b]Measured in rat cortical homogenates membranes, according to Laruelle et al. (1988); n = 4.

[c]Measured in baboon striatum with SPECT and Logit-log transform of displacement data (see Methods).

Radiolabeling

The radiolabeling yield averaged 65.2±2.3 percent (n = 18), and overall radiochemical yield averaged 54.4±2.2 percent. The radiolabeled product was stable for at least 28 h at room temperature in normal saline containing about 5 percent ethanol and 0.1 mM ascorbic acid; radiochemical purity averaged 97.5±0.5 percent immediately after preparation and 96.0±0.6 percent measured 21.1±0.8 h later. The specific activity of the final product was estimated to be 500-1,200 Ci/mmol, due to the presence in the tributylstannyl precursor of about 7 mol percent ß-CIT that was carried through the radiosynthesis and detected by HPLC of the tributylstannyl precursor.

Pharmacokinetics and Plasma Metabolites Analysis

Protein Binding. Plasma protein binding of [^{123}I]ß-CIT measured in vitro by ultrafiltration was 74.8±l.4 percent (n = 6), whether incubated in plasma or in whole blood for up to 22 h. Control binding of tracer to the ultrafiltration membrane in the absence of plasma was 6.2±0.2 percent (n = 6).

Metabolites. Plasma metabolites were characterized by solvent extraction followed by HPLC of the organic extract. The major metabolite was a polar, nonextractable fraction that increased to > 50 percent of the plasma activity by 30-45 min postinjection (p.i.). An extractable metabolite, less lipophilic than ß-CIT on HPLC, also was observed, increasing to about 4 percent of the plasma activity after 2-3 h.

Plasma Kinetics. After IV administration of [^{123}I]ß-CIT, peak arterial plasma levels of total ^{123}I and of unmetabolized parent were reached within 40-80 sec. In two experiments in which both arterial and venous samples were taken, venous plasma levels initially were lower than arterial levels but converged within 2 min in one experiment and within 30 min in the other. Arterial plasma concentration of parent compound was observed to match a triexponential function, with a terminal half-life of 77-166 min in baboons and 108-153 min in vervets.

Brain Uptake

Brain activity was concentrated in two areas. The most superior activity concentrations overlaid the right and left striatum. A second area of activity was detected consistently on the midline about 15 mm below the level of the striatal slice. This activity extended inferiorly and posteriorly over about 12 mm. This area was identified by reference to brain atlas diagrams and MRI coregistered scans (Malison et al., in press), as located at the level of the lower diencephalon (including the hypothalamus) and the mesencephalon (including the substantia nigra, the raphe nuclei, and the colliculi). Since the anatomical resolution of the camera did not allow differentiating the individual contributions of each of these structures to the activity, the ROI placed on the anterior/superior part of this area was labeled as

hypothalamic/midbrain ROI. Typical time activity curves in the striatum, hypothalamic/midbrain, occipital, frontal, and cerebellar regions are shown in figure 2.

Striatum. Striatum time activity curves were characterized by a prolonged phase of increasing activity, peaking at about 142±10 min and followed by an almost negligible washout (0.6±0.2 percent/h). The target-to-background (i.e., striatal-to-cerebellar) ratio increased consistently over the course of the experiments reaching 7.33±0.88 at 300 min. Despite the stability of the striatal plateau phase, [^{123}I]ß-CIT uptake was found to be reversible as the injection of an excess dose of nonradioactive ß-CIT at 180 min (figure 3) induced a displacement of striatal activity to a level similar to the cerebellar activity. This experiment showed that, at 180 min, more than 75 percent of striatal activity was associated with saturable sites.

Hypothalamic/Midbrain Area. Activity in the hypothalamic/midbrain area reached a peak at 47±2 min at a level equivalent to 63±3 percent of the striatal peak activity. Activity decreased thereafter at a rate of 14.4±0.9 percent/h. Despite the fact that the absolute number of counts reached a peak value at 47±2 min, the target-to-background ratio continued to increase for a longer period to 1.69±0.10 at 60 min, 2.57±0.18 at 180 min, and 2.32±0.38 at 300 min. Injection of nonradioactive ß-CIT at 180 min displaced at least 50 percent of the activity in the hypothalamic/midbrain area (figure 3).

Occipital, Frontal, and Cerebellar Areas. The time course of activities in these three regions was similar. Activities peaked within the first 30 min. Peak activities in these regions also were within a similar range; the occipital had values (46±3 percent) slightly higher than the cerebellar and frontal regions (36+3 percent and 38±3 percent, respectively). The washout rate was high in all three regions (20 to 30 percent/h). The injection of nonradioactive ß-CIT at 180 min did notaffect the activity in these cortical areas, suggesting that, at that time, most of the activity was not associated with saturable sites.

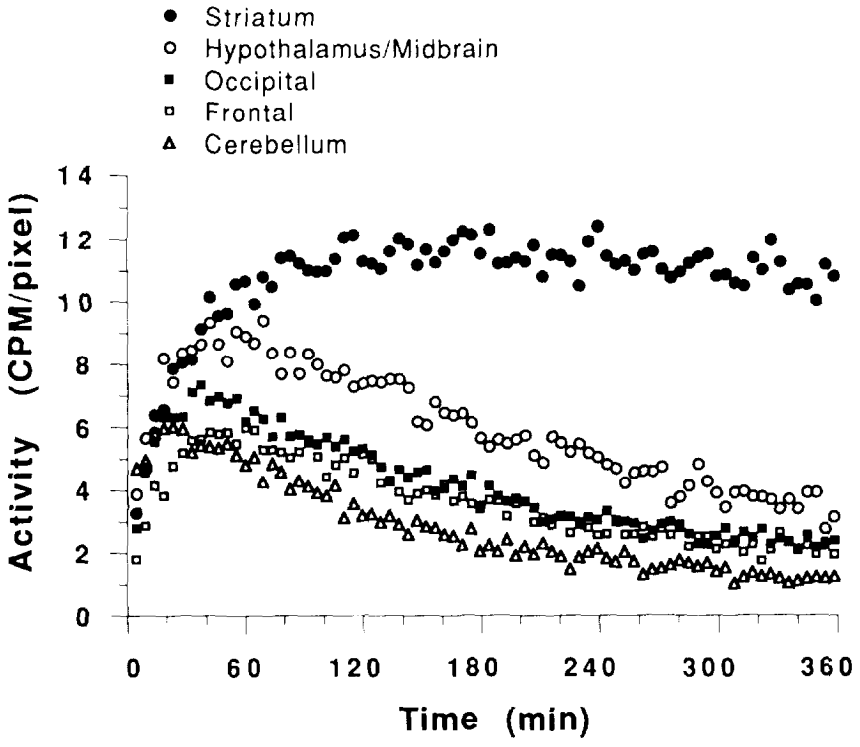

FIGURE 2. *Kinetic of brain uptake of [^{123}I]ß-CIT in various regions of the baboon's brain, following the injection of 3.2 mCi [^{123}I]ß-UT: striatum, average of left and right (closed circles), hypothalamic/midbrain area (open circles), occipital pole (closed squares), frontal pole (open squares), and cerebellum (open triangles). The striaral activity increased during the first three hours and remained stable thereafter. Hypothalamic/midbrain activity exhibited a peak between 45 and 60 min and then washed out at a rate of 14 percent of the peak value per h. Occipital, frontal, and cerebellar activities displayed similar kinetics, characterized by an early peak (20-30 min), followed by a rapid washout (20-30 percent of peak value per h). Data were acquired on the CERASPECT camera and are expressed in CPM/pixel.*

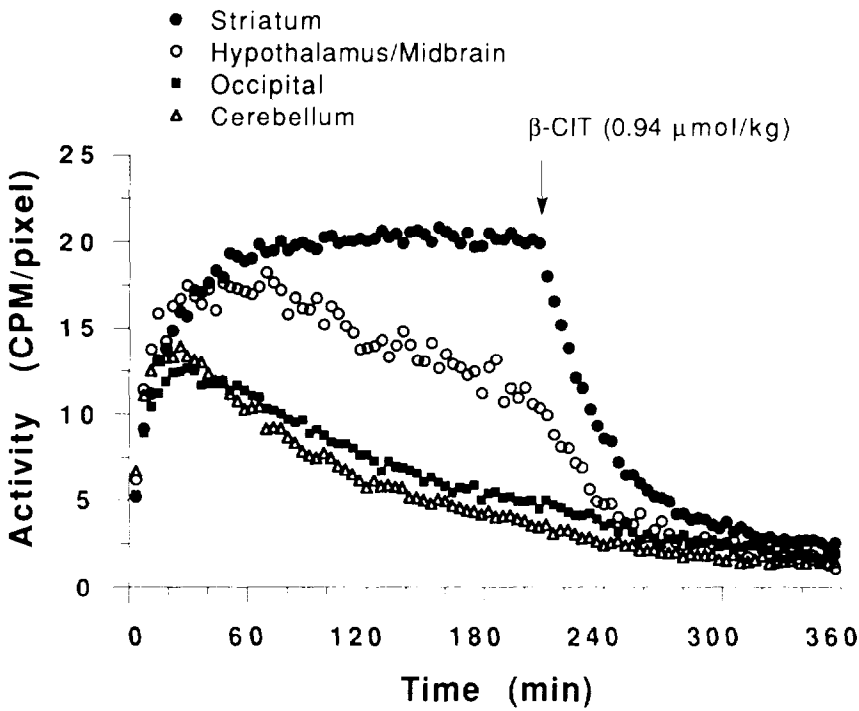

FIGURE 3. *Effects of injection of receptor saturating dose of ß-CIT on [^{123}I]ß-CIT uptake in baboon. Nonradioactive ß-CIT (0.94 μmol/kg IV) was injected IV 210 min (arrow) following the injection of 6.0 mCi [^{123}I]ß-CIT and caused displacement of 70-80 percent striatal activity and 50-60 percent of hypothalamic/midbrain activity. No effects were observed in the cortical and cerebellar regions. Data were acquired on the CERASPECT camera and are expressed in CPM/pixel.*

Pharmacological Selectivity

The pharmacological identity of the saturable sites associated with [^{123}I]ß-CIT uptake in the striatum was studied by injection of non-radioactive drugs during the plateau phase of the striatal uptake (180-200 min, "late injections"). Uptake in the hypothalamic/midbrain

area was investigated more specifically by injections performed shortly after peak time (60 min, “early injections”).

LU 19-005. Injection of LU 19-005 (3 µmol/kg IV), a nonspecific uptake inhibitor, at 180 min displaced both the striatal and hypothalamic/midbrain activities.

GBR 12909. Injections of GBR 12909 (3.4 and 6.8 µmol/kg IV) were performed at 200 min in two experiments and induced 47-50 percent displacement of striatal [^{123}I]ß-CIT (figure 4). The hypothalamic/midbrain [^{123}I]ß-CIT binding was unaffected, as demonstrated by an unchanged washout rate after the injection (13.3 percent/h).

Citalopram. Injection of citalopram (7.4 µmol/kg IV) at 180 min had no noticeable affect on striatal activity. However, it induced a marked increase in washout rate of the hypothalamic/midbrain area from 13.6 percent/h before the injection to 35.5 percent/h during the 60 min following the injection (figure 5). In three other experiments, citalopram was injected after 60 min at 7.4, 11.1, and 14.8 µmol/kg IV, respectively. The hypothalamic/midbrain washout rates, calculated during 60 min following the injection, increased to 45, 34, and 41 percent/h, respectively.

Maprotiline. Injection of maprotiline (13.9 µmol/kg IV) at 60 min failed to induce apparent changes in the uptake kinetics in either striatal or hypothalamic/midbrain areas.

In Vivo Potencies of Cocaine Analogs

The prolonged phase of stable striatal uptake allowed the authors to perform up to three displacements in a single experiment. Since thespontaneous washout was negligible, no correction was needed in computing the percentage of displacement. Striatal specific binding was defined operationally as the difference between striatal and cerebellar activity. The validity of this subtraction technique in the late phase of the scan was supported by displacement experiments with high doses of ß-CIT, as the level of nondisplaceable striatal activity was similar to the cerebellar activity (figure 3).

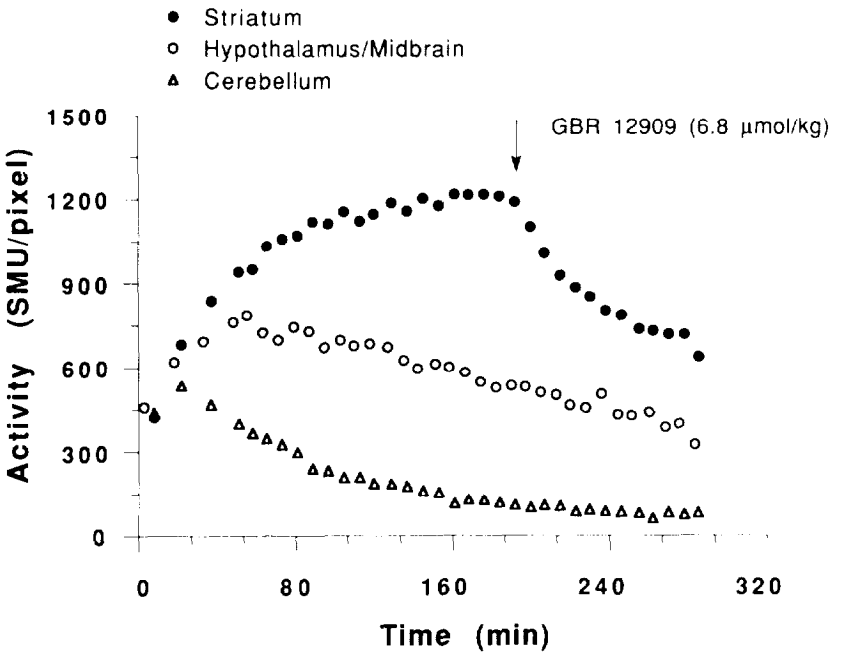

FIGURE 4. *Effects of the selective DA uptake inhibitor GBR 12909 on [^{123}I]ß-CIT uptake in baboon. GBR 12909 (6.8 µmol/kg) was injected IV 180 min after in injection of 4.1 mCi [^{123}I]b-CIT and induced a displacement of 49 percent of striatal activity. Hypothalamic/midbrain area was unaffected by the injection of GBR 12909, as the washout rate was unchanged by the injection. Cerebellum activity was unaffected. Data were acquired on the 810X Brain Imager camera and are expressed in SMU/pixel, with SMU corresponding to the count rate recorded from a untform flood source containing 100 Bq/ml of ^{99}mTc point source.*

Results of five experiments with a total of eight injections of various doses of nonradioactive cocaine were analyzed with the logit-log plot method (figure 6). Linear regression (r^2 = 0.92) allowed calculation of the ED_{50} as the inverse logarithm of the x-axis intercept (cocaine ED_{50} = 9.6 µmol/kg). The ED_{50} of ß-CIT and CFT were calculated with a

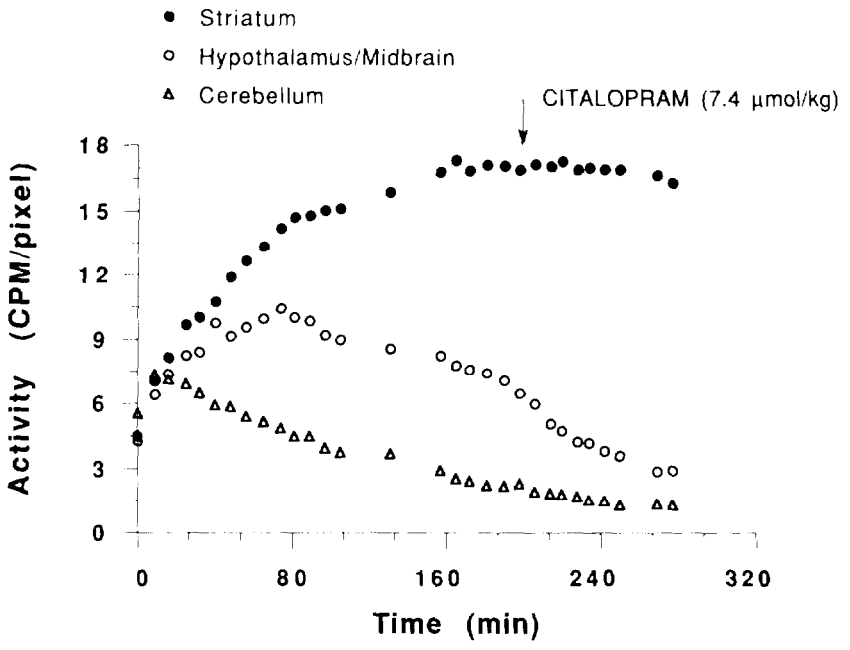

FIGURE 5. *Effects of the selective 5-HT uptake inhibitor citalopram on [^{123}I]ß-CIT uptake in baboon striatum (closed circles), hypothalamic/midbrain area (open circles), and cerebellum (open triangles). Citalopram (7.4 µmol/kg) was injected IV 180 min after the injection of 13.5 mCi [^{123}I]ß-CIT and induced an increase in the hypothalamic/midbrain activity washout from 13.6 percent/h before the injection to 35.5 percent/h during the 60 min period after the injection. Striatal and cerebellar activities were unaffected by the injection of citalopram. Data were acquired on the CERASPECT camera and are expressed in CPM/pixel.*

similar method and found to be 0.11 and 0.40 µmol/kg, respectively. The relationship between the in vivo ED_{50} of the three investigated cocaine-like drugs and their in vitro IC_{50} for displacing [^{3}H]CFT from DA transporters in monkey striatum appeared linear (r^2 = 0.96; figure 7). There was no apparent relationship with their in vitro IC_{50} for displacing [^{3}H]paroxetine from 5-HT transporters in rat cortical membranes (r^2 = 0.27).

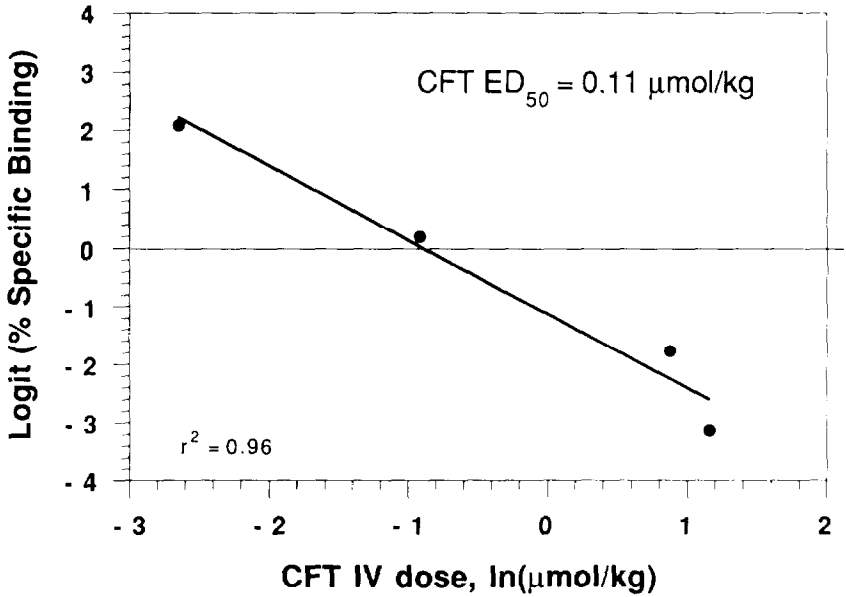

FIGURE 6. *Logit-log plot of four displacements performed with various doses of CFT. Data were acquired during four scanning experiments. To linearize the relationship between the injected dose and site occupancy, the percent displacement (P) was logit transformted as ln[P/(100-P)] and plotted versus ln dose. In this graph, 50 percent site occupancy corresponded to the 0 value on the y axis. Data were analyzed by linear regression (r^2 = 0.96). The inverse logarithm of the x intercept of the regression line was used as the estimation of the ED_{50} (0.40 µmol/kg).*

DISCUSSION

These studies suggest that [^{123}I]ß-CIT is a potentially useful ligand to label DA and 5-HT transporters in the living human brain.

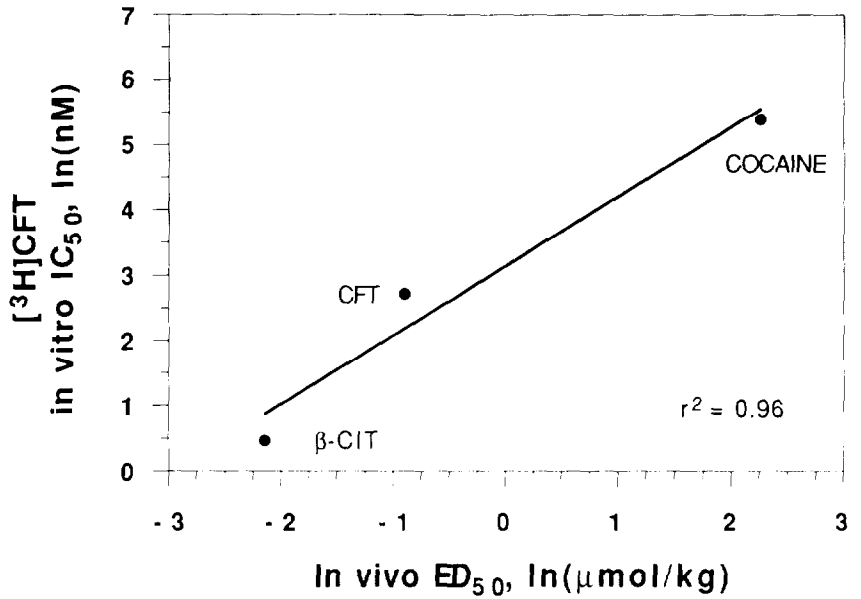

FIGURE 7. *Relarionship between the in vivo ED_{50} (μmol/kg) of cocaine, CFT, and ß-UT for displacing [^{123}I]ß-CIT binding in monkey striatum and their in vitro IC_{50}(nM) for displacing [^{3}H]CFT from DA transporters in monkey striatum. There was a significant relationship between in vivo ED_{50} values and in vitro [^{3}H]CFT IC_{50} values (r^2 = 0.96). Such a relationship was not found between the in vivo ED_{50} values and [^{3}H]paroxetine IC_{50} values (r^2 = 0.27).*

Binding Studies

ß-CIT displayed a similar high affinity for both DA and 5-HT transporters. Further pharmacological characterization with [^{125}I]ß-CIT demonstrated a good correlation between the potency of various drugs to inhibit DA uptake and to displace [^{125}I]ß-CIT binding in rat striatum (Boja et al. 1992). In the cortex, a similar correlation was found with the potency of various drugs to inhibit 5-HT uptake (Boja et al. 1992). The authors recently observed that displacement of [^{125}I]ß-CIT binding in rat and monkey striatum by citalopram was best fit with a two-site model, the first site corresponding to 5-10 percent of the binding

(Laruelle et al., in press- *b*). Since the IC_{50} of this first site was close to the affinity of citalopram for 5-HT transporter, the authors believethat 5-10 percent of [^{125}I]ß-CIT in vitro striatal binding is related to the 5-HT transporter. This value is in accordance with the density ratio of [^{3}H]GBR 12909 and [^{3}H]paroxetine binding sites in human striatum (Laruelle et al. 1988; Marcusson and Erikson 1988; Backstrom et al. 1989; De Keyser et al. 1989).

Pharmacokinetics

Studies of clearance from arterial plasma of the parent compound showed slow terminal half-lives (77-166 min in baboons and 108-153 min in vervets). Misra and colleagues (1977) reported a plasma terminal half-life of [^{3}H]cocaine in rhesus monkey of 79 min. Thus, these data suggested that ß-CIT might be metabolized more slowly than cocaine. The major metabolite was a polar, nonextractable fraction, and, thus, is expected not to cross the blood-brain barrier. This was confirmed by experiments in which monkeys (n = 3 [2 vervets and 1 baboon]) were euthanized 90-120 min after [^{125}I]ß-CIT injection. The parent compound represented 75 to 90 percent of the activity in the caudate but only 10 to 30 percent of the activity in the plasma.

Brain Uptake

The total brain uptake of the tracer was high, as attested by a high count rate within the field of view. The high brain uptake was measured more accurately with whole body dosimetry (Baldwin et al. 1993) that showed that 6 to 7 percent of the activity was present in the brain during the first h postinjection.

The activity was concentrated in the striatum and the midbrain/ hypothalamic area. This localization was confirmed with ex vivo autoradiographic studies in three animals performed at 120 min after injection of [^{123}I]ß-CIT. In these experiments, the authors found high levels of activities in the striatum, the hypothalamus, the colliculi, the substantia nigra, and the raphe nuclei.

The striatal activity increased for a prolonged period (2 to 3 h) and showed a remarkably stable plateau phase thereafter, with a negligible

washout phase (< 1 percent/h). As a result, the striatum-to-cerebellum ratio was very high at the end of the study (about 7 to 1). In contrast, the hypothalamic/midbrain activity peaked and washed out more quickly.

Pharmacological Specificity

Displacement experiments performed with unlabeled ß-CIT and the nonselective monoamine inhibitor LU 19-005 demonstrated that activity in the striatum and midbrain/hypothalamic area was associated with binding to saturable sites. Selective monoamine uptake inhibitors were then used to define the pharmacological identity of these sites.

At 300 min, the striatal activity was displaceable by GBR 12909, a DA selective drug, but not by citalopram, a 5-HT selective drug. This indicates that, at 300 min, the striatal uptake was primarily associated with DA transporters. The inverse was observed in the hypothalamic/ midbrain area, showing that the activity in this region was associated predominantly with 5-HT transporters. These results confirmed similar in vivo observations in rodents (Cline et al. 1992; Scheffel et al. 1992).

The absence of a citalopram effect in the striatum contrasted with in vitro experiments in which citalopram displaced about 10 percent of [^{125}I]ß-CIT equilibrium binding in the monkey caudate. The in vivo conditions are, however, very different from the in vitro equilibrium conditions. The rapid washout of the midbrain/hypothalamic area suggested that the uptake associated with 5-HT transporters washed out more quickly than the uptake associated with DA transporter. Thus, the component of striatal uptake associated with 5-HT transporter might have washed away at 300 min when the displacement experiments were performed.

Citalopram was the only drug found to be effective in increasing the washout rate in the hypothalamic/midbrain area. This is consistent with the fact that 5-HT transporters are more abundant than DA transporters in this region (Cortes et al. 1988; Laruelle et al. 1988; De Keyser et al. 1989). DA transporters are, however, present in the substantia nigra, but [^{123}I]ß-CIT binding to these sites was not demonstrated by the GBR 12909 injections. The interpretation of displacement experiments was more difficult in the hypothalamic/midbrain area

than in the striatum because of the absence of a prolonged plateau phase. This difficulty could be overcome by inducing a state of prolonged equilibrium by a constant infusion of the radiotracer. This paradigm, applied successfully for [^{123}I]iomazenil (Laruelle et al. 1993*b*), does allow a stable baseline of activity that increases the sensitivity to displacement experiments.

In Vivo Potencies of Cocaine Analogs

The stable baseline of [^{123}I]ß-CIT activity in the striatum allowed calculating the receptor occupancy ED_{50} of three related compounds: ß-CIT, cocaine, and CFT. There was a good relationship between the in vivo ED_{50} of these compounds and their in vitro IC_{50} for displacing [^{3}H]CFT ($r^2 = 0.96$) but not with their IC_{50} for displacing [^{3}H]paroxetine ($r^2 = 0.27$). Several conclusions can be made from this series of experiments. First, in vivo [^{123}I]ß-CIT binding in striatum is associated predominantly with DA transporters. Second, the affinity for the DA transporters is the main factor that explains the differences in ED_{50} between these drugs. Differences in peripheral clearance and blood-brain barrier permeability, if any, do not seem to have a significant contribution to the observed ED_{50} differences. Third, this paradigm has potential useful applications in humans to the study of the relationship between behavioral effects of cocaine-related drugs and kinetics of transporter occupancy.

[^{123}I]ß-CIT as a SPECT Radiotracer

[^{123}I]ß-CIT appears to be a promising SPECT radiotracer for labeling DA and 5-HT transporters. Some of the characteristics of the ligand are clearly advantageous: high brain uptake, slow peripheral clearance, low levels of metabolites in the brain, and low nonspecific binding and corresponding high levels of target-to-background ratio. Other characteristics (e.g., selectivity and high affinity) can be interpreted as positive or negative, depending on the intended application.

The lack of specificity for either the DA or the 5-HT transporter is not an ideal situation for the quantification of these sites in each brain region. However, it appears that binding to these transporters has a different kinetic profile, such that the striatal signal becomes predominantly associated with DA transporters after 180 min, and the peak of

uptake in the hypothalamic/midbrain activity is predominantly associated with 5-HT transporters. Thus, binding to each of these sites can be distinguished both anatomically and kinetically. If this observation is replicated in humans, it opens the opportunity to obtain information on both systems in one scanning session. This might be cost effective in clinical situations when alterations of both sites have been described, as in Parkinson's disease or in chronic cocaine abuse. More specific ligands, such as [^{123}I]isopropyl-CIT ([^{123}I]RTI-121; Scheffel et al. 1993) or [^{123}I]5-iodo-6-nitroquipazine (Mathis et al. 1992), are presently under development and might broaden the range of options available to the clinician.

The high affinity of [^{123}I]ß-CIT for the DA transporter, inducing a prolonged plateau phase in the striatum, is an ideal situation for pharmacological challenge tests, as performed here with cocaine analogs. This kinetic profile, however, creates a difficulty for the quantification of the binding sites. A ligand with a high tissue equilibrium volume of distribution (i.e., a high maximal number of binding sites (B_{max})-to-equilibrium binding constant [K_D] ratio) is not likely to reach equilibrium during the timeframe of the imaging session (Gjedde and Wong 1990), and equilibrium is required for measurement of B_{max} and K_D. In the absence of equilibrium, only the rate of association to the receptor can be measured (the product B_{max} k_{on}, with k_{on} being the association rate constant).

Furthermore, if equilibrium is not reached and if the association to the receptor is rapid as compared to the blood-brain barrier permeability, the activity in the region of interest reflects the blood flow more than the density of receptors, as observed with high affinity ligands like [^{123}I]qunuclidinyl benzilate (QNB) (Gibson et al. 1984) and [N-methyl-^{11}C]scopolamine (Vora et al. 1983; Frey et al. 1987). Under these conditions, little quantitative information can be gained by empirical methods, such as ratio methods, as opposed to model-based methods (Carson 1991) that are more difficult to implement in the clinical setting. Additional experiments comparing empirical methods to model-based methods with [^{123}I]ß-CIT are needed to explore this issue.

CONCLUSION

In conclusion, [^{123}I]ß-CIT appears to be a promising ligand for visualization and pharmacological studies of DA and 5-HT transporters. More experiments are needed to assess the protocol and methods necessary for measurement of the density and affinity of these sites. Development of these methods and evaluation of the tracer in humans currently are being performed in the authors' laboratory.

REFERENCES

Allard, P.; Alafuzoff, I.; Carlsson, A.; Erikson, K.; Ericson, E.; Gottfries, C.G.; and Marcusson, J.O. Loss of dopamine uptake sites labeled with [^{3}H]GBR-12935 in Alzheimer's disease. *Eur Neural* 30:181-185, 1990.

Andersen, P.H. The dopamine uptake inhibitor GBR 12909: Selectivity and molecular mechanism of action. *Eur J Pharmacol* 166:493-504, 1989.

Azizian, H.; Eabom, C.; and Pidcock, A. Synthesis of organotrialkylstannanes. The reaction between organic halides and hexaalkyldistannanes in the presence of palladium complexes. *J Organomet Chem* 215:49-58, 1981.

Bäckström, I.; Bergstrom, M.; and Marcusson, J. High affinity [^{3}H]paroxetine binding to serotonin uptake sites in human brain. *Brain Res* 486:261-265, 1989.

Baldwin, R.M.; Zea-Ponce, Y.; Zoghbi, S.S.; Laruelle, M.; Al-Tikriti, M.S.; Sybriska, E.H.; Malison, R.T.; Neumeyer, J.L.; Milius, R.A.; Wang, S.; Stabin, M.; Smith, E.O.; Chamey, D.S.; Hoffer, P.B.; and Innis, R.B. Evaluation of the monoamine uptake site ligand [^{123}I]methyl 3ß-(4-iodophenyl)tropane-2ß-carboxylate ([^{123}I]ß-CIT) in nonhuman primates: Pharmacokinetics, biodistribution, and SPECT imaging coregistered with MRI. *Nucl Med Biol* 20:597-606, 1993.

Balster, R.L.; Caroll, F.I.; Graham, J.H.; Mansbach, R.S.; Rahman, M.A.; Philip, A.; Lewin, A.H.; and Showalter, V.M. Potent substituted-3-ß-phenyltropane analogs of cocaine have cocaine-like discriminative stimulus effects. *Drug Alcohol Depend* 29:145-151, 1991.

Boja, J.W.; Mitchell, W.M.; Patel, A.; Kopajtic, T.A.; Carroll, F.I.; Lewin, A.H.; Abraham, P.; and Kuhar, M.J. High-affinity binding of [^{125}I]RTI-55 to dopamine and serotonin transporters in rat brain. *Synapse* 12:27-36, 1992.

Boja, J.W.; Patel, A.; Carroll, F.I.; Rahman, M.A.; Philip, A.; Lewin, A.H.; Kopajtic, T.A.; and Kuhar, M.J. [^{125}I]RTI-55: A potent ligand for dopamine transporters. *Eur J Pharmacol* 194: 133-134, 1991.

Carroll, F.I.; Gao, Y.; Rahman, M.A.; Abraham, P.; Parham, K.; Lewin, A.H.; Boja, J.W. and Kuhar, M.J. Synthesis, ligand binding, QSAR, and CoMFA study of 3ß-(p-substituted phenyl)tropane-2ß-carboxylic acid methyl esters. *J Med Chem* 34:27 19-2725, 1991.

Carson, R.E. Precision and accuracy considerations of physiological quantitation in PET. *J Cereb Blood Flow Metab* 11:A45-A50, 1991.

Cash, R.; Raisman, R.; Ploska, A.; and Agid, A. High and low affinity ^{3}H-imipramine binding sites in control and Parkinsonian brains. *Eur J Pharmacol* 117:71-80, 1985.

Chang, L.T. A method for attenuation correction in computed tomography. *IEEE Trans Natl Sci* NS-25:638-643, 1987.

Clarke, R.L.; Daum, S.J.; Gambino, A.J.; Aceto, M.D.; Pearl, J.; Levitt, M.; Cumiskey, W.R.; and Bogado, E.F. Compounds affecting the central nervous system: IV. 3ß-Phenyltropane-2-carboxylic esters and analogs. *J Med Chem* 16:1260-1267, 1973.

Cline, E.J.; Scheffel, U.; Boja, J.W.; Mitchell, W.M.; Caroll, F.I.; Abraham, P.; Lewin, A.H.; and Kuhar, M.J. In vivo binding of [^{125}I]RTI-55 to dopamine transporters: Pharmacology and regional distribution with autoradiography. *Synapse* 12:37-46, 1992.

Cortes, R.; Soranoi, E.; Pazos, A.; Probst, A.; and Palacios, J.M. Autoradiography of antidepressant binding sites in the human brain: Localization using [^{3}H]imipramine and [^{3}H]paroxetine. *Neuroscience* 27:473-496, 1988.

Crow, T.J.; Cross, A.J.; Cooper, S.J.; Deakin, J.F.W.; Ferrier, I.N.; Johnson, J.A.; Joseph, M.H.; Owen F.; Poulter, M.; Lofthouse, R.; Corsellis, J.A.N.; Chambers, D.R.; Blessed, G.; Perry, E.K.; and Perry, E.H. Neurotransmitter receptors and monoamine metabolites in the patients with Alzheimer-type dementia and depression and suicides. *Neuropharmacology* 23:1561-1569, 1984.

De Keyser, J.; De Baecker, J.P.; Ebinger, G.; and Vauquelin, G. [^{3}H]GBR 12935 binding to dopamine uptake sites in the human brain. *J Neurochem* 53:1400-1404, 1989.

Eckelman, W.C.; Rzeszotarski, W.J.; Gibson, R.E.; Francis, B.; and Reba, R.C. Use of 3-quinulidinyl 4-iodobenzilate as a receptor binding radiotracer. *J Nucl Med* 26:637-642, 1985.

Frey, K.A.; Hichwa, R.D.; Ehrenkaufer, R.L.E.; and Agranoff, B.W. Quantitative in vivo receptor binding: III. Tracer kinetic modeling of muscarinic cholinergic receptor binding. *Proc Natl Acad Sci U S A* 82:6711-6715, 1987.

Gibson, R.E.; Weckstein, D.J.; Jagoda, E.M.; Rzeszotarski, W.J.; Reba, R.C.; and Eckelman, W.C. The characteristics of I-125 4-IQNB and H-3 QNB in vivo and in vitro. *J Nucl Med* 25:214-222, 1984.

Gjedde, A., and Wong, D.F. Modeling neuroreceptor binding of radioligands in vivo. In: Frost, J.J., and Wagner, H.N., Jr., eds. *Quantitative Imaging: Neuroreceptors, Neurotransmitters, and Enzymes.* New York: Raven Press, 1990. pp. 51-79.

Glowinsky, J., and Axelrod, J. Inhibition of uptake of tritiated noradrenaline in intact rat brain by imipramine and structurally related compounds. *Nature* 204:107-114, 1964.

Hirai, M.; Kitamura, N.; Hashumoto, T.; Nakai, T.; Mita, T.; Shirakawa, O.; Yamadori, T.; Amano, T.; Noguchi-Kuno, S.A.; and Tanaka, C. [^{3}H]GBR-12935 binding sites in human striatal membranes: Binding characteristics and changes in Parkinsonians and schizophrenics. *Jpn J Pharmacol* 47:237-243, 1988.

Holman, B.L.; Carvalho, P.A.; Zimmerman, R.E.; Johnson, K.A.; Tumeh, S.S.; Smith, A.P.; and Genna, S. Brain perfusion SPECT using an annular single crystal camera: Initial clinical experience. *J Nucl Med* 31:1456-1461, 1990.

Hyttel, J. Citalopram: Pharmacological profile of a specific serotonin uptake inhibitor with antidepressant activity. *Prog Neuropsychopharmacol Biol Psychiatry* 6:277-295, 1982.

Hyttel, J., and Larsen, J.-J. Neurochemical profile of Lu 19-005 a potent inhibitor of uptake of dopamine, noradrenaline, and serotonin. *J Neurochem* 44:1615-1621, 1985.

Innis, R.; Baldwin, R.; Sybirska, E.; Zea, Y.; Laruelle, M.; Al-Tikriti, M.; Chamey, D.; Zoghbi, S.; Smith, E.; Wisniewski, G.; Hoffer, P.; Wang, S.; Milius, R.; and Neumeyer, J. Single photon emission computed tomography imaging of monoamine reuptake sites in primate brain with [^{123}I]CIT. *Eur J Pharmacol* 200:369-370, 1991*b*.

Innis, R.; Zoghbi, S.; Johnson, E.; Woods, SW.; Al-Tikriti, M.; Baldwin, R.; Seibyl, J.; Malison, R.; Zubal, G.; Chamey, D.; Heninger, G.; and Hoffer, P. SPECT imaging of the benzodiazepine receptor in non-human primate brain with [^{123}I]Ro 16-0154. *Eur J Pharmacol* 193:249, 1991*a*.

Janowsky, A.; Vocci, F.; Berger, P.; Angel, I.; Zelnick, N.; Kleinman, J.; Skolnick, P.; and Paul, S.M. [^{3}H]GBR-12935 binding to the dopamine transporter is decreased in the caudate nucleus in Parkinson's disease. *J Neurochem* 49:617-621, 1987.

Joyce, J.N.; Shane, A.; Lexow, N.; Winokur, A.; Casanova, M.F.; and Kleinman, J. E. Serotonin uptake sites and serotonin receptors are altered in the limbic system of schizophrenics. *Neuropsychopharmacology* 8:315-336, 1993.

Kaufman, M.J., and Madras, B.K. Severe depletion of cocaine recognition sites associated with the dopamine transporter in Parkinson's diseased striatum. *Synapse* 49:43-49, 1991.

Kuhar, M.J.; Ritz, M.C.; and Boja, J.W. The dopamine hypothesis of the reinforcing properties of cocaine. *Trends Neurosci* 14:299-302, 1991.

Kung, M.-P.; Kung, H.F.; Billings, J.; Yang, Y.; Murphy, R.A.; and Alavi, A. Characterization of IBF as a new selective dopamine D-2 receptor imaging agent. *J Nucl Med* 31:648-654, 1990.

Kung, H.F.; Pan, S.; Kung, M.-P.; Billings, J.; Kasliwal, R.; Reilley, J.; and Alavi, A. In vitro and in vivo evaluation of [^{123}I]IBZM: A potential CNS D-2 dopamine receptor imaging agent. *J Nucl Med* 30:88-92, 1989.

Laruelle, M.; Abi-Dargham, A.; Casanova, M.F.; Toti, R.; Weinberger, D.R.; and Kleinman, J.E. Selective abnormalities of prefrontal serotonergic receptors in schizophrenia: A postmortem study. *Arch Gen Psychiatry,* in press-*a*.

Laruelle, M.; Abi-Dargham, A.; Rattner, Z.; Al-Tikriti, M.; Zea-Ponce, Y.; Zoghbi, S.S.; Chamey, D.S.; Price, J.; Frost, J.J.; Hoffer, P.B.; Baldwin, R.M.; and Innis, R.B. Single photon emission computed tomography measurement of benzodiazepine receptor number and affinity in primates brain: a constant infusion paradigm with [^{123}I]iomazenil. *Eur J Pharmacol* 230:119-123, 1993*b*.

Laruelle, M.; Baldwin, R.M.; Malison, R.T.; Zea-Ponce, Y.; Zoghbi, S.S.; Al-Tikriti, M.; Sybriska, E.H.; Zimmerman, R.C.; Wisnieski, G.; Neumeyer, J.L.; Milius, R.A.; Wang, R.A.; Smith, E.O.; Roth, R.H.; Chamey, D.; Hoffer, P.B.; and Innis, R.B. SPECT imaging of dopamine and serotonin transporters with [^{123}I]ß-CIT: Pharmacological characterization of brain uptake in nonhuman primates. *Synapse* 13:295-309, 1993*a*.

Laruelle, M.; Giddings, S.S.; Zea-Ponce, Y.; Chamey, D.S.; Neumeyer, J.L.; Baldwin, R.M.; and Innis, R.B. [^{125}I]ß-CIT in vitro binding to dopamine and serotonin transporters under "physiological" conditions. *J Neurochem,* in press-*b*.

Laruelle, M.; Vanisberg, M.-A.; and Maloteaux, J.-M. Regional and subcellular localization in human brain of [^{3}H] paroxetine binding a marker of serotonin uptake sites. *Biol Psychiatry* 24:299-309, 1988.

Madras, B.K.; Fahey, M.A.; Bergman, J.; Canfield, D.R.; and Spealman, R.D. Effects of cocaine and related drugs in non human primates: I. [^{3}H]Cocaine binding sites in caudate-putamen. *J Phannacol Exp Ther* 251:131-141, 1989*a*.

Madras, B.K.; Spealman, R.D.; Fahey, M.A.; Neumeyer, J.L.; Saha, J.K.; and Milius, R.A. Cocaine receptors labeled by [^{3}H]-2ß-carbomethoxy-3ß-(4-fluorophenyl)tropane. *Mel Pharmacol* 36:5 18-524, 1989*b*.

Malison, R.T.; Miller, E.G.; Greene, R.; Hoffer, P.B.; McCarthy, G.; and Innis, R.B. Computer-assisted coregistration of multislice SPECT and MRI images by fixed external fiducials. *J Comput Assist Tomogr,* in press.

Maloteaux, J.M.; Vanisberg, M.A.; Laterre, C.; Javoy-Agid, F.; Agid, Y.; and Laduron, P.M. [^{3}H]GBR-12935 binding to dopamine uptake sites: Subcellular localization and reduction in Parkinson's disease and progressive supranuclear palsy. *Eur J Pharmacol* 156:331-340, 1988.

Marcusson, J., and Erikson, K. [^{3}H]GBR-12935 binding to dopamine uptake sites in the human brain. *Brain Res* 457:122-129, 1988.

Mathis, C.A.; Biegon, A.; Taylor, S.E.; Enas, J.E.; and Hanrahan, SM. [^{125}I]5-Iodo-6-nitro-2-piperazinylquino1ine: A potent and selective ligand for the serotonin uptake complex. *Eur J Pharmacol* 210:103-104, 1992.

Misra, A.L.; Giri, V.V.; Patel, M.N.; Alluri, V.R.; and Mule, S.J. Disposition and metabolism of [^{3}H]cocaine in acutely and chronically treated monkeys. *Drug Alcohol Depend* 2:261-272, 1977.

Neumeyer, J.L.; Wang, S.; Milius, R.A.; Baldwin, R.M.; Zea-Ponce, Y.; Hoffer, P.B.; Sybirska, E.; Al-Tikriti, M.; Laruelle, M.; and Innis, R.B. [^{123}I]2ß-carbomethoxy-3ß-(4-iodophenyl)tropane (ß-CIT): High affinity SPECT radiotracer of monoamine reuptake sites in brain. *J Med Chem* 34:3144-3146, 1991.

Niznik, H.B.; Fogel, E.F.; Fassos, F.F.; and Seeman, P. The dopamine transporter is absent in Parkinsonian putamen and reduced in the caudate nucleus. *J Neurochem* 56:192-198, 1991.

Paul, S.M.; Rehavi, M.; Skolnick, P.; and Goodwin, F.K. High affinity binding of antidepressants to a biogenic amine transport site in human brain and platelet: Studies in depression. In: Post, R.M., and Ballinger, J.C., eds. *Neurobiology of Mood Disorders.* Baltimore: Williams & Wilkins, 1984. pp. 846-853.

Perry, E.K.; Marshall, E.F.; Blessed, G.; Tomlinson, B.E.; and Perry, R.H. Decreased imipramine binding in the brains of patients with depressive illness. *Br J Psychiatry* 142:188-192, 1983.

Raisman, R.; Cash, R.; and Agid, Y. Parkinson's disease: Decreased density of ^{3}H-imipramine and ^{3}H-paroxetine binding sites in putamen. *Neurology* 36:556-560, 1986.

Reith, M.E.A.; Sershen, H.; Allen, D.L.; and Lajtha, A. A portion of [^{3}H]cocaine binding in brain is associated with serotonergic neurons. *Mol Pharmacol* 23:600-606, 1983.

Reith, M.E.A.; Sershen, H.; and Lajtha, A. Saturable [^{3}H]cocaine binding in central nervous system of mouse. *Life Sci* 27:1055-1062, 1980.

Riche, D.; Hantraye, P.; Guibert, B.; Naquet, R.; Loch'h, C.; and Mazière, M. Anatomical atlas of the baboon's brain in the orbito-meatal plane used in experimental positron emission tomography. *Brain Res Bull* 20:283-301, 1988.

Ritz, M.C.; Cone, E.J.; and Kuhar, M.J. Cocaine inhibition of ligand binding at dopamine, norepinephrine, and serotonin transporters: A structure activity study. *Life Sci* 46:635-645, 1990.

Scheffel, U.; Dannals, R.F.; Cline, E.J.; Ricaurte, G.A.; Carrel, F.I.; Abraham, P.; Lewin, A.H.; and Kuhar, M.J. [$^{123/125}$I]RTI-55, an in vivo label for the serotonin transporter. *Synapse* 11:134-139, 1992.

Scheffel, U.; Dannals, R.F.; Wong, D.F.; Yokoi, F.; Carroll, F.I.; and Kuhar, M.J. Dopamine transporter imaging with novel, selective cocaine analogs. *Neuroreport* 3:969-972, 1993.

Shaya, E.K.; Scheffel, U.; Dannals, R.F.; Ricaurte, G.A.; Carrol, F.I.; Wagner, H.N.; Kuhar, M.J.; and Wong, D.F. In vivo imaging of dopamine reuptake sites in the primate brain using single photon emission computed tomography (SPECT) and Iodine- 123 labeled RTI-55. *Synapse* 10:169-172, 1992.

Stanley, M.; Virgilio, J.; and Gershon, S. Tritiated imipramine binding sites are decreased in the frontal cortex of suicides. *Science* 216:1337-1339, 1982.

Stoddart, H.F., and Stoddart, H.A. A new development in single gamma transaxial tomography Union Carbide focused collimator scanner. *IEEE Trans Nucl Sci* 26:2710-2712, 1979.

Vora, M.M.; Finn, R.D.; Boothe, D.R.; Liskowsky, D.R.; and Potter, L.T. [*N*-methyl-^{11}C]-scopolamine: synthesis and biodistribution in rat brain. *J Labelled Comp Radiopharm* 20:1229-1236, 1983.

ACKNOWLEDGMENTS

The authors gratefully acknowledge the help of members of the Neurochemical Brain Imaging Program, Department of Psychiatry and Section of Nuclear Medicine, Yale School of Medicine, and Research Biochemicals Int. (Natick, MA) for providing the stannyl precursor of [^{123}I]ß-CIT.

AUTHORS

Marc Laruelle, M.D.
Assistant Professor

Ronald M. Baldwin, Ph.D.
Research Scientist

Robert B. Innis, M.D., Ph.D.
Associate Professor
Department of Psychiatry
Yale School of Medicine
West Haven VA Medical Center/116A2
West Haven, CT 06516

Cerebral Blood Flow Changes With Acute Cocaine Intoxication: Clinical Correlations With SPECT, CT, and MRI

I. Mena, R.J. Giombetti, B.L. Miller, K. Garrett, J. Villanueva-Meyer, C. Mody, and M.A. Goldberg

INTRODUCTION

Fourteen consecutive patients with acute cocaine intoxication and neurological symptoms were studied using computerized axial tomography (CT) and single photon emission computerized tomography (SPECT). Symptoms included transient ischemic attacks, stroke, seizures, and confusional states. Cerebral blood flow (CBF) was imaged with 99mTechnetium [99mTc] d,l, hexamethylpropyleneamine-oxime (HMPAO) and was measured using Xenon-133 (133Xe). Focal, multifocal, or diffuse areas of hypoperfusion were found in all 14 patients with either [99mTc]HMPAO SPECT or 133Xe. Multiple small, superficial, or deep areas of hypoperfusion causing a "scalloped" appearance on SPECT were seen in 12 patients, and this pattern is observed frequently in cocaine abuse. The mean CBF measured with 133Xe was diminished at 43.6+3.4 ml/100 g/min compared to 55.1+1.4 ml/100 g/mm in normals. Brain SPECT was useful in the evaluation of patients who were symptomatic from cocaine abuse, and cortical and subcortical vascular abnormalities not seen on CT or magnetic resonance imaging (MRI) were often found with SPECT.

Cocaine continues to be a major public health problem in the United States, with as many as 5 million daily users (U.S. Department of Health and Human Services 1990). While the general medical complications of cocaine have been reported extensively, neurological disease has received less attention and only recently have cocaine-induced seizures, transient ischemic attacks (TIA), and strokes been described (Brust and Richter 1977; Caplan et al. 1981; Mody et al. 1988; Levine and Welch 1988; Levine et al. 1990; Root and Rowbotham 1988).

Although vasospasm has been proposed as a possible mechanism for cocaine-induced TIA and ischemic stroke, angiography is often normal in these patients (Mody et al. 1988). The combined use of the 133Xe washout to quantify CBF and [99mTc]HMPAO SPECT to obtain a high-resolution image of CBF may help delineate the pathophysiological mechanisms associated with cocaine-induced neurological disease.

The authors evaluated CBF changes in 14 patients with neurological symptoms due to acute cocaine intoxication. CBF was assessed quantitatively with 133Xe, while high-resolution tomographic images of CBF were obtained with [99mTc]HMPAO. Clinical diagnoses were correlated with CT, MRI, and SPECT.

PATIENTS

Patients entering the emergency room at the Harbor-University of California, Los Angeles (UCLA) Medical Center with cocaine intoxication and neurological symptomatology were referred for study. In all, cocaine abuse (mostly "crack" cocaine) had occurred within the past 48 hours, and subjects with a history of polysubstance abuse were excluded. The history of cocaine abuse was obtained from the patient and relatives or friends, and urine toxicology was performed. All patients were evaluated with neurological examinations, CT or MRI, and SPECT. Cerebral angiography and lumbar puncture were performed when clinically indicated.

Regional CBF (rCBF)

133Xe was used for absolute measurements of rCBF. 1110 Megabecquerel (MBq) (30 millicuries [mCi]) of 133Xe was injected intravenously, and CBF was measured using a lo-probe system in a self-contained bedside structure. After intravenous injection of 133Xe, measurements were performed for 10 minutes. The slow and fast component of the cerebral washout was calculated, beginning at the time when the exhaled air dropped to 20 percent of maximum. The slow exponential was subtracted from the observed brain curves, and a fast component was defined. CBF was derived using the inert gas equation as defined initially by Kety and Schmidt (1945), and the

results were expressed in ml/100 g/min. CBF was calculated for all patients, and a mean and standard error of the 10-probe measurements was reported.

The authors used [99mTc]HMPAO as a cerebral perfusion imaging molecule for the study (Neirinckx et al. 1987; Sharp et al. 1986). Each patient received 740 MBq (20 mCi) of [99mTc]HMPAO, injected intravenously within 20 minutes after reconstitution. SPECT scanning started 2 hours after injection to clear soft tissue background activity. [99mTc]HMPAO brain SPECT was performed using a large field-of-view rotating gamma camera with a truncated detector. The camera was equipped with a high-resolution parallel-hole collimator and operated on a step-and-shoot modality. The orbit was circular-360 degrees. Sixty images (one image for every 6-degree step) were gathered. Each image took 30 seconds, and total acquisition time was 30 minutes. Reconstruction was performed using backprojection reconstruction with Hanning filtering. Transaxial, coronal, and sagittal sets of images were obtained. Each set had 14 to 16 images, depending on the volume of the brain. The images were displayed using a color scale that denoted abnormally diminished uptake-defined by a drop below 60 percent of maximal brain activity.

The [99mTc]HMPAO brain SPECT lesions were categorized as demon-strating: no abnormalities, multiple superficial cortical lesions, multi-focal deep periventricular lesions (periventricular scalloping), or focal wedge-shaped hypoperfusion. Lesions also were defined as to their location. Abnormalities were described qualitatively by a radiologist blinded to the patients' clinical state. A data base collection of 10 age-matched normal volunteers (age 32±5 years) was used as a reference.

RESULTS

Clinical Description

Fourteen patients were enrolled in the study. The patients' problems included ischemic stroke (4), TIA (3), brain hemorrhage (2), generalized seizures (2), and confusional states (3). The mean patient age was 32.9±2.7 standard error of the mean (SEM) years, and there were

eight females and six males. Overall, the patients were free of pre-existing medical conditions, although one had chronic hypertension (patient #1) and another had a history of migraine headaches (patient #5).

Ischemic Stroke. Three patients with ischemic strokes had cerebral localization verified by CT or MRI (patients #2, #3, and #4) while a fourth (patient #1) had normal CT and MRI but an abnormal SPECT. Patient #3 had a right frontal (anterior cerebral artery distribution) infarct, patient #2 had bilateral occipital (posterior cerebral artery) infarcts, and patient #4 had a pontine infarct. Patient #1 had a suspected right hemispheric stroke because he developed left hemiparesis with hemisensory loss to pinprick. However, head CT, MRI, and cerebral angiography were all normal, and focal abnormalities that correlated with clinical symptoms were evident only on SPECT.

T/A. Two patients developed symptoms of middle cerebral artery distribution TIA (patients #6 and #7). Symptoms and focal deficits had resolved by the time of neurological consultation in both patients (within 8 hours). Patient #6 had both a CT and cerebral angiography that were normal. Patient #7 also had a normal CT, but angiography was not performed. In both, SPECT was abnormal.

A third patient (#5) had TIA-like symptoms minutes after intranasal cocaine abuse. The episode started with scintillating scotoma described as "clear, moving needles" and was followed by right visual field loss, word-finding difficulty, and right upper extremity numbness that lasted 20 minutes. No headache was associated with this episode, but the patient had a history of two previous episodes of visual disturbances followed by hemicranial headaches not associated with cocaine abuse. The patient's CT was normal, and a diagnosis of cocaine-induced migraine versus TIA was made.

Cerebral Hemorrhage. Two patients (#8 and #9) had large bleeds in the basal ganglia (#8) and thalamus (#9) demonstrated with CT. Although the hemorrhages occurred in places typical for hypertensive hemorrhage, neither patient had a history of hypertension.

Confusional States. Three patients (#10, #11, and #12) presented with confusional states characterized by drowsiness, inattention, and

fluctuating level of consciousness. All had normal head CT, and all improved to baseline mental status within 48 hours.

Seizures. Two patients (#13 and #14) came to the hospital due to generalized tonic-clonic seizures. Neither patient had a history of seizures, and both the neurological examination, electroencephalogram, and head CT were normal.

SPECT

Absolute CBF was measured in all patients with 133Xe. Mean CBF was 43.6+3.4 ml/100 g/min compared to a CBF of 55.1+1.4 ml/100 g/min in a group of age-matched normals. Nine patients had markedly diminished CBF (< 45 ml/100 g/min) while in five it was > 45 ml/100 g/min. All 14 patients had abnormal cerebral perfusion with [99mTc]HMPAO SPECT. Multiple superficial or deep lesions (periventricular scalloping) occurred in 12 patients (86 percent). The most common focal cortical lesions were unilateral parietal-occipital lesions (43 percent) and bilateral frontal lesions (29 percent). The SPECT results are summarized in table 1.

Two patients did not demonstrate cortical scalloping, one had a pontine stroke (patient #4) and the other had a confusional state (patient #10). Patient #10 came to the hospital in a stupor, but she was alert and oriented when her SPECT was performed 10 hours after the onset of symptoms. At that time, she was irritable, hostile, and disinhibited. These symptoms resolved within 48 hours. On SPECT, scalloping was not found, although CBF measured with 133Xe was extremely low at 21 ml/100 g/min and brain SPECT revealed large areas of frontal hypoperfusion bilaterally.

There was not a one-to-one correlation between clinical symptoms, CT, MRI, and SPECT, although SPECT appeared extremely sensitive to symptoms of focal ischemia. In only one stroke patient (#2) did findings on CT, MRI, and SPECT strongly correlate, although SPECT also revealed temporal hypoperfusion and diffuse scalloping. Patient #1 had a grossly abnormal SPECT with marked right parietal

TABLE 1. *Demographic data*

PT	AGE	DIAGNOSIS	CT	MRI	rCBF*	HMPAO SPECT*
#1 RM	34	L HEMISPHERE STROKE	NL	NL	38	SCALLOPING, R PAR, B/L TEMPORAL, L FRONTAL
#2 RC	54	BL OCCIPITAL STROKE	R > L PCA INFARCT	R > L PCA INFARCT	46	SCALLOPING, B/L PAR-OCC, B/L TEMP
#3 RC	35	R FRONTAL STROKE	R ACA INFARCT	R ACA INFARCT, LACUNES, R CAUDATE, L PONS	41	SCALLOPING, L FRONTAL, B/L PAR
#4 JD	24	L PONTINE STROKE	L PONTINE INFARCT	ND	49	B/L PAR
#5 KG	27	L PCA TIA MIGRAINE	NL	ND	46	SCALLOPING, L OCC-PAR, L TEMP
#6 JH	38	R MCA TIA	NL	ND	48	SCALLOPING, L PAR, B/L TEMP, L > R
#7 AN	26	L MCA TIA	NL	ND	43	SCALLOPING, B/L FRONTAL, B/L TEMP, B/L PAR
#8 SH	41	CEREBRAL HEMORRHAGE	HEMATOMA, L PUTAMEN	ND	38	SCALLOPING, L PAR-OCC
#9 RJ	42	CEREBRAL HEMORRHAGE	HEMATOMA, L THALAMUS	ND	40	SCALLOPING, L PAR
#10 EA	21	CONFUSIONAL STATE	NL	ND	43	B/L FRONTAL
#11 CB	45	CONFUSIONAL STATE	NL	ND	47	SCALLOPING, B/L PAR-OCC, R TEMP

PT	AGE	DIAGNOSIS	CT	MRI	rCBF[a]	HMPAO SPECT[b]
#12 KK	24	CONFUSIONAL STATE	NL	ND	44	SCALLOPING, L PAR
#13 RR	24	GENERALIZED TONIC-CLONIC SEIZURE	NL	ND	43	SCALLOPING, L PAR-OCC, L TEMPORAL
#14 SG	25	GENERALIZED TONIC-CLONIC SEIZURE	NL	ND	42	SCALLOPING, B/L FRONTAL, B/L PARIETAL

[a]rCBF in ml/100 g/min

[b]HMPAO SPECT location of hypoperfusion

KEY: L = left; R = right; NL = normal; B/L = bilateral; ND = not done; PAR = parietal; TEMP = temporal; PCA = posterior cerebral artery; OCC = occipital; ACA = anterior cerebral artery; MCA = middle cerebral artery

hypoperfusion that corresponded to his clinical stroke, even though his CT and MRI were normal. Also, severe periventricular scalloping and small cortical perfusion deficits were seen. Patient #3 had multiple deficits on SPECT, but the findings did not correlate with abnormalities on CT and MRI, which fit better with his clinical syndrome. Patient #4 had posterior circulation hypoperfusion on SPECT that was consistent with the pontine stroke seen on CT. All three patients (#5, #6, and #7) with TIA had cerebral hypoperfusion that correlated with clinical symptoms, although CT was normal in all three. In patients with cerebral hemorrhage (#8 and #9), diffuse cerebral hypoperfusion was seen in addition to the decreased flow at the site of hemorrhage.

In those patients with confusional states or seizures (#10 to #14) diffuse and multifocal deficits were found in all, except in patient #10. There were no clinical symptoms or neurological deficits to correspond to brain SPECT abnormalities, but rather these findings appear to be evidence of the diffuse cerebral effects of cocaine.

DISCUSSION

Acute cocaine intoxication caused both generalized and focally diminished CBF. Mean CBF was 43.6 ml/100 g/min, and in nine it was diminished markedly at < 45 ml/100 g/min. In all 14 patients abnormalities were visualized with [99mTc]HMPAO. The most striking abnormalities seen were multifocal small cortical and sometimes deep areas of hypoperfusion. A characteristic and unusual scalloping pattern of periventricular perfusion was noted. The authors previously had seen this perfusion pattern in patients with both cerebral vasculitis and with acquired immunodeficiency syndrome (AIDS) dementia syndrome. It was not present in any of the control patients.

Recent findings show vasoconstriction in coronary vessels during catheterization after small doses of cocaine (Lange et al. 1989; Kaye and Fainstat 1987; Krendel et al. 1990), and brain SPECT appears to be a sensitive way to detect similar phenomena in cerebral vessels. The authors suspect that this periventricular subcortical hypoperfusion (scalloping) is the manifestation of cerebral vasoconstriction and is a characteristic of vasoconstrictive agents such as cocaine. The scalloping may be due to the constriction of small- and medium-sized arteries, although for reasons that are still undetermined. The deep white matter appears to show selective involvement with cocaine. A second hypothesis is that focal areas of hypoperfusion are secondary to clusters of cells damaged during the acute, intense, prolonged vasoconstriction induced by cocaine. Primary hypofunction will induce a focal secondary hypoperfusion.

Also, large wedge-shaped cortical perfusion defects were seen frequently. These deficits appeared to be caused by vasoconstriction of larger arteries or confluence of multiple constricted smaller arteries, This pattern was found in three of four stroke patients and two patients with TIA. Unlike the scalloping and multifocal cortical deficits that had uncertain clinical significance, these large SPECT deficits corresponded to focal clinical symptomatology. These wedge-shaped areas of hypoperfusion are seen in patients with other causes of cerebral ischemia.

Frontal lobe hypopetfusion was found in over one-quarter of the patients, and the patients with this abnormality were irritable and disinhibited-characteristics of patients with frontal lobe dysfunction (Stuss and Benson 1986; Miller et al. 1989). A previous study of CBF in cocaine abusers was performed by Volkow and colleagues (1988), who used positron emission tomography (PET) to assess cerebral perfusion with oxygen-labeled water. Patients for that study were recruited from a drug rehabilitation center and were, by definition, without major medical or neurological illness. The patients in this study differed in this respect because all had neurological symptoms. In Volkow's study, diffuse patchy areas of hypoperfusion were observed, and marked hypoperfusion was seen in the prefrontal cortex. Repeat scans performed 10 days later revealed persistent deficits. The authors' findings of multifocal hypoperfusion and frontal hypoperfusion appear consistent with this earlier PET work. More recent studies by Volkow and colleagues (1991) in subjects during the first week of withdrawal from cocaine showed increased metabolism of glucose in the orbital-frontal cortex and basal ganglia.

Like Volkow and colleagues (1991), the authors found a substantial group of patients with frontal hypoperfusion. Although these changes may have been secondary to alterations in metabolism induced by the cocaine, it is possible that ischemia vasospasm involving frontal lobes may have been the primary event responsible for these patients' behavioral changes (Miller et al. 1989). Cocaine intoxication often leads to behavioral disinhibition, and it is conceivable that these behavioral disturbances are due to frontal lobe dysfunction induced by focal ischemia. Alternately, the frontal hypoperfusion could have been a premorbid characteristic of the subjects who will abuse cocaine, although this seems unlikely. A third explanation would be that the hypoperfusion was secondary to a metabolic disturbance induced by changes in neurotransmitters associated with cocaine.

Both of the patients with seizures had brief generalized tonic-clonic spells, but both were clinically normal by the time that SPECT was performed. The SPECT findings in these patients were nonspecific and revealed diffuse areas of hypoperfusion and scalloping-abnormalities that were seen in patients with other diagnoses. Neither

of the patients had focal seizures where SPECT has been reported to show focal hypoperfusion in the postictal state (Katz et al. 1990).

SUMMARY AND CONCLUSIONS

In summary, these data suggest that widespread primary or secondary cerebral vasoconstriction is common in patients with neurological complications from cocaine. In most patients, SPECT showed widespread hypoperfusion in regions that had no clear clinical significance (e.g., the periventricular area). In many, the SPECT was performed more than 24 hours after the onset of neurological symptomatology. These findings raise several questions.

It has been assumed that these SPECT changes in patients with acute neurological symptoms are temporary, although it will be important to determine whether these areas of hypoperfusion persist after symptoms have abated. Recently, Holman and colleagues (1991) found multifocal and deep areas of hypoperfusion with SPECT in 16 of 18 patients with a history of chronic cocaine abuse. Although most of the subjects tested positive for cocaine, several had abstained from cocaine use for weeks prior to the study. All 18 subjects had neuropsychological deficits, 13 mild and 5 moderate. Similarly, Pascual-Leone and colleagues (1991) have shown that CT scan atrophy strongly correlates with the duration of cocaine abuse, suggesting that brain injury may occur with continued use of cocaine. It is the authors' concern that cocaine abuse might produce permanent changes in cerebral perfusion.

In conclusion, brain SPECT was found to be a useful procedure in the evaluation of acute cocaine intoxication. Brain SPECT revealed focal cortical lesions not seen on head CT or MRI, which corresponded to clinical deficits. In addition, [99mTc]HMPAO brain SPECT had a characteristic scalloped appearance, and this may be a marker for acute intoxication with cocaine. This study further supports the contention that cocaine causes neurological disease by its vasoconstrictive action.

REFERENCES

Brust, J., and Richter, R.W. A stroke associated with cocaine abuse. *N Y State J Med* 77:1473-1475, 1977.

Caplan, L.R.; Hier, D.B.; and Banks, G. Stroke and drug abuse. *Stroke* 13:869-872, 1981.

Cregler, L.L., and Mark, H. Medical complications of cocaine abuse. *N Engl J Med 3* 15:1495-1500, 1986.

Holman, B.L.; Carvalho, P.A.; Mendelson, J.; Teoh, S.K.; Nardin, R.; Hallgring, E.; Hebben, N.; and Johnson, K.A. Brain perfusion is abnormal in cocaine-dependent polydrug users: A study using technetium-99m-HMPAO and ASPECT. *J Nucl Med* 32:1206-1210, 1991.

Katz, A.; Bose, A.; Lind, S.J.; and Spencer, S.S. SPECT in patients with epilepsia partialis continua. *Neurology* 40:1848-1850, 1990.

Kaye, B.R., and Fainstat, M. Cerebral vasculitis associated with cocaine abuse. *JAMA* 258:2104-2106, 1987.

Kety, S.S., and Schmidt, C.F. The determination of cerebral blood flow in man by the use of nitrous oxide in low concentrations. *Am J Physiol* 143:53-66, 1945.

Krendel, D.A.; Ditter, S.M.; Frankel, M.R.; and Ross, W.K. Biopsy-proven cerebral vasculitis associated with cocaine abuse. *Neurology* 40:1092-1094, 1990.

Lange, R.A.; Cigarroa, R.G.; Yancy, C.W. Jr.; Willard, J.E.; Popma, J.J.; Sills, M.N.; McBride, W.; Kim, A.S.; and Hillis, L.D. Cocaine-induced coronary-artery vasoconstriction. *N Engl J Med* 321:1557-1562, 1989.

Levine, S.L., and Welch, K.M.A. Cocaine and stroke. *Stroke* 19:779-783, 1988.

Levine, S.R.; Brust, J.C.M.; Futtrell, N.; Ho, K.L.; Blake, D.; Millikan, C.H.; Brass, L.M.; Fayad, P.; Schultz, L.R.; and Selwa, J.F. Cerebrovascular complications of the use of the "crack" form of alkaloidal cocaine. *N Engl J Med* 323:699-704, 1990.

Miller, B.L.; Garrett, K.; Leedom, L.; and Djenderedjian, A. Neuro-spect in cocaine abuse: rCBF and HMPAO findings. *Clin Nucl Med* 14:12, 1989.

Mody, C.K.; Miller, B.L.; McIntyre, H.B.; Cobb, S.K.; and Goldberg, M.A. Neurological complications of cocaine abuse. *Neurology* 38:1189-1193, 1988.

Neirinckx, R.D.; Canning, L.R.; Piper, I.M.; Nowotnik, D.P.; Pickett, R.D.; Holmes, R.A.; Volkert, W.A.; Forster, A.M.; Weisner, P.S.; Marriott, J.A.; and Chaplin, S.B. Technetium-99md,l HMPAO: A new radiopharmaceutical for SPECT imaging of regional cerebral blood perfusion. *J Nucl Med* 28:191-202, 1987.

Pascual-Leone, A.; Dhuna, A.; and Anderson, D.C. Cerebral atrophy in habitual cocaine abusers: a planimetric CT study. Neurology 41:34-38, 1991.

Pitts, D.K., and Marwah, J. Autonomic effects of cocaine. *Can J Physiol Pharmacol* 67:1167-1176, 1989.

Root, R.K., and Rowbotham, M. Neurologic aspects of cocaine abuse. *West J Med* 149:442-448, 1988.

Sharp, P.F.; Smith, F.W.; Gemmell, H.G.; Lyall, D.; Evans, N.T.; Gvozdanovic, D.; Davidson, J.; Tyrrell, D.A.; Pickett, R.D.; and Neirinckx, R.D. Technetium-99m HM-PAO steroisomers as potential agents for imaging regional cerebral blood flow: Human volunteer studies. *J Nucl Med 27:* 171-177, 1986.

Stuss, D.T., and Benson, D.F. *The Frontal Lobes. New* York: Raven Press, 1986.

U.S. Department of Health and Human Services. Cocaine induces vascular changes in brain: Demonstration by SPECT. News Release. August 31, 1990.

Volkow, N.D.; Fowler, J.S.; and Wolf, A.P. Changes in brain glucose metabolism in cocaine dependence and withdrawal. *Am J Psychiatry* 148:621-626, 1991.

Volkow, N.D.; Mullani, N.; Gould, K.; Adler, S.; and Krajewski, K. Cerebral blood flow in chronic cocaine users: a study using positron emission tomography. *Br J Psychiatry* 152:641-648, 1988.

AUTHORS

I. Mena, M.D.
Division of Nuclear Medicine

R.J. Giombetti, M.D.
Department of Neurology

B.L. Miller, M.D.
Department of Neurology

K. Garrett, CNMT
Division of Nuclear Medicine

J. Villanueva-Meyer, M.D.
Division of Nuclear Medicine

C. Mody, M.D.
Department of Neurology

M.A. Goldberg, Ph.D., M.D.
Department of Neurology
UCLA School of Medicine
Harbor-UCLA Medical Center
Torrance, CA 90509

An Introduction to Magnetic Resonance Methods for Clinical Research

Gerald G. Blackwell

INTRODUCTION

Nuclear magnetic resonance (NMR) analytical methods have been an integral part of basic biochemistry laboratories since NMR's introduction approximately 40 years ago. In recent years, however, these powerful methods have found a niche in diagnostic medical imaging and basic biomedical research. The purpose of this brief chapter is to introduce the reader to basic NMR methods so as to foster thought for applications in the arena of drug development.

BASIC PRINCIPLES

NMR methods exploit the magnetic properties of certain atomic nuclei (Saini et al. 1988). Nuclei possessing an odd number of protons, neutrons, or both have a small electromagnetic field associated with their nuclear spin. Different nuclear species spin at different frequencies, but, importantly, all nuclei of a given element will spin at precisely the same frequency. This frequency is described by the Larmor equation: frequency = gyromagnetic ratio x magnetic field strength. The Larmor frequency for atomic nuclei occurs in the radiofrequency range of the electromagnetic spectrum, and specialized instruments enable researchers to interact with atomic nuclei using this nonionizing radiation (Doyle and Blackwell 1992).

The instruments designed to acquire magnetic resonance images and spectra are composed of a magnet set, a coil capable of both transmitting and receiving radiofrequency signals, and a computer that coordinates and integrates instructions to the instrument. The magnet set determines the external field strength and also can be manipulated to produce transient gradients that allow spatial localization. The

radiofrequency coil is "tuned" to interrogate the desired nuclear species, and the computer faithfully records the resultant signal (Doyle and Blackwell 1992).

The nucleus most easily interrogated by NMR methods is hydrogen. The hydrogen nucleus is widely distributed in all organic compounds, and its electromagnetic signal can be detected easily. Other species that are NMR "visible" and of potential medical relevance are given in table 1. Specialized techniques can produce three-dimensional displays of nuclear magnetic resonance distribution (magnetic resonance imaging-MRI) or, alternatively, displays of nuclear composition and concentration (magnetic resonance spectroscopy). Most medical research to date has focused on the imaging of hydrogen nuclei and spectroscopy of phosphorus nuclei.

TABLE 1. *NMR "visible" nuclei of potential medical relevance*

Isotopes With Spin	Molar Concentration	Gyromagnetic Ratio (MHz/T)*	NMR Sensitivity
^{1}H	99	42.58	1
^{14}N	1.6	3.08	--
^{31}P	0.35	17.24	0.066
^{13}C	0.10	10.71	0.016
^{23}Na	0.078	11.26	0.093
^{39}K	0.045	1.99	0.0005
^{17}O	0.031	5.77	0.029
^{2}H	0.015	6.53	0.0096
^{19}F	0.0066	40.05	0.830

*MHz/T = Megahertz/Tesla

It must be recognized that the appearance of magnetic resonance images and spectra is dependent upon a complex interaction between equipment acquisition parameters and the local chemical environment of the nucleus in question. Detailed descriptions of these principles are beyond the scope of this article, and the interested reader can consult several comprehensive reviews and texts (Higgins et al. 1992; Bottomley et al. 1984; Pykett 1982; Horowitz 1989; Nelson et al. 1984).

MAGNETIC RESONANCE IMAGING

The first human magnetic resonance images were obtained approximately 20 years ago, but, through the collaboration of basic scientists and clinicians, MRI applications have expanded rapidly (Lauterbur 1973). The clarity and resolution of magnetic resonance images are unparalleled, and MRI is established firmly as the imaging method of choice for diseases involving many organ systems. The advantages of MRI, compared with other imaging techniques, include the ability to manipulate image contrast by changing acquisition parameters and the ability to assess function and flow. Tissue contrast also can be improved in certain situations by the use of paramagnetic contrast agents (Canby et al. 1987). Most clinical imaging to date has focused on central nervous system (CNS) and musculoskeletal applications. Magnetic resonance images are degraded by motion, and applications to organ systems such as the cardiovascular system have been slower to develop. Gating techniques and ultrafast imaging sequences reduce motion artifact, and applications for this technology are expanding (Lotan et al. 1988; Blackwell et al. 1992).

The CNS is well suited for study by MRI. Unprecedented insight into both normal and abnormal brain structure has been provided using current clinical instruments. Preliminary work in the author's laboratory using a very high field strength 4.1 tesla instrument offers hope that new frontiers in human CNS imaging will be opened. The tissue contrast and spatial resolution achieved at this high field strength may exceed what is obtainable on standard clinical instruments (figure 1). Continued research may add to existing knowledge of structure and function relationships within the CNS.

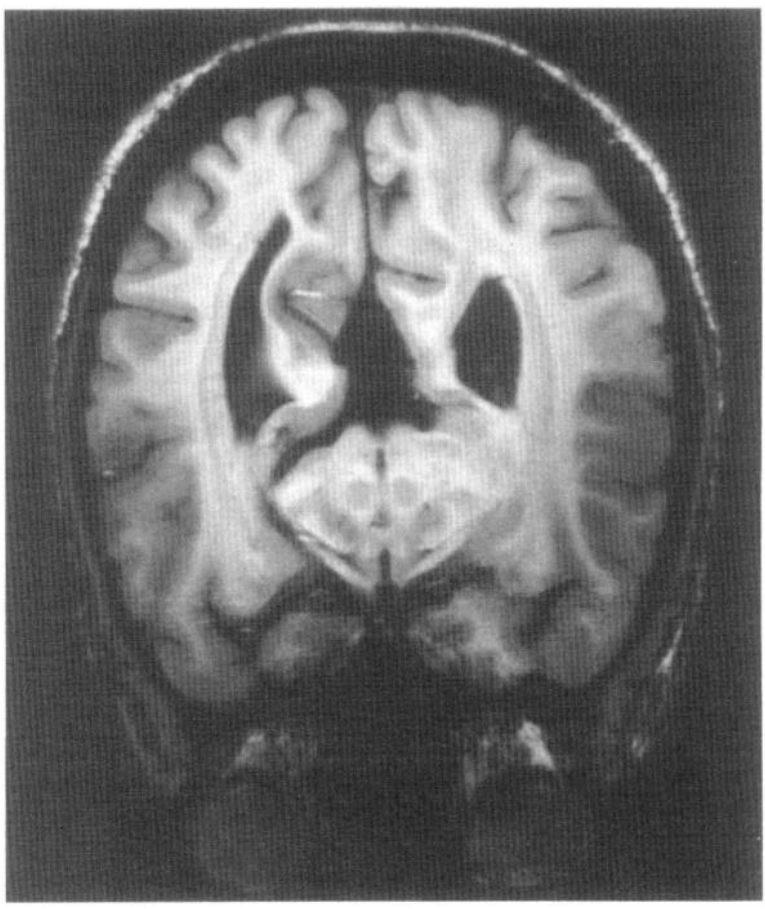

FIGURE 1. *Inversion recovery gradient echo image of the human brain obtained at a field strength of 4.1 tesla. Slice thickness is 3 mm with an in-plane resolution of 450 microns. Tissue contrast and spatial resolution may be improved using this highfield strength.*

SOURCE: *Image courtesy of Dr. Hoby Hetherington, Center for Nuclear Imaging Research, University of Alabama at Birmingham.*

MAGNETIC RESONANCE SPECTROSCOPY

In addition to providing high-resolution images, biochemical information also can be obtained noninvasively using magnetic resonance spectroscopy. Many chemical moieties can be interrogated using the nuclei shown in table 1. Because of the central role of phosphorus-containing compounds in cellular energetics, much of the work to date has focused on phosphorus-31 spectroscopy (Bottomley et al. 1990; Robitaille et al. 1989; Schaefer et al. 1989). Using magnetic resonance techniques, measurements can be made of compounds such as phosphocreatine (PCr), inorganic phosphate (Pi), and adenosine triphosphate (ATP). Figure 2 is an example of a normal in vivo phosphorus spectrum from human myocardium.

In vivo and in vitro spectroscopy research also is being performed utilizing compounds that contain hydrogen, ^{13}C, and ^{23}Na (Barany et al. 1988; Evanochko et al. 1987; Reeves et al. 1989). Many organic compounds (e.g., lipids and lactate) can be studied through hydrogen and carbon spectroscopy, and sodium spectroscopy may facilitate insight into intracellular and extracellular fluid distribution and membrane integrity.

Realizing that acquisitions may be manipulated to obtain either images or spectra, researchers recently have focused on providing images of different compounds, so-called spectroscopic imaging. Figure 3 is an example of such an image. With spectroscopic imaging, anatomic maps can be derived of a specific chemical moiety. Much work has been carried out at lower field strengths, but research using high field strength instruments with their inherently improved signal-to-noise ratio is ongoing in the author's laboratory and other laboratories. It is anticipated that the combination of high field strength instruments and better radiofrequency coil design will greatly advance these techniques.

SUMMARY

It is very early in the era of exploiting the power of magnetic resonance methods. Great strides have been made in both diagnostic medical imaging and spectroscopy. Using high field strength instruments, normal and abnormal biochemistry within specific CNS

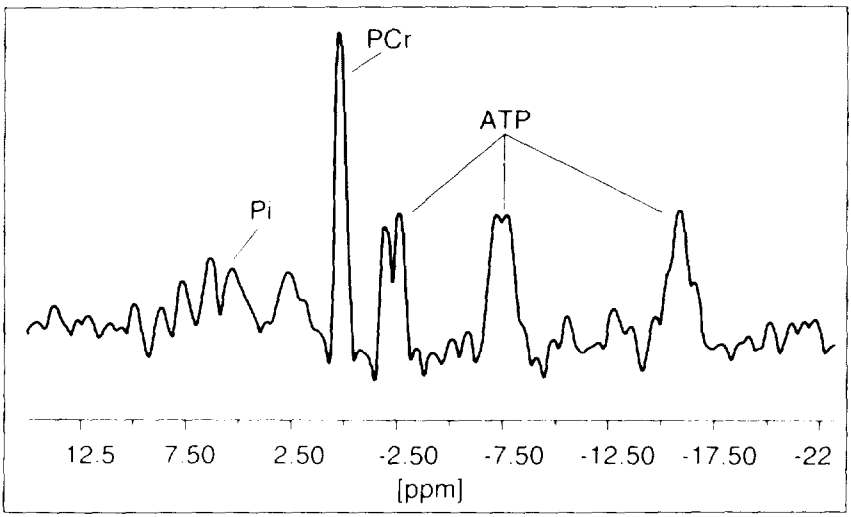

FIGURE 2. *Normal phosphorous spectrum from the human myocardium obtained at 1.5 tesla. Note separate peaks for the three phosphorus atoms in ATP.*

KEY: Pi = inorganic phosphate; PCr = phosphocreatine; ATP = adenosine triphosphate

SOURCE: Reproduced from Blackwell, G.; Cranney, G.; and Pohost, G., eds. MRI: Cardiovascular System. New York: Gower Medical Publishing, 1992.

regions and their response to interventions ultimately may be discernible. With technological improvements, it is to be expected that image quality will improve, and in vivo spectroscopy may move rapidly from the research environment into the clinical arena.

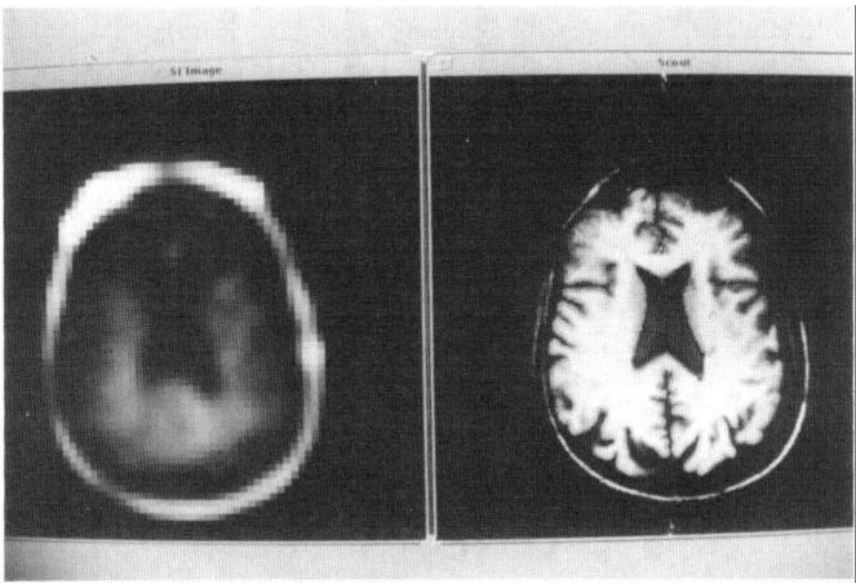

FIGURE 3. *Spectroscopic image of the human brain obtained at 4.1 tesla. The right panel is a standard transverse scout image. The left panel represents distribution of the compound N-acetylaspartate within this slice. Voxel resolution 0.5 cm^3. Using this technology, anatomic distribution of many different compounds can be discerned.*

SOURCE: Image courtesy of Dr. Hoby Hetherington, Center for Nuclear Imaging Research, University of Alabama at Birmingham.

REFERENCES

Barany, M.; Langer, B.G.; Glick, R.P.; Venkatasubramonion, P.N.; Wilbur, A.C.; and Spigos, D.G. In vivo H-l spectroscopy in humans at 1.5 T. *Radiology* 167:839-844, 1988.

Blackwell, G.; Doyle, M.; and Cranney, G. Cardiovascular MRI techniques. In: Blackwell, G.; Cranney, G.; and Pohost, G., eds. *MRI: Cardiovascular System.* New York: Gower Medical Publishing, 1992.

Bottomley, P.A.; Foster, T.H.; Argersinger, R.E.; and Pfeifer, L.M. A review of normal tissue hydrogen NMR relaxation times and mechanisms from 1-100 MHz: Dependence on tissue type, NMR frequency, temperature, species, excision, and age. *Am Assoc Phys Med* 11:425-448, 1984.

Bottomley, P.A.; Hardy, C.J.; and Roemer, P.B. Phosphate metabolite imaging and concentration measurements in human heart by nuclear magnetic resonance. *Magn Reson Med* 14:425-434, 1990.

Canby, R.C.; Elgavish, G.A.; and Pohost, G.M. Paramagnetic NMR contrast agents for cardiovascular imaging. *New Concepts Card Imaging* 3:315-342, 1987.

Doyle, M., and Blackwell, G. Basic principles of MRI. In: Blackwell, G.; Cranney, G.; and Pohost, G. eds. *MRI: Cardiovascular System.* New York: Gower Medical Publishing, 1992.

Evanochko, W.T.; Reeves, R.C.; Sakai, T.T.; Canby, R.C.; and Pohost, G.M. Proton NMR spectroscopy in myocardial ischemic insult. *Magn Reson Med* 5:23-31, 1987.

Higgins, C.B.; Hricak, H.; and Helms, C.A., eds. *Magnetic Resonance Imaging* of *the Body.* New York: Raven Press, 1992.

Horowitz, A.L. *MRI Physics for Physicians.* New York: Springer-Verlag, 1989.

Lauterbur, P.C. Image formation by induced local interactions: Examples employing nuclear magnetic resonance. Nature 242: 190, 1973.

Lotan, C.S.; Cranney, G.B.; and Pohost, G.M. Cine NMR: An emerging technology. *Echocardiography* 5:373-382, 1988.

Nelson, T.R.; Hendrick, R.E.; and Hendee, W.R. Selection of pulse sequences producing maximum tissue contrast in magnetic resonance imaging. *Magn Reson Imaging* 2:285-294, 1984.

Pykett, I.L. NMR imaging in medicine. *Sci Am* 246:78-89, 1982.

Reeves, R.C.; Evanochko, W.T.; Canby, R.C.; McMillin, J.B.; and Pohost, G.M. Demonstration of increased myocardial lipid with postischemic dysfunction ("myocardial stunning") by proton nuclear magnetic resonance spectroscopy. *J Am Coll Cardiol* 13:739, 1989.

Robitaille, P.M.; Lew, B.; Merkle, H.; Sublett E.; Lindstrom, P.; From, A.H.; Garwood, M.; Bache, R.J.; and Ugurbil, K. Transmural metabolite distribution in regional myocardial ischemia as studied with ^{31}P NMR. *Magn Reson Med* 10:108-110, 1989.

Saini, S.; Frankel, R.B.; Stark, D.D.; and Ferrucci, J.T. Magnetism: A primer and review. *AJR* 150:735-744, 1988.

Schaefer, S.; Camacho, A.; Gober, J.M.; Obregon, R.G.; DeGroot, M.A.; Botvinick, E.H.; Massie, B.; and Weiner, M.W. Response of myocardial metabolites to graded regional ischemia: ^{31}P NMR spectroscopy of porcine myocardium in vivo. *Circ Res* 64:968-976, 1989.

AUTHOR

Gerald G. Blackwell, M.D.
1808 Seventh Avenue South
Cardiovascular NMR Laboratory
D105 Diabetes Hospital
University of Alabama at Birmingham
Birmingham, AL 35294-0012

National Institute on Drug Abuse Research

monograph series

While limited supplies last, single copies of the monographs may be obtained free of charge from the National Clearinghouse for Alcohol and Drug Information (NCADI). Please contact NCADI also for information about availability of coming issues and other publications of the National Institute on Drug Abuse relevant to drug abuse research.

Additional copies may be purchased from the U.S. Government Printing Office (GPO) and/or the National Technical Information Service (NTIS) as indicated. NTIS prices are for paper copy; add $3.00 handling charge for each order. Microfiche copies are also available from NTIS. Prices from either source are subject to change.

Addresses are:

NCADI
National Clearinghouse for Alcohol and Drug Information
P.O. Box 2345
Rockville, MD 20852
(301) 468-2600
(800) 729-6686

GPO
Superintendent of Documents
U.S. Government Printing Office
P.O. Box 371954
Pittsburgh, PA 15220-7954
(202) 738-3238
FAX (202) 512-2233

NTIS
National Technical Information Service
U.S. Department of Commerce
Springfield, VA 22161
(703) 487-4650

For information on availability of NIDA Research Monographs from 1975-1993 and those not listed, write to NIDA, Community and Professional Education Branch, Room 10A-39, 5600 Fishers Lane, Rockville, MD 20857.

26 THE BEHAVIORAL ASPECTS OF SMOKING. Norman A. Krasnegor, Ph.D., ed. (Reprint from 1979 Surgeon General's Report on Smoking and Health.)
NCADI #M26 NTIS PB #80-118755/AS $23

42 THE ANALYSIS OF CANNABINOIDS IN BIOLOGICAL FLUIDS. Richard L. Hawks, Ph.D., ed.
NCADI #M42 NTIS PB #83-136044/AS $23

50 COCAINE: PHARMACOLOGY, EFFECTS, AND TREATMENT OF ABUSE. John Grabowski, Ph.D., ed.
NCADI #M50 NTIS PB #85-150381/AS $23

52 TESTING DRUGS FOR PHYSICAL DEPENDENCE POTENTIAL AND ABUSE LIABILITY. Joseph V. Brady, Ph.D., and Scott E. Lukas, Ph.D., eds.
NCADI #M52 NTIS PB #85-150373/AS $23

53 PHARMACOLOGICAL ADJUNCTS IN SMOKING CESSATION. John Grabowski, Ph.D., and Sharon M. Hall, Ph.D., eds.
NCADI #M53 NTIS PB #89-123186/AS $23

54 MECHANISMS OF TOLERANCE AND DEPENDENCE. Charles W. Sharp, Ph.D., ed.
NCADI #M54 NTIS PB #89-103279/AS $39

56 ETIOLOGY OF DRUG ABUSE: IMPLICATIONS FOR PREVENTION. Coryl LaRue Jones, Ph.D., and Robert J. Battjes, D.S.W., eds.
NCADI #M56 NTIS PB #89-123160/AS $31

61 COCAINE USE IN AMERICA: EPIDEMIOLOGIC AND CLINICAL PERSPECTIVES. Nicholas J. Kozel, MS., and Edgar H. Adams, M.S., eds.
NCADI #M61 NTIS PB #89-131866/AS $31

62 NEUROSCIENCE METHODS IN DRUG ABUSE RESEARCH. Roger M. Brown, Ph.D., and David P. Friedman, Ph.D., eds.
NCADI #M62 NTIS PB #89-130660/AS $23

63 PREVENTION RESEARCH: DETERRING DRUG ABUSE AMONG CHILDREN AND ADOLESCENTS. Catherine S. Bell, MS., and Robert J. Battjes, D.S.W., eds.
NCADI #M63 NTIS PB #89-103287/AS $31

64 PHENCYCLIDINE: AN UPDATE. Doris H. Clouet, Ph.D., ed.
NCADI #M64 NTIS PB #89-131858/AS $31

65 WOMEN AND DRUGS: A NEW ERA FOR RESEARCH. Barbara A. Ray, Ph.D., and Monique C. Braude, Ph.D., eds.
NCADI #M65 NTIS PB #89-130637/AS $23

69 OPIOID PEPTIDES: MEDICINAL CHEMISTRY. Rao S. Rapaka, Ph.D.; Gene Bamett, Ph.D.; and Richard L. Hawks, Ph.D., eds.
NCADI #M69 NTIS PB #89-158422/AS $39

70 OPIOID PEPTIDES: MOLECULAR PHARMACOLOGY, BIOSYNTHESIS, AND ANALYSIS. Rao S. Rapaka, Ph.D., and Richard L. Hawks, Ph.D., eds.
NCADI #M70 NTIS PB #89-158430/AS $45

72 RELAPSE AND RECOVERY IN DRUG ABUSE. Frank M. Tims, Ph.D., and Carl G. Leukefeld, D.S.W., eds.
NCADI #M72 NTIS PB #89-151963/AS $3 1

74 NEUROBIOLOGY OF BEHAVIORAL CONTROL IN DRUG ABUSE. Stephen I. Szara, M.D., D.Sc., ed.
NCADI #M74 NTIS PB #89-151989/AS $23

78 THE ROLE OF NEUROPLASTICITY IN THE RESPONSE TO DRUGS. David P. Friedman, Ph.D., and Doris H. Clouet, Ph.D., eds.
NCADI #M78 NTIS PB #88-245683/AS $31

79 STRUCTURE-ACTIVITY RELATIONSHIPS OF THE CANNABINOIDS. Rao S. Rapaka, Ph.D., and Alexandros Makriyannis, Ph.D., eds.
NCADI #M79 NTIS PB #89-109201/AS $31

80 NEEDLE SHARING AMONG INTRAVENOUS DRUG ABUSERS: NATIONAL AND INTERNATIONAL PERSPECTIVES. Robert J. Battjes, D.S.W., and Roy W. Pickens, Ph.D., eds.
NCADI #M80 NTIS PB #88-236138/AS $31

82 OPIOIDS IN THE HIPPOCAMPUS. Jacqueline F. McGinty, Ph.D., and David P. Friedman, Ph.D., eds.
NCADI #M82 NTIS PB #88-245691/AS $23

83 HEALTH HAZARDS OF NITRITE INHALANTS. Harry W. Haverkos, M.D., and John A. Dougherty, Ph.D., eds.
NCADI #M83 NTIS PB #89-125496/AS $23

84 LEARNING FACTORS IN SUBSTANCE ABUSE. Barbara A. Ray, Ph.D., ed.
NCADI #M84 NTIS PB #89-125504/AS $31

85 EPIDEMIOLOGY OF INHALANT ABUSE: AN UPDATE. Raquel A. Crider, Ph.D., and Beatrice A. Rouse, Ph.D., eds.
NCADI #M85 NTIS PB #89-123178/AS $31

87 OPIOID PEPTIDES: AN UPDATE. Rao S. Rapaka, Ph.D., and Bhola N. Dhawan, M.D., eds.
NCADI #M87 NTIS PB #89-158430/AS $45

88 MECHANISMS OF COCAINE ABUSE AND TOXICITY. Doris H. Clouet, Ph.D.; Khursheed Asghar, Ph.D.; and Roger M. Brown, Ph.D., eds.
NCADI #M88 NTIS PB #89-125512/AS $39

89 BIOLOGICAL VULNERABILITY TO DRUG ABUSE. Roy W. Pickens, Ph.D., and Dace S. Svikis, B.A., eds.
NCADI #M89 NTIS PB #89-125520/AS $23

92 TESTING FOR ABUSE LIABILITY OF DRUGS IN HUMANS. Marian W. Fischman, Ph.D., and Nancy K. Mello, Ph.D., eds.
NCADI #M92 NTIS PB #90-148933/AS $45

94 PHARMACOLOGY AND TOXICOLOGY OF AMPHETAMINE AND RELATED DESIGNER DRUGS. Khursheed Asghar, Ph.D., and Errol De Souza, Ph.D., eds.
NCADI #M94 NTIS PB #90-148958/AS $39

95 PROBLEMS OF DRUG DEPENDENCE, 1989. PROCEEDINGS OF THE 5 1 ST ANNUAL SCIENTIFIC MEETING. THE COMMITTEE ON PROBLEMS OF DRUG DEPENDENCE, INC. Louis S. Harris, Ph.D., ed.
NCADI #M95 NTIS PB #0-237660/AS $67

96 DRUGS OF ABUSE: CHEMISTRY, PHARMACOLOGY, IMMUNOLOGY, AND AIDS. Phuong Thi Kim Pham, Ph.D., and Kenner Rice, Ph.D., eds.
NCADI #M96 NTIS PB #90-237678/AS $31

97 NEUROBIOLOGY OF DRUG ABUSE: LEARNING AND MEMORY. Lynda Erinoff, Ph.D., ed.
NCADI #M97 NTIS PB #90-237686/AS $31

98 THE COLLECTION AND INTERPRETATION OF DATA FROM HIDDEN POPULATIONS. Elizabeth Y. Lambert, MS., ed.
NCADI #M98 NTIS PB #90-237694/AS $23

99 RESEARCH FINDINGS ON SMOKING OF ABUSED SUBSTANCES. C. Nora Chiang, Ph.D., and Richard L. Hawks, Ph.D., eds.
NCADI #M99 NTIS PB #91-141119/AS $23

100 DRUGS IN THE WORKPLACE: RESEARCH AND EVALUATION DATA. VOLUME II. Steven W. Gust, Ph.D.; J. Michael Walsh, Ph.D.; Linda B. Thomas, B.S.; and Dennis J. Crouch, M.B.A., eds.
GPO Stock #017-024-01458-3 $8 NCADI #M100

101 RESIDUAL EFFECTS OF ABUSED DRUGS ON BEHAVIOR. John W. Spencer, Ph.D., and John J. Boren, Ph.D., eds.
GPO Stock #017-024-01426-7 $6 NTIS PB #91-172858/AS $31
NCADI #M101

102 ANABOLIC STEROID ABUSE. Geraline C. Lin, Ph.D., and Lynda Erinoff, Ph.D., eds.
GPO Stock #017-024-01425-7 $8 NTIS PB #91-172866/AS $31
NCADI #M 102

106 IMPROVING DRUG ABUSE TREATMENT. Roy W. Pickens, Ph.D.; Carl G. Leukefeld, D.S.W.; and Charles R. Schuster, Ph.D., eds.
GPO Stock #017-024-01439-7 $12 NTIS PB #92-105873
NCADI #M106 Paperback $50 Microfiche $19

107 DRUG ABUSE PREVENTION INTERVENTION RESEARCH: METHODOLOGICAL ISSUES. Carl G. Leukefeld, D.S.W., and William J. Bukoski, Ph.D., eds.
GPO Stock #017-024-01441-9 $9 NTIS PB #92-160985
NCADI #M107 Paperback $35 Microfiche $17

108 CARDIOVASCULAR TOXICITY OF COCAINE: UNDERLYING MECHANISMS. Pushpa Thadani, Ph.D., ed.
GPO Stock #017-024-01446-0 $7 NTIS PB #92-106608
NCADI #M108 Paperback $35 Microfiche $17

109 LONGITUDINAL STUDIES OF HIV INFECTION IN INTRAVENOUS DRUG USERS: METHODOLOGICAL ISSUES IN NATURAL HISTORY RESEARCH. Peter Hartsock, Dr.P.H., and Sander G. Genser, M.D., M.P.H., eds.
GPO Stock #017-024-01445-l $4.50 NTIS PB #92-106616
NCADI #M109 Paperback $26 Microfiche $12.50

111 MOLECULAR APPROACHES TO DRUG ABUSE RESEARCH: VOLUME I. RECEPTOR CLONING, NEUROTRANSMITTER EXPRESSION, AND MOLECULAR GENETICS. Theresa N.H. Lee, Ph.D., ed.
NCADI #M111 NTIS PB #92-135743
Paperback $35 Microfiche $17

112 EMERGING TECHNOLOGIES AND NEW DIRECTIONS IN DRUG ABUSE RESEARCH. Rao S. Rapaka, Ph.D.; Alexandros Makriyannis, Ph.D.; and Michael J. Kuhar, Ph.D., eds.
GPO Stock #017-024-01455-9 $11 NTIS PB #92-155449
NCADI #M112 Paperback $44 Microfiche $17.50

113 ECONOMIC COSTS, COST EFFECTIVENESS, FINANCING, AND COMMUNITY-BASED DRUG TREATMENT. William S. Cartwright, Ph.D., and James M. Kaple, Ph.D., eds.
NCADI #M113 NTIS PB #92-155795
Paperback $35 Microfiche $17

114 METHODOLOGICAL ISSUES IN CONTROLLED STUDIES ON EFFECTS OF PRENATAL EXPOSURE TO DRUG ABUSE. M. Marlyne Kilbey, Ph.D., and Khursheed Asghar, Ph.D., eds.
GPO Stock #017-024-01459-1 $12 NTIS PB #92-146216
NCADI #M114 Paperback $43 Microfiche $17

115 METHAMPHETAMINE ABUSE: EPIDEMIOLOGIC ISSUES AND IMPLICATIONS. Marissa A. Miller, D.V.M., M.P.H., and Nicholas J. Kozel, M.S., eds.
GPO Stock #017-024-01460-5 $4 NCADI #M115

116 DRUG DISCRIMINATION: APPLICATIONS TO DRUG ABUSE RESEARCH. Richard A. Glennon, Ph.D.; Torbjörn U.C. Järbe, Ph.D.; and Jerry Frankenheim, Ph.D., eds.
GPO Stock #017-024-01470-2 $13 NCADI #M116

117 METHODOLOGICAL ISSUES IN EPIDEMIOLOGY, PREVENTION, AND TREATMENT RESEARCH ON DRUG-EXPOSED WOMEN AND THEIR CHILDREN. M. Marlyne Kilbey, Ph.D., and Khursheed Asghar, Ph.D., eds.
GPO Stock #017-024-01472-9 $12 NCADI #M117

118 DRUG ABUSE TREATMENT IN PRISONS AND JAILS. Carl G. Leukefeld, D.S.W., and Frank M. Tims, Ph.D., eds.
GPO Stock #017-024-01473-7 $16 NCADI #M118

120 BIOAVAILABILITY OF DRUGS TO THE BRAIN AND THE BLOOD-BRAIN BARRIER. Jerry Frankenheim, Ph.D., and Roger M. Brown, Ph.D., eds.
GPO Stock #017-024-01481-8 $10 NCADI #M120

121 BUPRENORPHINE: AN ALTERNATIVE TREATMENT FOR OPIOID DEPENDENCE. Jack D. Blaine, Ph.D., ed.
GPO Stock #017-024-01482-6 $5 NCADI #M121

123 ACUTE COCAINE INTOXICATION: CURRENT METHODS OF TREATMENT. Heinz Sorer, Ph.D., ed.
GPO #017-024-01501-6 $6.50 NCADI #M123

124 NEUROBIOLOGICAL APPROACHES TO BRAIN-BEHAVIOR INTERACTION. Roger M. Brown, Ph.D., and Joseph Fracella, Ph.D. eds.
GPO Stock #017-024-01492-3 $9 NCADI #M124

125 ACTIVATION OF IMMEDIATE EARLY GENES BY DRUGS OF ABUSE. Reinhard Grzanna, Ph.D., and Roger M. Brown, Ph.D., eds.
GPO #017-024-01503-2 $7.50 NCADI #M125

126 MOLECULAR APPROACHES TO DRUG ABUSE RESEARCH. VOLUME II: STRUCTURE, FUNCTION, AND EXPRESSION. Theresa N.H. Lee, Ph.D., ed. NCADI #M126

127 PROGRESS AND ISSUES IN CASE MANAGEMENT. Rebecca Sager Ashery, D.S.W., ed.
GPO Stock #017-024-01490-7 $14 NCADI #M127

128 STATISTICAL ISSUES IN CLINICAL TRIALS FOR TREATMENT OF OPIATE DEPENDENCE. Ram B. Jain, Ph.D., ed.
GPO Stock #017-024-01491-5 $6.50 NCADI #M128

129 INHALANT ABUSE: A VOLATILE RESEARCH AGENDA. Charles W. Sharp, Ph.D.; Fred Beauvais, Ph.D.; and Richard Spence, Ph.D., eds.
GPO Stock #017-024-01496-6 $12 NCADI #M129

130 DRUG ABUSE AMONG MINORITY YOUTH: ADVANCES IN RESEARCH AND METHODOLOGY. Mario R. De La Rosa, Ph.D., and Juan-Luis Recio Adrados, Ph.D., eds.
GPO #017-024-01506-7 $14 NCADI #M130

131 IMPACT OF PRESCRIPTION DRUG DIVERSION CONTROL SYSTEMS ON MEDICAL PRACTICE AND PATIENT CARE. James R. Cooper, Ph.D.; Dorynne J. Czechowicz, M.D.; Stephen P. Molinari, J.D., R.Ph.; and Robert C. Peterson, Ph.D., eds.
GPO #017-024-01505-9 $14 NCADI #M131

132 PROBLEMS OF DRUG DEPENDENCE, 1992: PROCEEDINGS OF THE 54TH ANNUAL SCIENTIFIC MEETING OF THE COLLEGE ON PROBLEMS OF DRUG DEPENDENCE. Louis Harris, Ph.D., ed.
GPO Stock #017-024-01502-4 $23 NCADI #M132

133 SIGMA, PCP, AND NMDA RECEPTORS. Errol B. De Souza, Ph.D.; Doris H. Clouet, Ph.D.; and Edythe D. London, Ph.D., eds.
NCADI #M133

134 MEDICATIONS DEVELOPMENT: DRUG DISCOVERY, DATABASES, AND COMPUTER-AIDED DRUG DESIGN. Rao S. Rapaka, Ph.D., and Richard L. Hawks, Ph.D., eds.
GPO #017-024-01511-3 $11 NCADI #M134

135 COCAINE TREATMENT: RESEARCH AND CLINICAL PERSPECTIVES. Frank M. Tims, Ph.D., and Carl G. Leukefeld, D.S.W., eds.
GPO #017-024-01520-2 $11 NCADI #M135

136 ASSESSING NEUROTOXICITY OF DRUGS OF ABUSE. Lynda Erinoff, Ph.D., ed.
GPO #017-024-01518-1 $11 NCADI #M136

137 BEHAVIORAL TREATMENTS FOR DRUG ABUSE AND DEPENDENCE. Lisa Simon Onken, Ph.D.; Jack D. Blaine, M.D.; and John J. Boren, Ph.D., eds.
GPO #017-024-01519-9 NCADI #M137

☆ U.S. GOVERNMENT PRINTING OFFICE: 1994 300-973/80006

NIH Publication No. 94-3728
Printed 1994